DSPACE

https://dspace.org/

Geostatistical modelling and simulation of uncertainty of a kimberlite pipe.

Mjimba, Nqangi.

2014-02-03
http://hdl.handle.net10539/13633

Downloaded from a DSpace repository. https://dspace.org/

GEOSTATISTICAL MODELLING AND SIMULATION OF UNCERTAINTY OF A KIMBERLITE PIPE

Nqangi Mjimba

A research project submitted to the Faculty of Engineering and the Built Environment, University of the Witwatersrand, in partial fulfilment of the requirements for the degree of Master of Science in Mining Engineering.

Johannesburg, 2013

DECLARATION

I declare that this research report is my own, unaided work. It is being submitted in partial fulfilment of requirements for the Degree of Master of Science in Mining Engineering in the University of the Witwatersrand, Johannesburg. It has not been submitted before for any degree or examination in any other University. The information on which this dissertation is based was obtained from Murowa Diamond Mine after request and approval to use the mine for project purposes.

_____

(Signature of candidate)

_____ day of _____ _____

ABSTRACT

Understanding uncertainty associated with grades in resource models is an essential requirement for mineral resource evaluation. One of the most important considerations in diamond estimation is the use of an appropriate variable that represents the true variability of grades in the kimberlite. The Spm^3 variable used in the Murowa pipes expresses true the variability of the grades in the kimberlite pipes.

Kriging in the Normal Scores (NS) approach and conditional geostatistical simulations were used to investigate and quantify uncertainty of the grade in the KIMB4 unit of the K1 pipe. The kriging in NS approach did not perform well in demarcating areas that are truly high and those that are truly low in the estimates. Point realisations were then generated using the sequential gaussian simulation algorithm. The resultant conditional means and variances highlighted areas of high and low uncertainty in the grade estimates. The point scale realisations were then averaged to the blocks size used at Murowa (25m x 25m x 15m) to obtain the block conditional simulation model. Zones of high and low uncertainties in the grade estimates of KIMB4 of the Murowa K1 kimberlite were delineated and additional drilling was proposed to reduce the uncertainty in the grade estimates. The uncertainty in grade was also investigated down the pipe and this further identified the need for additional sampling at depth.

ACKNOWLEDGEMENTS

The author would like to thank Professor. R. Minnitt for his patience in supervising the research project and for assistance in administrative matters at the University of the Witwatersrand. Dr Chris Prins gave some valuable insight into the fundamentals of diamond deposit evaluation. Special thanks go to Mr Lovemore Chimuka for all his input and for supplying the data used in the study. Murowa Diamonds, the operating company of Murowa Diamonds Mine, is thanked for granting me the opportunity to conduct this study and the permission to publish this project report. I am grateful to Dr. Ina Dohm who first fanned my interest in geostatistics. Lastly, a special thanks to Dr Alexandre Boucher and his prompt assistance in matters relating to the availability and use of the SGeMS software.

For my Husband

Ignatious Ncube

CONTENTS

DECLARATION 2

ABSTRACT 3

CONTENTS 6

LIST OF FIGURES 9

LIST OF TABLES 12

LIST OF SYMBOLS 13

NOMENCLATURE 14

1 INTRODUCTION 16

1.1 General Geology 16

1.2 Kimberlite Geology 19

2 FORMULATION OF THE PROBLEM 23

2.1 Justification for the current study 26

2.2 Parameters used in diamond grade estimation 30

2.2.1 The appropriate variable for estimation 30

2.2.2 Modifications necessary to combine different data sources 32

2.2.3 The incorporation of calliper data for sample volume and density for sample mass 33

2.2.4 Inclusion or exclusion of incidental diamonds 33

3 EXPLORATORY DATA ANALYSIS 34

3.1 Data Validation 34

3.2 Data declustering 37

3.3 Variography of the domains of the K1 pipe 38

4 GEOSTATISTICAL ANALYSIS OF THE SPM^3 VARIABLE OF THE KIMB4 DOMAIN 42

4.1 Ordinary Kriging 42
4.2 Normal Scores variography of the KIMB4 domain 46
4.3 Indicator Kriging of Spm^3 variable....52
5 CONDITIONAL SIMULATION OF THE SPM^3 VARIABLE OF THE KIMB4 DOMAIN 57
5.1 The Theory of Sequential Gaussian Simulation....57
5.1.1 Validation of the simulations 60
5.2 The application of sequential gaussian simulation to the Spm3 variable....60
5.2.1 Validation of the Spm^3 variable simulation 62
6 ASSESSING UNCERTAINTY IN THE KIMB4 DOMAIN 67
6.1 Measures of uncertainty 68
6.2 Point kriging model 69
6.3 Quantile and Probability Maps....72
6.4 Point Simulation Model....74
6.5 Presentation of the block model 78
7 DISCUSSION 86
8 CONCLUSIONS AND RECOMMENDATIONS 90
8.1 Recommendations for Future Work 91
9 REFERENCES....92
APPENDIX I- EXTRACT FROM THE JORC CODE: REPORTING OF DIAMOND EXPLORATION RESULTS, MINERAL RESOURCES AND ORE RESERVES 96
APPENDIX II– EXPERIMENTAL HORIZONTAL VARIOGRAMS 99
APPENDIX III – INDICATOR VARIOGRAM MODELS FROM $SPM^3 > 5$ TO $SPM^3 >26$ THRESHOLDS 102
APPENDIX IV-PROGRESSIVE STATISTICS DATA 113

APPENDIX V-SUMMARY OF REALISATION STATISTICS 116

APPPENDIX VI- SELECTED INDIVIDUAL REALISATIONS.....118

APPENDIX V11 –15m BENCH INTERVAL AND BLOCK KRIGING MAPS OUTPUT COMPARED TO SIMULATED MAPS OUTPUT PER BENCH INTERVAL.....120

LIST OF FIGURES

Figure 1: Schematic map showing the location of Murowa kimberlites and the regional geology. 17
Figure 2: Location of the Murowa kimberlite pipes in relation to the main structural features; to the west a doleritic dyke and to the east a shear zone. Notation shows the K1-K5 pipes. 18
Figure 3: K1 geology model showing the internal geology domains. The KIMB4 domain outline is highlighted in red. 21
Figure 4: Inclined view of the K1 geology model 22
Figure 5: High grade vent surrounded by relatively low grade samples (left) and sample grades within K1 showing smoothing of grades with no recognition of feeder vent (right). Images from Platell (2011) 26
Figure 6: Plan view of the K1 pipe, showing the location of LD drill holes in K1and the MPZ domain (in pink) enveloping the other domains, and location of data points of the KIMB2/4 domain in relation to the entire K1 pipe. Image from Platell (2011) 35
Figure 7: Histograms for the KIMB1 domain (left); KIMB2/4 domains (middle) and MPZ domain (right) 36
Figure 8: Spherical model variogram for the Spm^3 variable for KIMB4 in the vertical direction....39
Figure 9: Radar chart of Horizontal variogram ranges of the KIMB4 domain....40
Figure 10: KIMB4 omni- directional spherical variogram model for the Spm^3 variable 41
Figure 11: Discretisation test used to determine the optimal block discretisation of 5x5x1 for the KIMB4 domain. 44
Figure 12: Cross validation of the Spm^3 estimates from the KIMB4 domain 45
Figure 13: The normal score transformation for data z_i. At the bottom is the anamorphosis function. Sourced from Ortiz and Deutsch (2003)....47
Figure 14: Calculation of the mean by numerical integration. Sourced from Oritz and Deutsch (2003) 48

Figure 15: Normal scores transformation process and resultant parameters of the KIMB4 Spm^3 variable.....49
Figure 16: Model variogram parameters for Spm^3 data from the domain, modelled in Gaussian space. 50
Figure 17: Comparison of untransformed OK (left) and gaussian (NS) back-transformed kriging map outputs (right).....51
Figure 18: KIMB4 domain OK results (right) and SK back-transformed kriging results (left) viewed from the SW.....52
Figure 19: Relationship between various cut-offs of Spm^3 and the proportion above cut-off (top) and the model indicator variogram at a cut-off of 12 Spm^3. 55
Figure 20: Kriged map of Spm^3 >12 viewed from the top, as well as the block model of the KIMB4 domain. 55
Figure 21: Cumulative frequency distribution of 10 randomly selected realisations in NS (in blue) compared to the cumulative frequency of the input data (in red) 63
Figure 22: The univariate statistical parameters of randomly selected histograms generated from the Sequential Gaussian simulation of Spm^3 compared to those of the sample data (bottom left). 64
Figure 23: Frequency distribution of 10 randomly selected back-transformed realisations (in blue) compared to the raw Spm3 data (in red) 65
Figure 24: Experimental variograms of randomly selected realisations (crosses) compared to the model of the input data (solid line) 66
Figure 25: Map outputs of back-transformed NS kriging (left) compared to kriging in NS with mean of zero (middle) and OK (right) showing the high grade area to the South West of the domain and low grades estimates elsewhere. 70
Figure 26: Back-transformed NS Variance (Left) compared to the Kriging variances in NS with mean of zero (middle) and OK(right) 71
Figure 27: NS Back-transformed mean map (right) compared to back-transformed variances (Left) 72
Figure 28: 0.05 (extreme left), 0.5 (middle left), 0.9 (middle right) probability maps and NS back-transformed map (extreme right).....73

Figure 29: Map of conditional means (left) and conditional variances (right) 75
Figure 30: Map outputs of probability maps at 0.1 quantile (extreme left), 0.5 quantile (middle left), 0.9 quantile (middle right) compared to the conditional mean map (extreme right).....76
Figure 31: P10 and P90 maps flagging areas that are surely high (right) and areas that are surely low in Spm^3 estimates (left). 77
Figure 32: Probability of Spm^3 values above 0.2ct/t cut-off.....78
Figure 33: Comparison of univariate statistical parameters of the Spm^3 sample data (top left) against those of the ordinary kriged estimates (top right) and mean of the simulations (bottom left). The output from the kriging and simulation is also compared using a quantile-quantile plot (bottom right) where ordinary kriged estimates are plotted on the X-axis and the Conditional mean of the simulations on the Y-axis.....79
Figure 34: Output from the different techniques generated by Kriging (left), SGS (middle) and indicator kriging results (Prob Z*>12) right 80
Figure 35: Map of Conditional means (left) and conditional variances (right) 81
Figure 36: P10 (left) and P90 (middle) maps flagging blocks that are surely high and blocks that are surely low in Spm^3 estimates blocks where there is high uncertainty - broken line (left) and conditional mean map (right). 82
Figure 37: Block coefficient of variation and resource classification.....83
Figure 38: Proposed LD holes (pink) and P10 and P90 maps flagging blocks that are surely high and blocks that are surely low in Spm^3 estimates and blocks where there is high uncertainty -broken line (middle and right). The magenta line outlines the KIMB domains, the yellow line- weathering and the blue the MPZ.....85
Figure 39: Post plots of Spm^3 values on the geological model and in relation to the areas of high and low uncertainty and resource classification based on COV. 86
Figure 40: Comparison of the output of nineteen individual conditional simulations. The ±15% envelope about the mean is shown as a reference. 88
Figure 41: Spm^3 Conditional simulated mean per bench along with the 95% confidence limits. 89

LIST OF TABLES

Table 1: Tabulation of findings that could have resulted in the deficit of 2009: Source from Platell (2011) 23
Table 2: Change in overall tonnes and carats between the 2010 and 2000 model (grey fill). Source from Platell (2011) 27
Table 3: Drillhole samples used for each domain 36
Table 4: The omni-directional semi variograms models from KIMB2/4 and MPZ domains 41
Table 5: Table showing a comparison of the estimates and actual values of the KIMB4 44
Table 6: Base statistics for CCOV and classification category 83

LIST OF SYMBOLS

Billion Years	Ga
Gamma	ɣ
Grams per Tonne	g/t
Greater than	>
Hectares	ha
Kilometre	km
Lamda	λ
Less than	<
Less than or equal to	≤
Metre	m
Nugget Effect	C0
Variogram Sill	C1
Percent	%
Tonnes	t

NOMENCLATURE

Carats per tonnne	ct/t
Carats per hundred tonnes	cpht
Coefficient of variation	COV
Cumulative distribution function	cdf
Conditional Cumulative distribution function	ccdf
East	E
Direct block simulation	DBSIM
Geostatistical Software Library	GSLIB
Hypabyssal kimberlite	HK
Injected granite	IG
Inverse power distance	IPD
Inter quartile range	IQR
Joint Ore Reserves Committee Code	JORC
Life of mine	LOM
Large diameter reverse circulation	LDRC
Murowa Expansion	MXP
Marginal Pipe Zone	MPZ
Mean Stone Size	MSS
Mantle Xenolith	MX
North	N
North North West	NNW
Normal Scores	NS
Selective Mining Unit	SMU
Sequential Gaussian Simulation	SGS
Stanford Geostatistical Modelling Software	SGeMS
Stones Per cubic metre	Spm^3
South South East	SSE
South West	SW

West	W
Dollars per carat	$/ct

1 INTRODUCTION

The Murowa kimberlite cluster is located in the South Eastern part of Zimbabwe, about 200km from the border of South Africa, 60 km South West of Masvingo and some 35 km South East of the town of Zvishavane. The Murowa kimberlite cluster was discovered and evaluated between 1997 and 2000 as part of the regional exploration program undertaken by Rio Tinto between 1994 and 2000 in Zimbabwe. The K1 (2.6ha) and K2 (0.8ha) pipes have been mined since late 2004 by conventional open-cast methods. Murowa Diamonds is the company that is responsible for mining the kimberlites. Murowa Diamonds is an unincorporated joint venture between Rio Tinto Zimbabwe (56% owned by Rio Tinto plc) and Tinto Holdings Zimbabwe (100% owned by Rio Tinto plc.). The beneficial ownership is, therefore, 78% Rio Tinto plc with the balance being held principally by investors through the Zimbabwe Stock Exchange.

1.1 General Geology

The kimberlites are of Cambrian age, situated on the Archean Zimbabwe Craton. The area lies at an elevation of 760m and is bounded immediately to the east by the Runde River. The nearest previously recorded kimberlites are Chingwizi, Sese and others in the Limpopo Mobile Belt.

Figure 1 is a schematic map of the regional geology around the Murowa Kimberlites. Regionally, the Murowa Kimberlites lie within an East North-easterly trending strip of the Chibi granites. The granites aged approximately 2.6Ga formed part of a regional batholith intrusive event into the basement Shabani Gneisses. The Murowa Kimberlites are bounded some 15km to the North by the Tokwe cratonic segment, which stabilised around 3.5Ga. The basement gneisses have been intruded by a set of

East South-easterly and East North-easterly trending dolerites, themselves cut by the Chibi Granites. To the South, also about 15km, lies the East North-easterly trending Mberengwa Greenstone belt of the Bulawayan System, which hosts a banded iron formation, exploited at Buchwa for iron up until the late 1980s. The greenstone formations were probably established by 2.8Ga and in the Buchwa area they are contained as remnants within the Mweza Schist Belt.

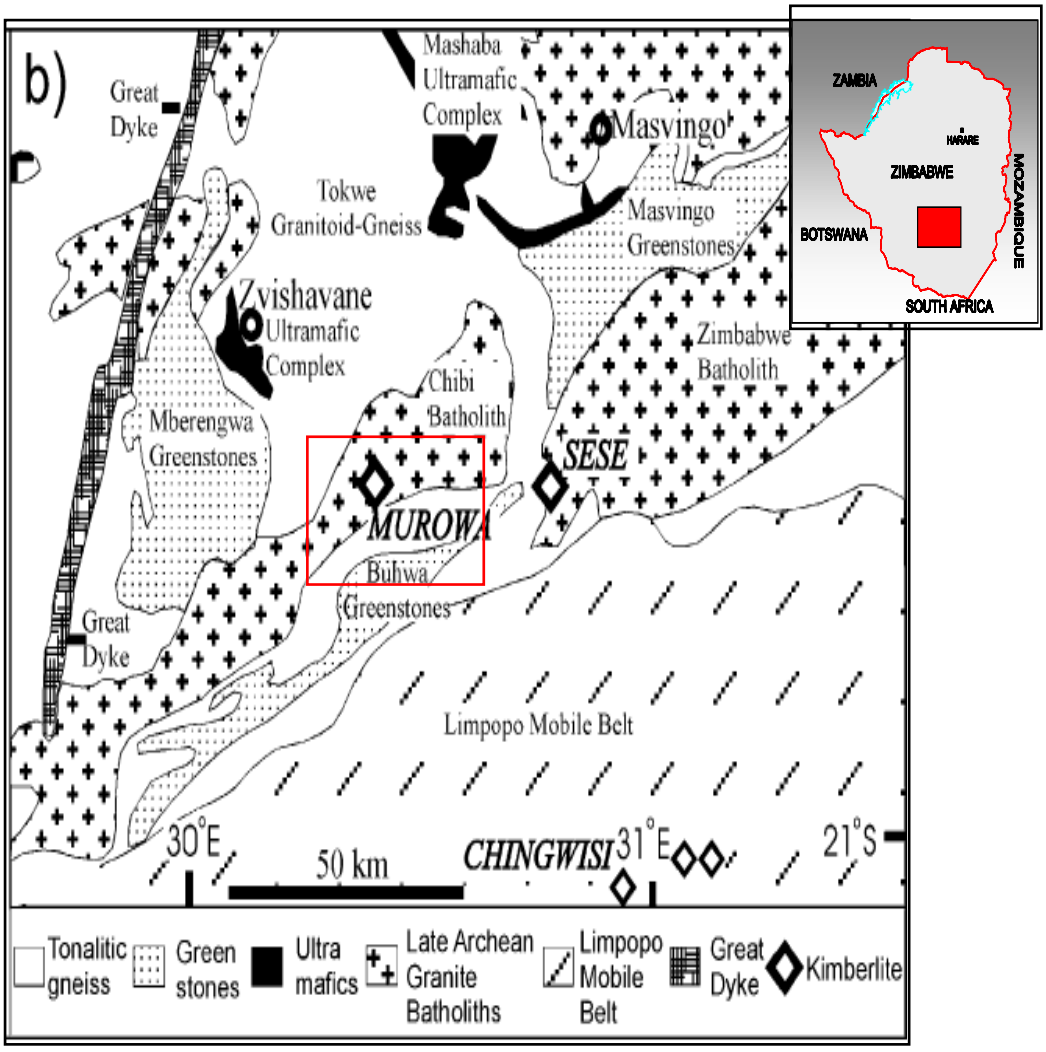

Figure 1: Schematic map showing the location of Murowa kimberlites and the regional geology.

A series of inselberg domes up to 250m high around Murowa, are said to attest to stripping of the weathering profile by more recent erosion. Buhwa Mountain, 12km south of Murowa and formed of banded ironstone, lies more than 600m above the surrounding Pliocene–Quaternary plain and forms a remnant of the older Pre- Karoo erosion surface (Mtetwa et al., 2002).

The Murowa Diamond deposit consists of a cluster of five kimberlite pipes and dykes. The pipes, labelled K1 to K5, lie between two structural features with a North-South trend (Figure 2). To the West is a doleritic dyke and to the east is a major shear zone.

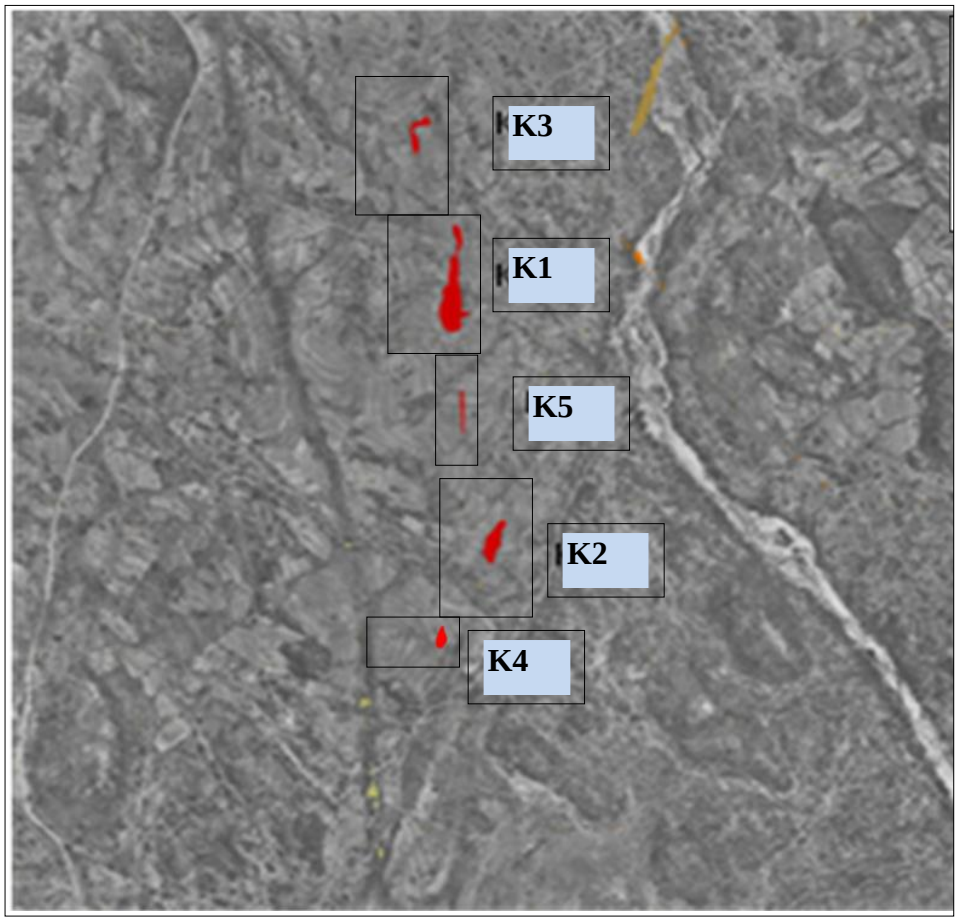

Figure 2: Location of the Murowa kimberlite pipes in relation to the main structural features; to the west a doleritic dyke and to the east a shear zone. Notation shows the K1-K5 pipes.

The K1 pipe is considered to be part of a complex blow along a North-South system of kimberlite dykes of which the smaller K3, K4 and K5 bodies are a part of the local controls on K1 are of North-South orientation. However K2's emplacement was more directly controlled by a reactivation along the shear zone.

The shape of the pipe of the K2 pipe, the eastern side of which is in direct contact with the shear, and the western wall which dips away to the west, is an inverted wedge. This shape is unusual for a kimberlite pipe and it is said almost certainly to result from a structural preparation of the ground. Detailed observation of some dyke contacts with the granite on the western side of K2 indicate that there was indeed some reactivation along the quartz shear occurring at the time of emplacement.

Only K1, K2 and K3 are considered economic based on the OoM estimates. K1 and K2 are currently being mined while K3, the smallest of the economic pipes with lowest value ore will be mined after the two larger pipes have been completed. K1 and K3 have similar grade profiles while K2 is somewhat different being significantly higher in grade. Of the three pipes, K2 pipe shows a clear boundary between ore and waste, whereas the ore in K1 and K3 has a halo of lower grade material referred to as the MPZ. This material will be stockpiled for later treatment. Waste rock material is predominantly granite.

1.2 Kimberlite Geology

The pipes themselves are exposed in the root zone at the current erosion level. The small complex multi-lobed bodies together with sills and dykes are characteristic of the basal part of kimberlite pipe development (Smith et al., 2004). The geology of the Murowa kimberlite pipes is complex comprising of inter-mixing of kimberlite lithologies and different phases of emplacement. The country rock is veined, brecciated and/or metasomatised and fenitised with kimberlitic fluid phases at the

kimberlite pipe contact (Moss, 2010). The K1 pipe (the main focus of this study) is modelled as a complex, steep sided multi-lobed kimberlite pipe. The contact zones around K1 vary in thickness, overall rock textures and the relative proportion of kimberlitic components. There are five kimberlite type domains in the K1 pipes namely KIMB1, KIMB2, KIMB3, KIMB4 and KIMB5 as well as additional MPZ and KDYKE-MX.

KIMB1 and KIMB5 consist of coherent kimberlite mainly a hypabyssal kimberlite. KIMB2 and KIMB4 consist mainly of volcaniclastic kimberlite and KDYKE-MX is a mantle xenolith-rich dyke. The MPZ is a granite-rich and kimberlite-poor or kimberlite absent domain that is spatially distinct from the main pipe-filling domains and it forms an envelope around the other domains. Figure 3 shows the geological domains of the K1 pipe and Figure 4, the inclined view of the K1 geology model.

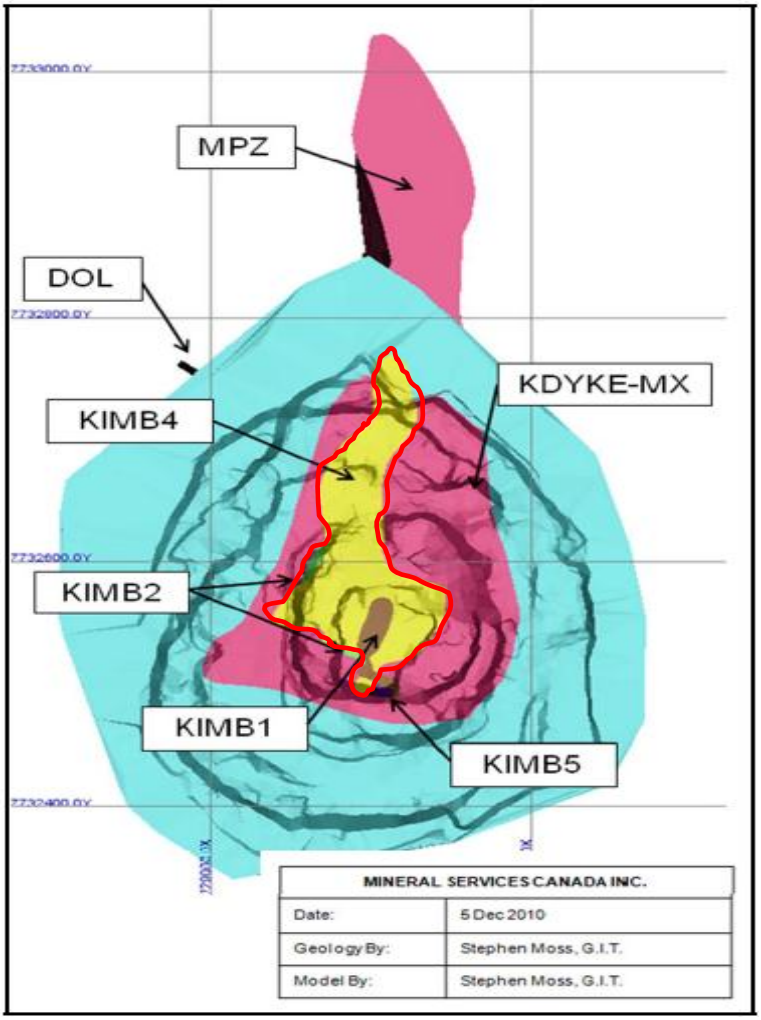

Figure 3: K1 geology model showing the internal geology domains. The KIMB4 domain outline is highlighted in red.

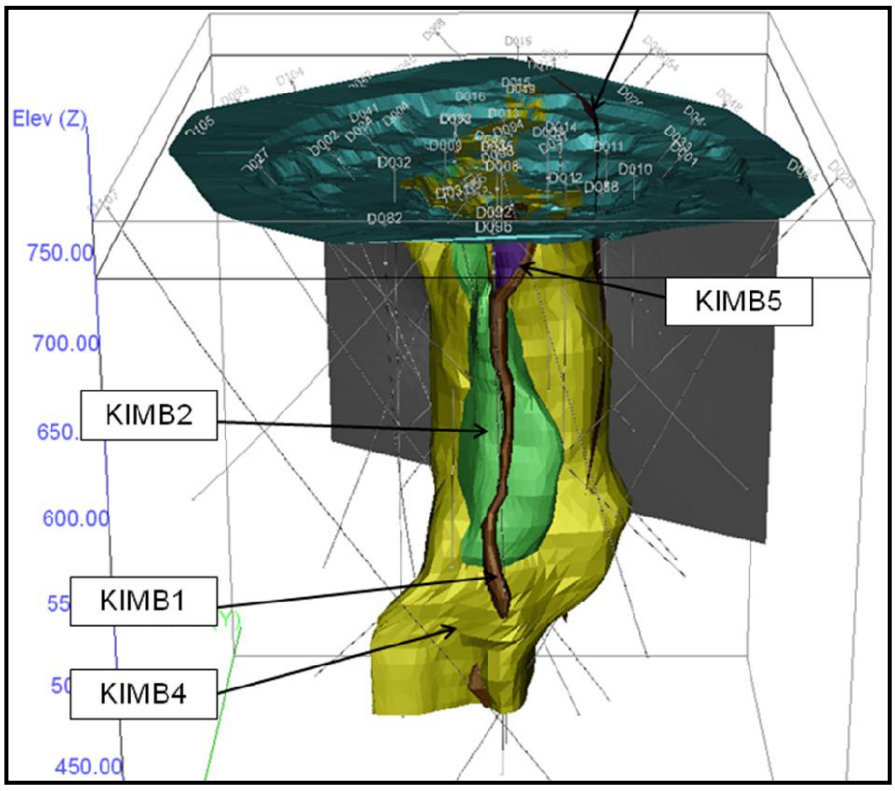

Figure 4: Inclined view of the K1 geology model

Of the K1 domains, KIMB4 is volumetrically dominant followed by KIMB1 and KIMB2. KIMB5 represents a comparatively minor volume within the modelled depth while KDYKE-MX is modelled as a surface, with no estimated volume. KIMB3 was not modelled as a separate domain due to the lack of spatial continuity, spatial overlap with other rock types, and the sub-mining scale (<5m) of most occurrences.

2 FORMULATION OF THE PROBLEM

During 2009, there was a shortfall in carats from the K1 pipe and Rio Tinto Technology and Innovation (T&I) in Perth, Australia was engaged to perform a desktop review of the existing K1 Murowa resource model that was constructed as part of the Murowa feasibility study of 2000. The aim of this review was to identify any potential issues with the existing model that may have caused an over-estimation of resource grade. The review identified several issues that may have led to an over-estimation of resource grade in this initial model. The findings are listed in Table 1.

Table 1: Tabulation of findings that could have resulted in the deficit of 2009: Source from Platell (2011)

Issue identified	**Description of the issue**
Conflicting lithology codes	There was little correlation between the domains as modelled in the 2000 model and the lithology codes contained within the database used. A large number of codes used within the internal pipe did not exhibit any clear internal domaining. There were numerous instances where adjacent or crossing holes were logged with conflicting codes, suggesting that there was an issue with the standard of core logging in the evaluation of 2000. This was observed both in the vent as well as elsewhere in the pipe.

The enriched vent	The majority of the high grade samples occurred at the southern end of K1 within a narrow feeder pipe, or "vent", with the remaining parts of the modelled pipe essentially very low grade.
Shielding of High Grade Samples	In the 2000 model, samples greater than 140 spm3 were shielded (capped) so that their influence was restricted to one parent block ($25m^2$). However, study of the sample grade histograms indicated that the MPZ domain and the KIMB4 domain contained outliers in the grade distribution. The outliers could have been left out in the production of the variograms but included in the kriging and not restricted
Weathering	During the 2000 study that a weathering (or oxidation) horizon may have a significant impact on the grade. The weathered kimberlite may have been enriched due to winnowing of non-diamond material. The weathering surface that was used for the 2000 estimate was inspected and found to be quite irregular, with many peaks and troughs which did not appear to be supported by the weathering code as logged in the drill hole database. A new weathering surface was created from the existing weathering data using the surface gridding technique in Vulcan. As in the 2000 estimate the weathered surface was not modelled as a separate domain due to the lack of spatial continuity. This issue will not be considered in this study as only the fresh un-mined material will be used in the estimate
Eastern Dykes	Within the MPZ domain, only three samples showed significant grade. These samples were all located on the

	eastern margin of the pipe and appeared to be aligned on a north-south trend. T&I postulated that these samples represented intersections of relatively narrow grade-bearing dykes. This interpretation was supported by delineation hole logging which indicated narrow intersections of kimberlite in this area.
Density Media Separation Plant Issues	Issues were also identified in the process plant, such as Density Media Separation efficiency and weightometer accuracy but these issues were considered outside the scope of the both the investigation by T&I as well as in the study that will be undertaken.

The failure to recognise the feeder/enriched vent had the most significant influence on the over estimation of the resource grade. This factor influenced the smoothing of grades in the southern end of the K1 kimberlite pipe as shown on Figure 5. The enriched vent was not recognised in the 2000 evaluation. The result was that high and low grade samples within the major domain were smoothed at the southern end of the pipe. The smoothing approach could have resulted in an over-estimation of grade as blocks outside of the vent would be unduly influenced by high grade samples within the vent.

Conversely the low grade samples outside the vent would cause blocks within the vent to be under-estimated, if the high grade vent was of a small volume relative to the surrounding low grade area, this would lead to an overall over-estimation in grade (Platell, 2011).

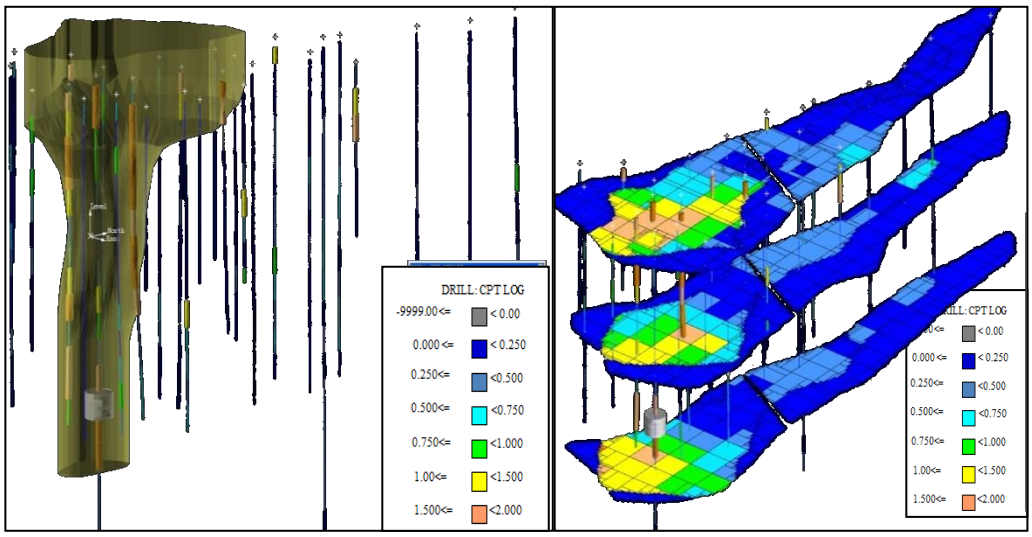

Figure 5: High grade vent surrounded by relatively low grade samples (left) and sample grades within K1 showing smoothing of grades with no recognition of feeder vent (right). Images from Platell (2011)

Mineral Services Canada Inc. (MSC) was then engaged in March 2010 to re-evaluate the geological core logging and to re-model the internal geology of the K1 pipe. This resulted in a revised geological model already discussed above in Section 1. T&I then created a revised resource estimate based on this new interpretation. This new model was expected to give a more realistic prediction of grade and consequently to give an improved reconciliation once the new estimate is used during mine planning.

2.1 Justification for the current study

The detailed work by MSC indicated that the KIMB1 (vent) was much narrower than had been modelled by T&I. The overall tonnage estimated decreased by over 5% in K1, due to the changes in the interpretation kimberlite pipe. This was coupled with a decrease of over 40% in carats within K1 (Table 2).

Table 2: Change in overall tonnes and carats between the 2010 and 2000 model (grey fill). Source from Platell (2011)

Pipe	Unit	Tonnes (Million)	Carats (Million)	Unit	Tonnes (Million)	Carats (Million)
K1	KIMB1	0.64	1.08	HK	19.51	9.98
	KIMB2	0.10	0.06			
	KIMB4	8.16	3.10			
	MPZ	19.01	2.04	IG	14.79	2.03
	Total	27.91	6.28	Total	34.30	12.01

Based on the new resource model, T&I classified the KIMB1 and KIMB4 units as Indicated Resource above the 545m elevation. There is economic uncertainty on the end-of-mine-life processing costs of the MPZ unit. However the sample density in this unit is sufficient for the mineralised blocks to be classified as Indicated Resource. Below this elevation to 425m, none of the units in K1 have been classified according to the JORC schema and any mineralised material has been assigned to Mineralised Inventory only (Platell, 2011).

With the significant reduction of the K1 resource and the planned expansion, understanding the risk associated with the diamond grade is imperative going forward to avoid deficit in the reconciliation, such as what happened in 2009. The quantification of grade uncertainty would provide focus areas that may require decisions relating to additional drilling so as to increase the confidence in the resource model and in the grade estimates. The KIMB4 unit being the most voluminous carries the bulk of the production tonnes for this pipe. It also forms the largest portion of the KIMB domains and therefore warrants further investigation not only to understand the risks associated with the grades but also to obtain deeper understanding of the variability of the grade in this unit. KIMB2 will be estimated together with KIMB4 due to insufficient data to model them separately and also the liberation characteristics of the ground within the two domains are considered not to be a hard boundary.

The implementation of a full-scale study which includes all the domains would require stricter investigation of the geological unit definitions, the treatment of the boundaries between these units, and the use of cut-off grades to distinguish ore from waste. These are beyond the scope of this study.

As in most mining operations, the methods (for example OK) that are used to provide the grade estimates in Murowa only produce single estimate values and their associated variances per mining block. The kriging variance depends only on the form of spatial continuity of the sample data and the spatial configuration of the sampling positions. Thus the error calculated using OK variance is independent from the data values and therefore imposing severe limitations on its use to quantify uncertainty

.

Kriging in Normal Scores (NS) provides conditional means and variances. The conditional variances can be used to assess uncertainty in the estimates at a point support. Besides the kriging conditional means and variances, conditional simulation is another method that can be used to quantify uncertainty around spatial variables such as grade and can be taken from point support to at higher supports (for example blocks and panels). The conditional simulation uses a Monte Carlo-type simulation approach where it generates multiple, equally probable realisations that provide a model of the spatial uncertainty of the grade in the in-situ ore body (Dimitrakopoulos et al., 2002). The resultant realisations are conditioned to the available sample data, match the same sample statistics and also reasonably reproduce the histogram and semi-variogram model of the sample data. Conditional simulation is generally a superior method of studying issues relating to variability and uncertainty in a way that estimates such as kriging do not. Besides uncertainty modelling, simulations have been used to evaluate and analyse issues relating to drill spacing, selectivity and sensitivity to different mine scheduling approaches.

The quantification of grade uncertainty will be vital in providing decisions about focus areas that require additional drilling to increase the confidence of the grade estimates

in the KIMB4 domain. It is hoped that a clearer picture of the variability of the grades in this unit will emerge and that the realisations obtained can also be utilised in pit optimisation algorithms in K1. Optimization in mine planning has been accepted as a set of techniques that introduce analytical mathematical methods into planning. The most common approach in open-pit design and planning is based on the Lerchs–Grossmann three-dimensional graph theory. It is implemented in most commercial mining industry applications as the nested Lerchs– Grossmann algorithm.

The reasons for investigating and modelling the variability and uncertainty associated with the grade estimates are therefore as follows:

- The KIMB4 domain being volumetrically the most dominant warrants further investigation of the variability of the grades. According to Goovaerts (1997), generating alternative realisations of the spatial distribution of an attribute is rarely the goal. Rather these alternative realisations can also serve as the input to other transfer functions, which in the open pit mining environment would comprise a mining process such as a pit optimisation algorithm.

Kriging in Normal Scores and the SGS method will be applied to the Murowa data, the spatial features will be accessed but the approach will largely follow a workflow devised by Deutsch (2011). The simulations will be compared to the NS kriging method.

- Once areas of high variances have been quantified, additional drilling can be planned and carried out thereby refining the model.

Techniques such as simulation and the resultant associated conditional variances may present indications of high variability within the KIMB4 unit than the use of kriging because in kriging only location plays a role and not the values of the samples.

2.2 Parameters used in diamond grade estimation

This section will briefly discuss the derivation of the variables used in diamond grade estimation and how these were used in the 2000 Murowa evaluation.

The discrete particle nature of diamonds makes resource estimation of diamonds not only more complex but also difficult compared to most other commodities. Diamond deposits and the estimation thereof, in kimberlitic (and placer) deposits are therefore considered sufficiently unique to warrant a sub-section in most reporting codes; e.g. the JORC Code clauses 40 to 43 (Appendix I) and the SAMREC code clauses 54 to 62. However the geostatistical approach to kimberlite diamond resource estimation is well established and follows fairly standard methodologies. It is vital to make optimal decisions prior to the evaluation process and the critical areas for consideration encompass the following:

• The appropriate variable for estimation such as stone or carat grade, volume or mass units
• The incorporation of calliper data for sample volume and density for sample mass
• The bottom cut-off and the inclusion or exclusion of incidental diamonds
• The modifications necessary to combine different data sources or address different recovery processes, liberation or lockup profiles etc.

2.2.1 The appropriate variable for estimation

Stone density is usually preferred as the principal grade variable in diamond grade estimation because it is less variable than cpt. The cpt variable tends to introduce more nugget effect and less confidence in the interpolation because of the positively skewed distribution of stone sizes or carats per stone (Roscoe and Postle, 2005). Another variable used in diamond grade estimation is the carat grade. This variable is an "accumulation", i.e. a combination of two variables namely the diamond content or

stone density such as stones per cubic meter (Spm^3) and the stone size or carats per stone. This variable is represented by the following formula:

$$\frac{cts}{m^3} = \frac{stn}{m^3} \times \frac{cts}{stn}$$

Diamond carat grade is therefore dependent on the number of stones per unit volume or mass and the diamond size distribution. The diamond size is described in terms of a size frequency distribution which lists the number of stones within particular size class. Size frequency distributions, like grade, are typically lognormal or positively skewed with a long positive tail. References made to average stone sizes are always accompanied by a stated bottom cut-off.

In general the stone density variable is used where samples are obtained by drilling or bulk samples such as trenches and shafts and diamond breakage is minimal. The carat grade estimate on the other hand is reliant on optimal diamond liberation (above the desired bottom cut-off). The revenue ($/ct) estimate is influenced by the size distribution thus optimal liberation without damage is important.

If grade is expressed in terms of tonnes, the density of the rock material is introduced. In most cases though, the overall kimberlite pipe grade is expressed in terms of carats per unit volume or mass, for mass the norm is ct/t or cpht (Bush, 2010).

The evaluation of 2000 and the review by T&I utilized the Spm^3 variable to estimate grade in the Murowa kimberlites although the final estimates were in cpt. The Spm^3 variable was built from a combination of parameters obtained during the 2000 evaluation. The derivation of cpt followed directly from the Spm^3, mean stone size (MSS) (+1mm bottom cut-off) and density variables using the formula,

$$cpt = Spm^3 \times \frac{MSS}{Density}$$

2.2.2 Modifications necessary to combine different data sources

The parameters incorporated sample volumes, stone counts from the LD(RC) drilling, stone distributions from the bulk sampling and shaft sampling programmes and specific gravity from the diamond drilling. Larger stone sizes within the size distribution of LD samples were under-represented and truncated; their frequency of occurrence became less as sample volumes became smaller. More representative stone distributions could only be attained through sampling larger volumes of material namely the bulk and shaft samples. The bulk and shaft samples therefore provided the Mean Stone Size (MSS) parameter derived using the formula,

$$\text{MSS} = \frac{\text{Total Number of Carats}}{\text{Number of Stones}}$$

The use of a MSS to derive a total carat figure had two major benefits namely:

- It allowed a smoothing of the data that otherwise would have suffered from high local variance due to the nugget effect of recovering occasional large stones from the LD samples.
- It provided a link between the stone size distribution of the domains and the grade estimated from the LD samples.

An assumption was made, which was justified from data available, that within each sub-domain, the stone size distribution remained the same. This assumption allowed a standard size frequency curve to be constructed from the bulk and shaft samples. The shaft and bulk samples were deemed to be representative of the domains. The primary driver behind the choice of the bulk and shaft samples to be include for the grade estimation adjustments came from the necessity of building up a recoverable distribution which could then also be used for the pricing from which the central estimate $/ct was derived (Duffin, 2000).

2.2.3 The incorporation of calliper data for sample volume and density for sample mass

The sample volumes were calculated from downhole data derived from a 3 arm caliper log. A number of intervals and LD holes did not have caliper runs made due to unsuitable ground conditions. For these intervals, average volumes were used. The density parameter was derived from the specific gravity and lithological proportions. The resultant density and the resource volumes then formed the basis of the tonnages:

$$\text{Tonnes} = \text{Volume } (m^3) \text{ x density } (t/m^3)$$

2.2.4 Inclusion or exclusion of incidental diamonds

Natural stone breakage will always be present in most diamond populations. Breakage induced additional stones were evaluated if they constituted more than 5% of the total carats of the interval.

Analysis of the data showed that the difference in density between each of the rock-types in K1 is within 5% and therefore in the region of 2.6 t/m^3. The MMS (bottom cut-off +1mm) obtained in the KIMB4 domain was 0.0767ct/stn. Therefore with stable MMS and densities in the KIMB4 domain, the cpt value can be easily obtained.

The current study therefore utilised the Spm^3 variable. Due to the sensitivity of the data, some of the axes and legends of graphs and charts will be removed and some figures will also be modified to protect the confidentiality of the data.

3 EXPLORATORY DATA ANALYSIS

3.1 Data Validation

A total of 289 LDRC sample data from K1 constitute the dataset used in the current study. The data file was obtained in the form of a Microsoft Excel spreadsheet from the Murowa Diamond operation. This incorporates samples obtained from 752m.a.s.l to about 465m.a.s.l. The K1 pit is currently sitting at between 740 and 415m.a.s.l.

Checks in the data were made for

- Duplicates in information
- Outliers in terms of coordinates and values
- Obvious mistakes
- Zero values or missing
- What may not be in the data

The data file was systematically scanned through to identify duplicates, obvious mistakes and missing values. No duplicate pair samples containing the same information in all data fields/columns, obvious mistakes and missing values were identified.

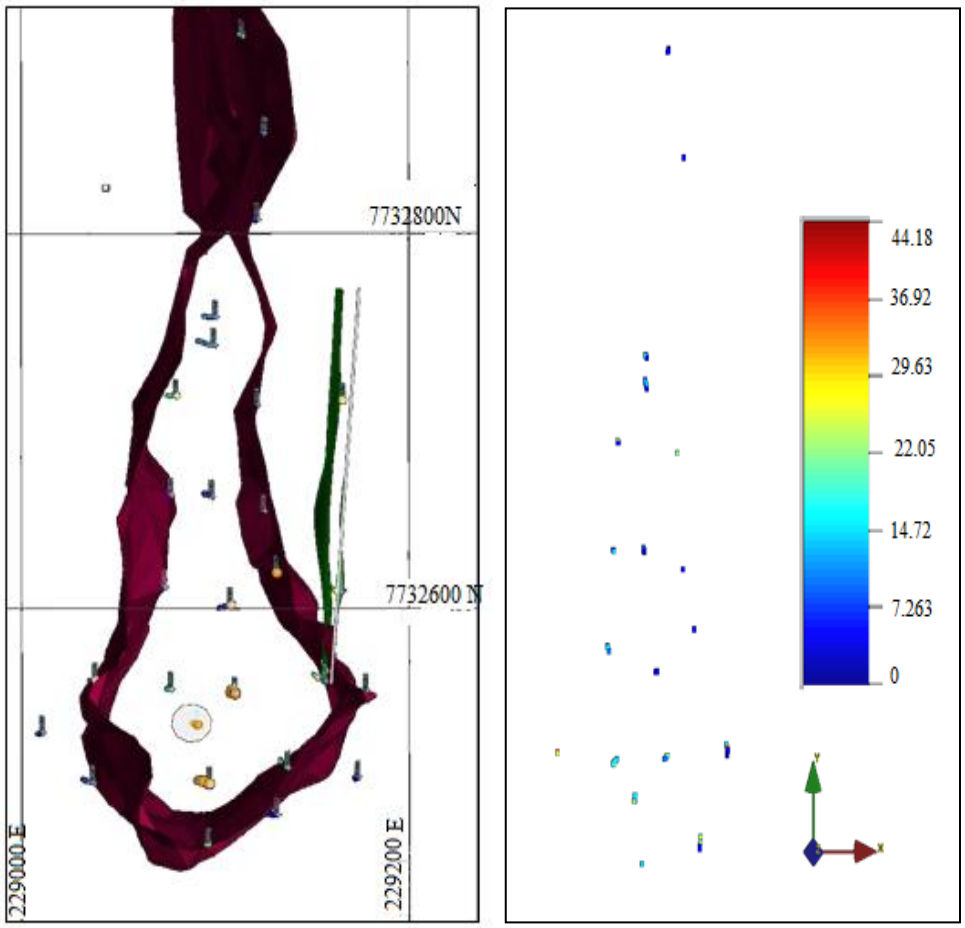

Figure 6: Plan view of the K1 pipe, showing the location of LD drill holes in K1and the MPZ domain (in pink) enveloping the other domains, and location of data points of the KIMB2/4 domain in relation to the entire K1 pipe. Image from Platell (2011)

Plots of sample locations (in this case drillhole locations) facilitate easier visual analysis for outliers in terms of coordinates. They also assist in looking for and delineating trends, locate areas with high values and low values. The sample positions in the KIMB4 domain are acceptable and generally well constrained within the domain boundaries (Figure 6).

The number of samples and drillholes which were used for each domain as well as the univariate Spm^3 statistical parameters are summarised in Table 3.

Table 3: Drillhole samples used for each domain

Domain	Number of samples	Mean of Spm^3	Minimum of Spm^3	Maximum of Spm^3	Median	Standard Deviation	COV
KIMB1	28	61.36	14.22	194.12	56.87	36.15	1.70
KIMB2/KIMB4	143	10.71	0.00	44.18	9.26	8.75	1.22
MPZ	118	3.48	0.00	26.40	2.05	5.53	0.63

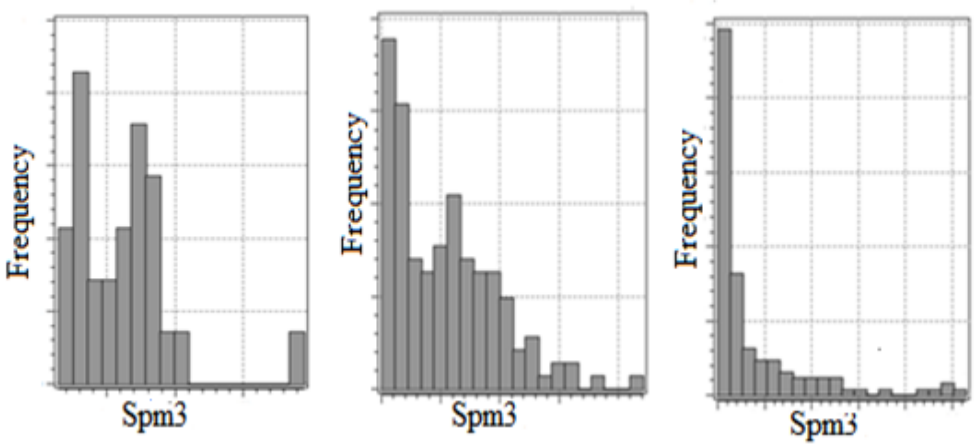

Figure 7: Histograms for the KIMB1 domain (left); KIMB2/4 domains (middle) and MPZ domain (right)

Figure 7 shows the distribution of the Spm^3 variable for the K1 domains. The KIMB2/KIMB4 and MPZ domain data are all positively skewed while KIMB1 has a bimodal distribution. KIMB1 and KIMB4 domains have outliers at 194.12Spm^3 and 44.18Spm^3 respectively. Inspection of data indicates that the outliers are not as a result of stone breakage. The outlier in KIMB4 will be excluded for the computation of the variogram but incorporated in the kriging and simulation part of the study. In

the 2000 model the outliers had a restricted radius of influence applied. In this study the restricted radius of influence will not be applied.

The outliers cannot be considered as anomalous data as the exploratory data analysis has sought for and removed or corrected any anomalous data. The high values typically come from heavy-tailed distributions, where a small number of samples can be responsible for a large proportion of the metal content or grade in the deposit. Parker (1991) reported a case where 4 out of 34 samples are responsible for 70% of the gold content, and 7 out of 34 for 90% of the gold content. He notes, even small changes in the grade near these assays or the proportion of high-grade material may be responsible for large differences between estimated and recovered reserves. Discarding the high grades completely creates a bias. The value of a deposit may just come from these high grades. In some cases, high grades are deliberately left out with the idea that it is more rewarding to revise estimates up than down. The problem is that this may lead to the abandonment of the project if it was a marginal one.

3.2 Data declustering

Geological sampling programs are not entirely spatially random hence the removal of potential bias or "declustering" the data is vital. The declustering process adjusts the summary statistics to be representative of the entire area of interest thereby removing potential bias, for example one area may have clustered sampled points compared to other portions (Deutsch and Journel, 1998). Since in conditional simulation the histograms and summary statistics of the conditioning data are an essential foundation for the accuracy of the resultant model they need to be representative of the volume of interest. Weights are assigned to each data point based on their proximity to surrounding data. An example of a declustering method termed cell declustering, divides the area of interest into regular cells at a given grid spacing. The weight for each cell, and all data points inside that cell, is calculated as:

$$\frac{1}{\text{Number of data points in a cell x Total Number of occupied cells}}$$

The correct cell size is determined by calculating the weights at multiple cell spacings and then plotting the cell sizes against the mean of the data with the weights applied (the declustered mean). The final grid size used is the grid size that either minimizes or maximises the mean. Often, the cell size that is roughly equal to the average sample spacing is an appropriate choice.

The Murowa data was not declustered in the current study because the samples that were used were taken at regular intervals of 15 m. The sample lengths of 15 m were chosen such that between 3 and 30 stones would be recovered given a grade range between 0.1 and 1 cpt and a sample tonnage of around 3 tonnes. This range of stone recoveries was recommended as a minimum for the statistical evaluation of grade in the 2000 evaluation. The sample lengths were kept at a consistent bench depth with no allowance for likely lithological or grade variations. This was done partly to keep the sample support consistent throughout the evaluation without the need to composite the data.

3.3 Variography of the domains of the K1 pipe

Data was read into the SGeMS software from where the variography was performed. A version of SGeMS which is still under development was obtained from the developer with additional algorithms that are able to simulate blocks.

The downhole (along the Z axis) semi- variogram of the KIMB2/4 domain (untransformed data) was first constructed to determine the nugget effect. A 15 m lag interval was chosen due to the 15 m sampling interval in the downhole direction. A nugget of 10 Spm^3 and a range of 53 m were modelled (Figure 8).

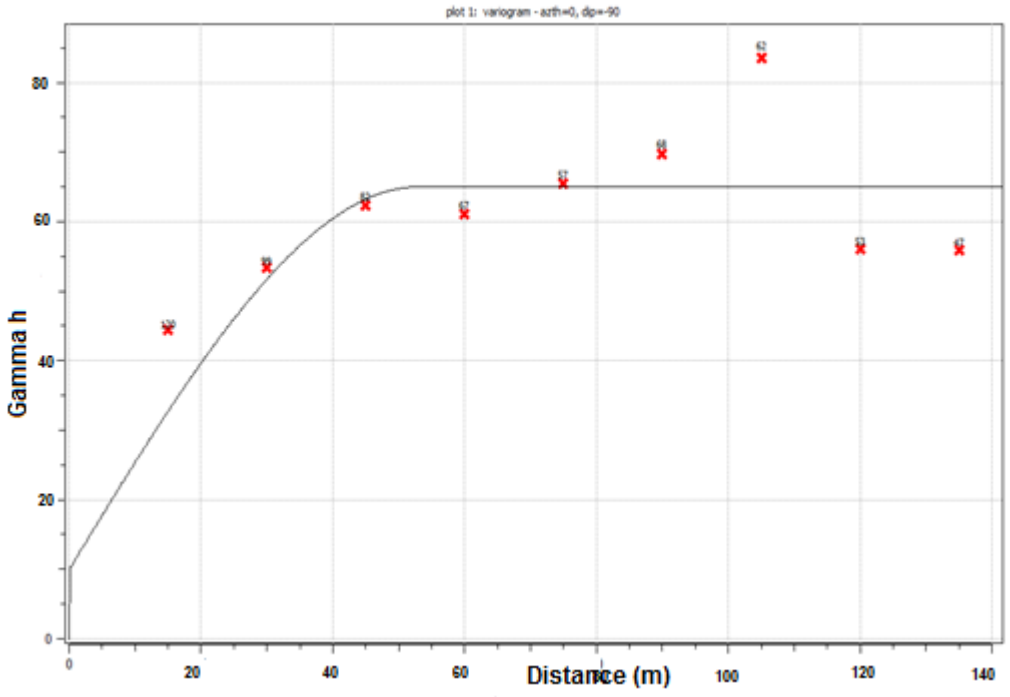

Figure 8: Spherical model variogram for the Spm^3 variable for KIMB4 in the vertical direction

The drift in the data was investigated. Variograms were obtained (where possible) for every 5 degrees azimuth in order to explore the pattern of anisotropy within the KIMB4 domain. A tolerance of 22.5 degrees was selected as it was large enough to allow sufficient pairs for more stable variograms in the horizontal directions. The ranges were plotted on a radar chart (Figure 9). A weak North North West-South South East trend emerged and this appeared to agree with higher grade area to the SW of the KIMB4 domain.

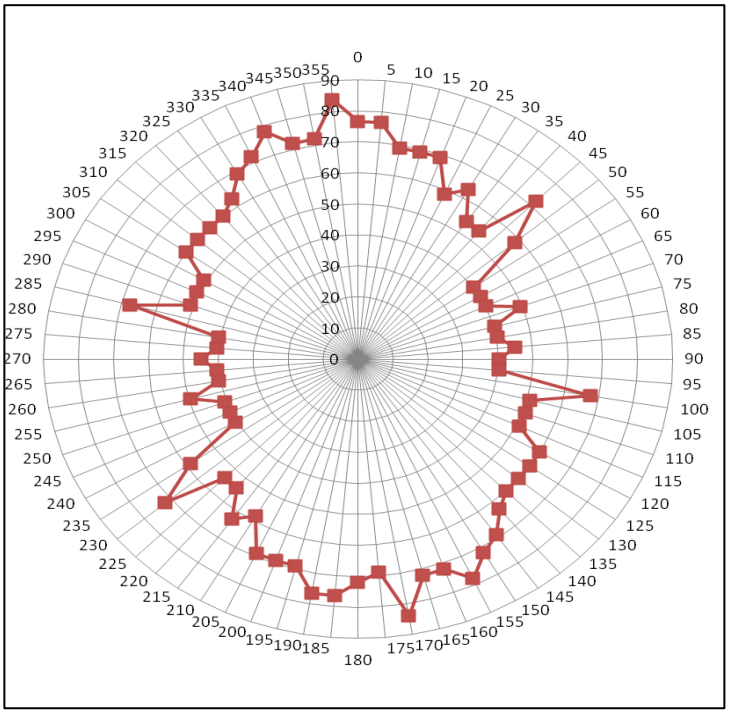

Figure 9: Radar chart of Horizontal variogram ranges of the KIMB4 domain

The directional horizontal variograms were investigated using both spherical and exponential variogram type models. The experimental variograms are presented in Appendix II. However the spherical type model fitted much more accurately to the omni-directional variogram. The omni-directional variogram also defined a better structure than the horizontal variograms and was therefore used during the estimation. A spherical omni-directional variogram for the MPZ domain also defined a better structure than the other directional variograms and therefore used as the final variogram. The resultant semi-variograms of the KIMB4 and MPZ obtained are summarised in Table 4 and the KIMB4 variogram is shown in Figure 10. KIMB1 domain was not investigated due to the small number of samples and therefore insufficient pairs in some directional variograms.

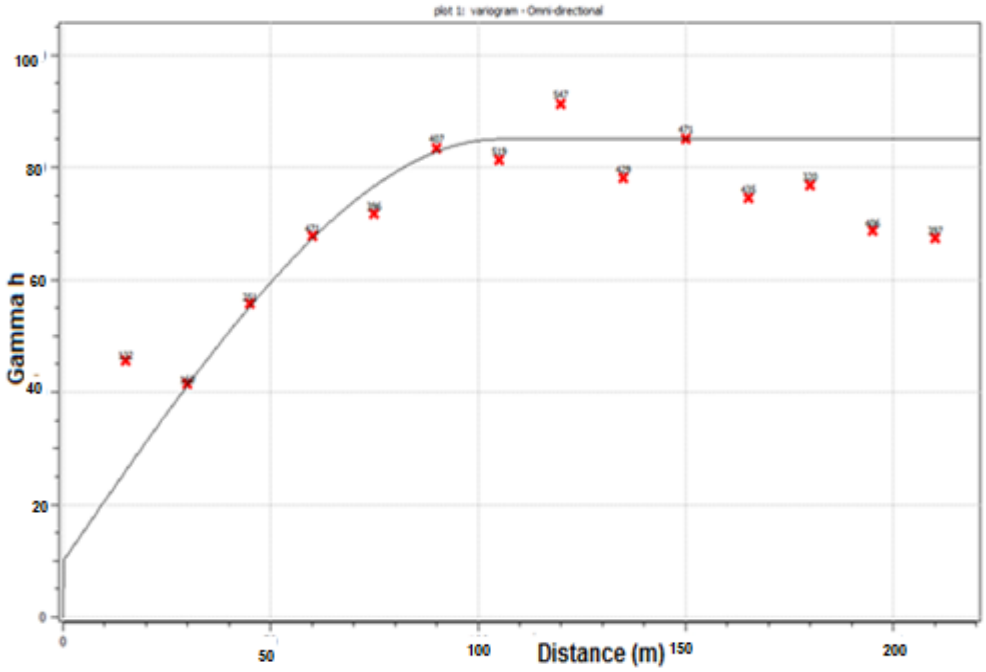

Figure 10: KIMB4 omni- directional spherical variogram model for the Spm^3 variable

Table 4: The omni-directional semi variograms models from KIMB2/4 and MPZ domains

Domain	**Variogram Type**	**C0**	**C1**	**Range**	**Azimuth/Dip**
				Omni directional	
KIMB2/4	Semi variogram (spherical)	10	75	105	00/00
MPZ	Semi Variogram (Spherical)	12	25	105	00/00

4 GEOSTATISTICAL ANALYSIS OF THE SPM^3 VARIABLE OF THE KIMB4 DOMAIN

Numerous authorities have discussed the fundamentals of geostatistics in detail (e.g. Deutsch and Journel, 1998 and Isaaks and Srivastava, 1989). Geostatistical estimation can be defined as the prediction of the value of an attribute at a location at which it is unknown from measured values of that characteristic at a number of known locations through a function defining the spatial correlation between values (Dohm, 2010). Both kriging and simulations have had much theoretical development and are well described in most geostatistical literature and are mostly used in the mining industry.

Most geostatistical methods rely on the assumptions of stationarity, which is seen as the decision to pool data within a given area or domain. Deutsch and Journel (1998) state the importance of making proper decisions about stationarity as they are critical for the representativeness and reliability of the geostatistical tools used. Samples from geozones or domains of similar geology be it rock type, chemical characteristic, structure, grade are grouped together. Dividing a dataset into areas that are acceptable with regards to stationarity is therefore essential in geostatistics.

4.1 Ordinary Kriging

Ordinary Kriging (OK) was developed by Matheron in the early 1960s based on the Master's thesis of Danie G. Krige, the pioneering plotter of distance-weighted average gold grades at the Witwatersrand reef complex in South Africa. Ordinary Kriging is the form of kriging used mostly because it works under simple stationarity assumptions and does not require knowledge of the mean (Chilès and Delfiner, 2012). A good estimator will be unbiased, that is, on average the estimated values will equal the unknown values and the estimation errors (Z-Z*) will be as small as possible.

In kriging (and simulation), the search volume or kriging neighbourhood can have significant impact on the outcome of the estimates and therefore a suitable neighbourhood has to be determined. Most criteria discussed by a number of authors e.g. Vann etal, (2003) to consider when evaluating a particular kriging neighbourhood include the following:

- Slope of regression of the data values vs. the estimates (Z/Z*)
- Weight of the mean in simple kriging
- The distribution of kriging weights
- Variance of the estimator Z*
- Percentage blocks filled
- Mean of the estimate vs. mean of the sample data
- The proportion of negative weights is kept relatively low

In the current study, a number of kriging neighbourhoods were evaluated and a neighbourhood of 120m, 225m and 15m in X, Y, Z directions was used.

Local point and block estimates of the variable were obtained using OK (unknown mean) and the variogram model shown in Figure 10. The blocks in the KIMB4 domain were discretised into 5x5x1 based on the stabilisation of the estimation variance at 5x5x1 in a discretisation test (Figure 11).

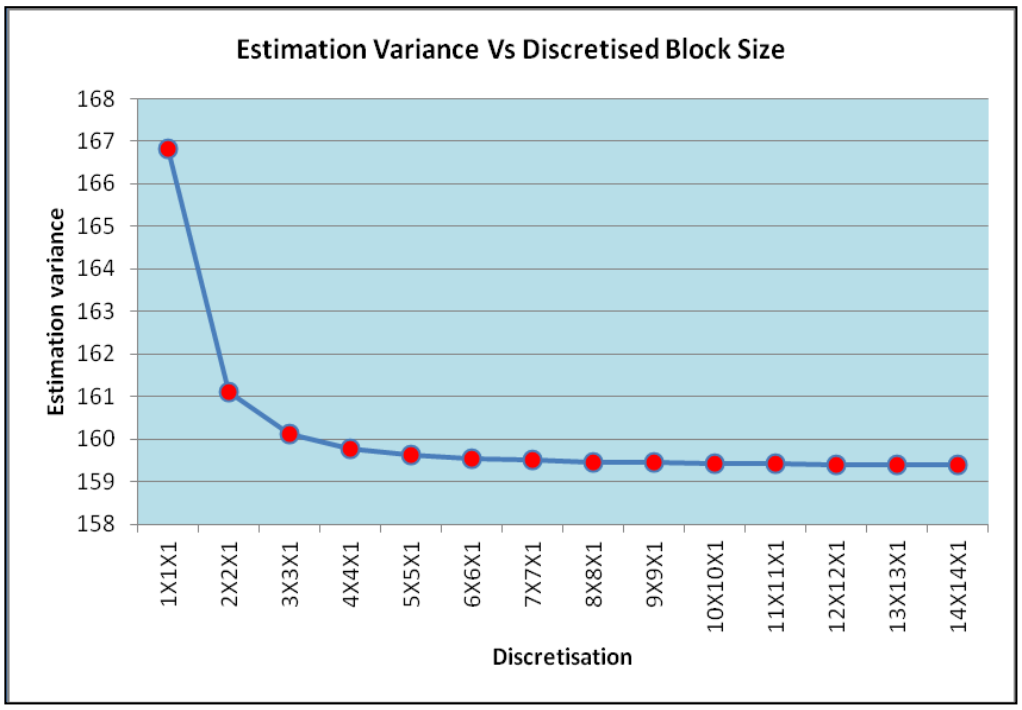

Figure 11: Discretisation test used to determine the optimal block discretisation of 5x5x1 for the KIMB4 domain

Table 5: Table showing a comparison of the estimates and actual values of the KIMB4

Estimate	**Actual Sample Value Average**	**Estimated Average**	**Actual Sample Value Standard Deviation**	**Estimated Standard Deviation**
Point Kriging	10.71	10.95	8.75	9.4
Block Kriging	10.71	11.38	8.75	7.33

The point and block estimates are very close (Table 5). However the estimated standard deviations differ with the point estimate being larger than the block estimate. This reduction of the standard deviation in the block estimate is expected in estimations such as kriging where the variance decreases with the size and volume of the unit being considered, in this case drillhole sample support versus block support.

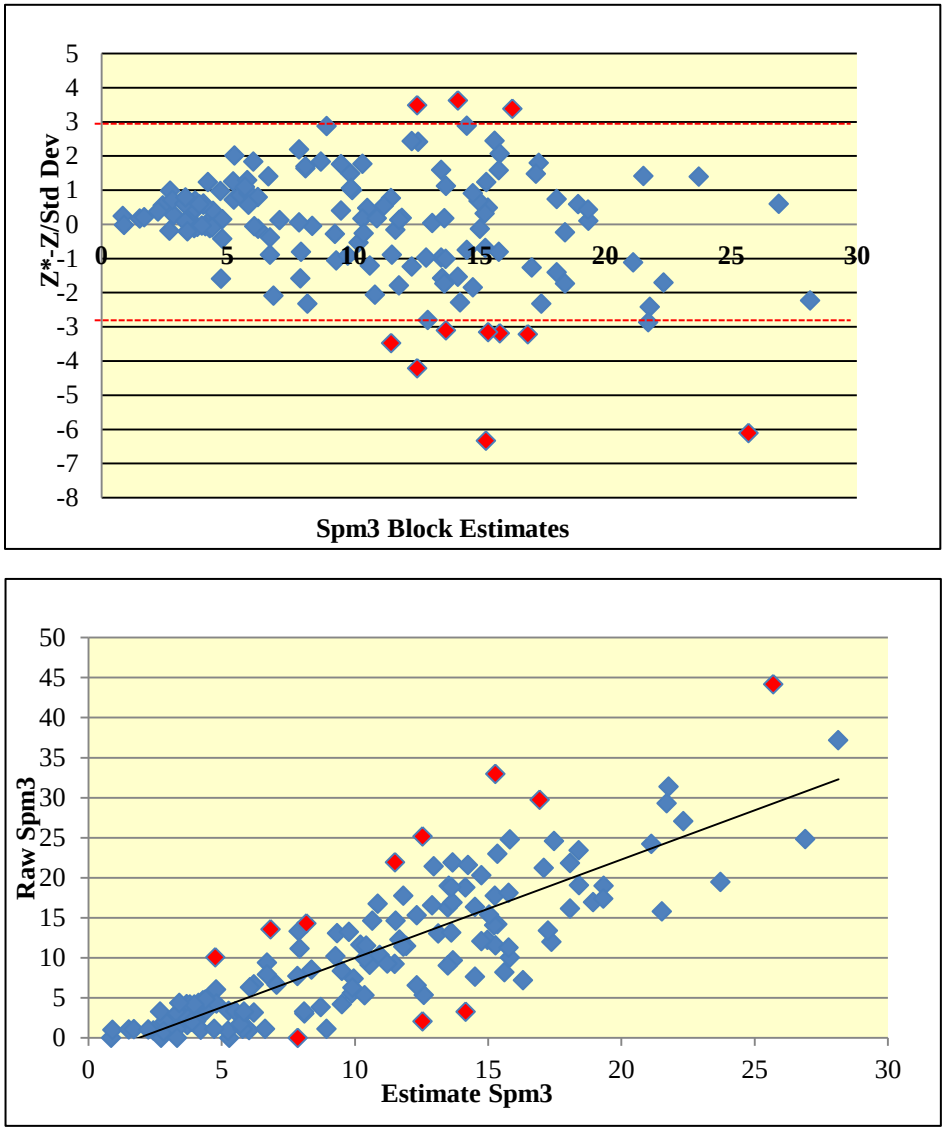

Figure 12: Cross validation of the Spm^3 estimates from the KIMB4 domain

Validation of the block estimates was performed using a combination of the Inverse Power Distance (IPD) estimates and a comparison of bench (15m interval) averaged estimates and sample data, comparison of mean of the estimate and mean of the sample data, (already seen from Table 5) and cross-validations shown in Figure 12. A total of 90% of the estimates tested as robust. The non-robust estimates are shown in red.

Both Simple Kriging (SK) and OK can be used as basis for conditional simulation. However according to strict stationarity theory, SK should be applied to Gaussian or NS transforms. The conditional simulation in this study will use SK.

4.2 Normal Scores variography of the KIMB4 domain

A NS transformation was performed in preparation for the simulation of the Spm^3 variable but also to compare point kriging results from this transformed data and the untransformed data. Normally, kriging data with skewed distributions can result in spurious estimates and such data would be transformed using transformations such as the Gaussian transformation into a normal distribution before variography is performed. This would then require back transformation to the original units. The main drawback of using kriging in NS or gaussian space is that the change of support is not always straightforward. Ortiz and Deutsch (2003) illustrated how the mean can be back-calculated using numerical integration. The illustration used considers that a spatially distributed dataset z (u_α), α = 1,..., n is declustered. The cumulative frequency (F(z)) is read from the original distribution and the value y_i of a standard normal distribution, corresponding to that cumulative frequency (G(y)) is assigned to the data location and a normal score transformation is performed, generating the normal/gaussian values $y(u_\alpha)$, α = 1, ..., n. This is illustrated in Figure 13.

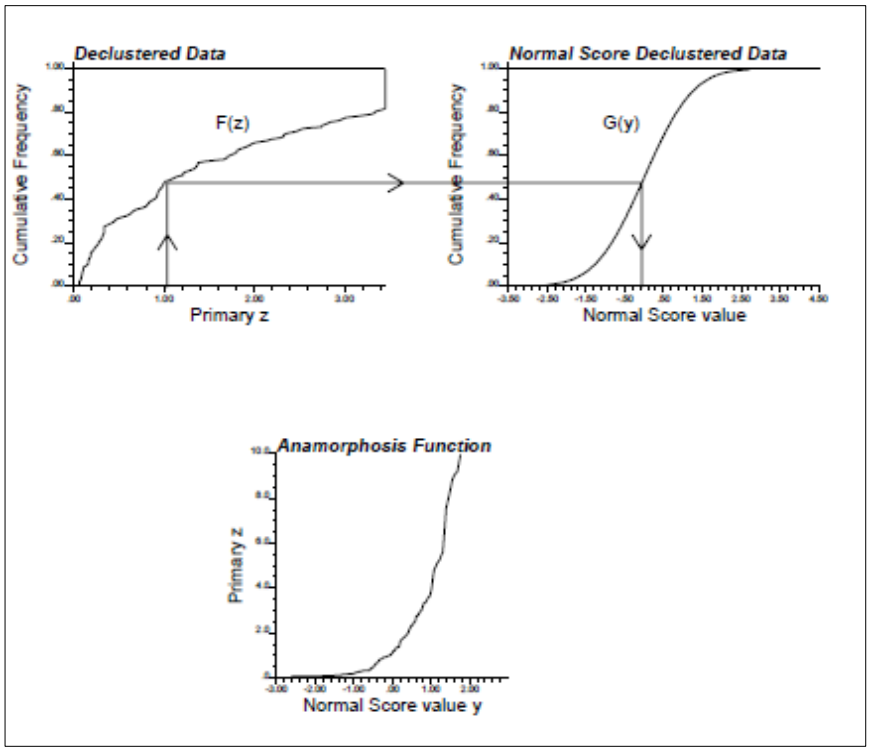

Figure 13: The normal score transformation for data z_i. At the bottom is the anamorphosis function. Sourced from Ortiz and Deutsch (2003)

Under the Gaussian assumption, the shape of the conditional distribution is Gaussian and therefore the full conditional distribution in the original units of the variable can be retrieved by back calculating the *z* values for several quantiles. This is illustrated in Figure 14. In this illustration nine deciles of the distribution, *y*1,..., *y*9, are back-transformed (top) and the corresponding values, *z*1, ..., *z*9, are used to calculate the mean. The full distribution in original units can be retrieved in the same manner. The estimation variances can also be back-transformed to express the local uncertainty but this requires additional processing. Deutsch and Lyster (2004) investigated the impact of the additional processing on back-transformed kriging means and variances using a program called PostMG developed within GSLIB. PostMG was specifically written to perform the back transform of kriged (multi)gaussian output. What became apparent

was that the PostMG did not improve the quality of kriged estimated mean but returned the correct variances for each estimated point. The kriged normal scores variances were properly back-transformed and could be used more reliably to analyse uncertainty.

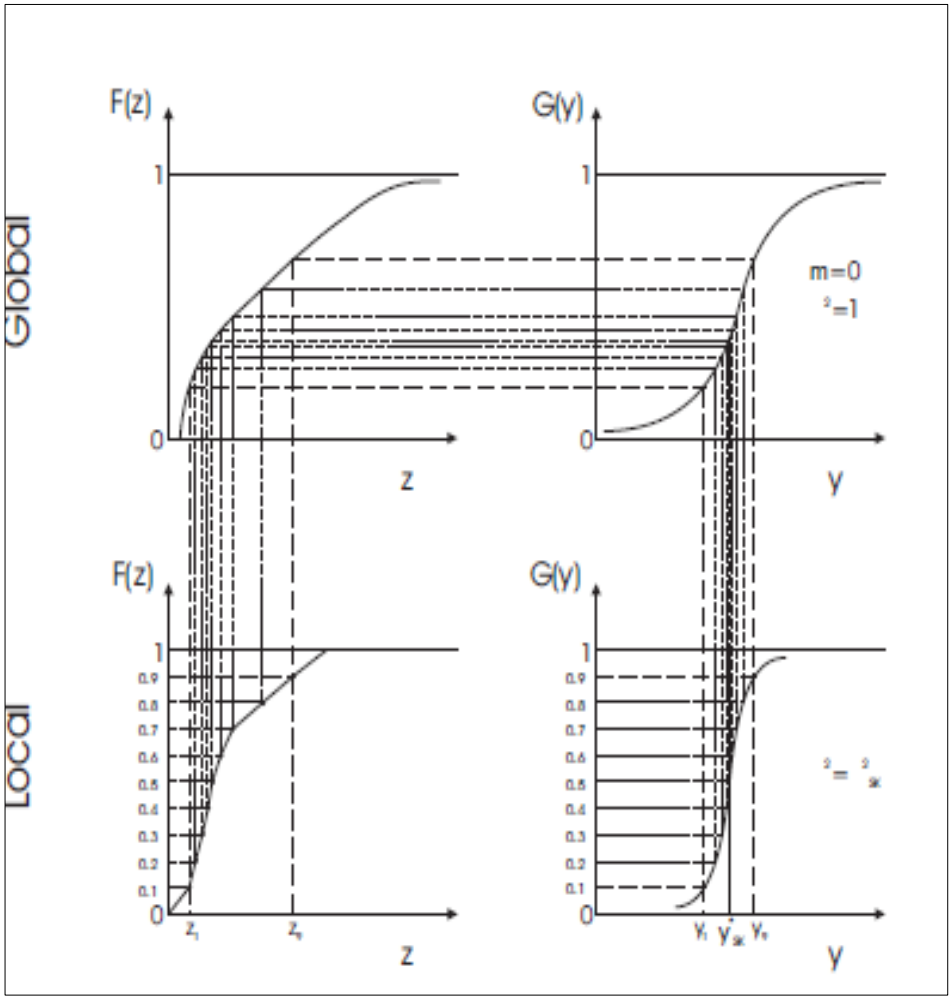

Figure 14: Calculation of the mean by numerical integration. Sourced from Oritz and Deutsch (2003)

The Spm[3] data was transformed using the Histogram transformation algorithm in SGeMS and the resultant data distribution and parameters shown in Figure 15 (bottom

right). It is vital that the standard normal simulations be back-transformed to match the histogram of the sample values after they are generated.

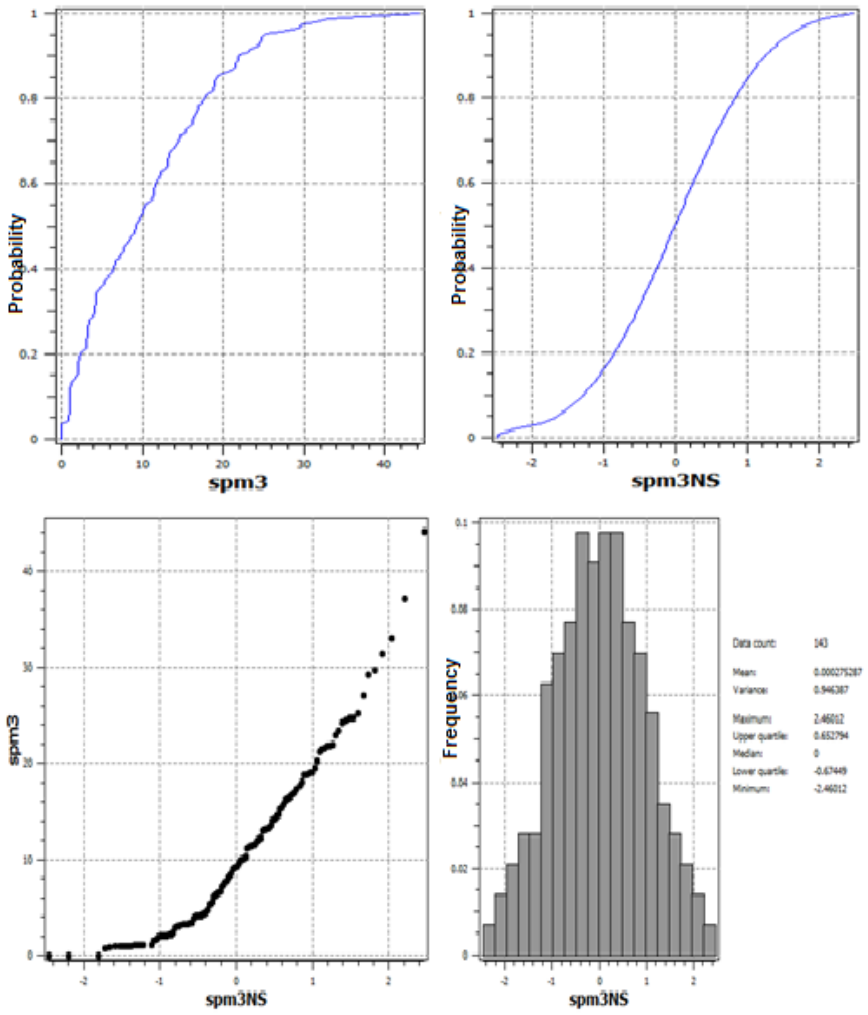

Figure 15: Normal scores transformation process and resultant parameters of the KIMB4 Spm^3 variable

The transformation also involves extrapolation of the tails of the distribution, for which the user sets the minimum and maximum allowed limits for the back-transformed values. 0 and 45 Spm^3 were used for the KIMB4 domain as these values were considered close to the limits of the actual data.

The aim of the Gaussian transformation is to get a mean of 0 and a unit variance of 1. In this case, the mean and the variance of the distribution obtained were 0 and 0.95 respectively. The distribution was acceptable for the variography and kriging purposes as the median of the distribution was 0 indicating that the distribution is symmetric. The resultant NS variogram also modelled a spherical model and the omni-directional variogram defined a better structure compared to the other horizontal variograms. The nugget effect obtained was 0.05 and the sill was modelled at 0.91 at a range of 82m (Figure 16).

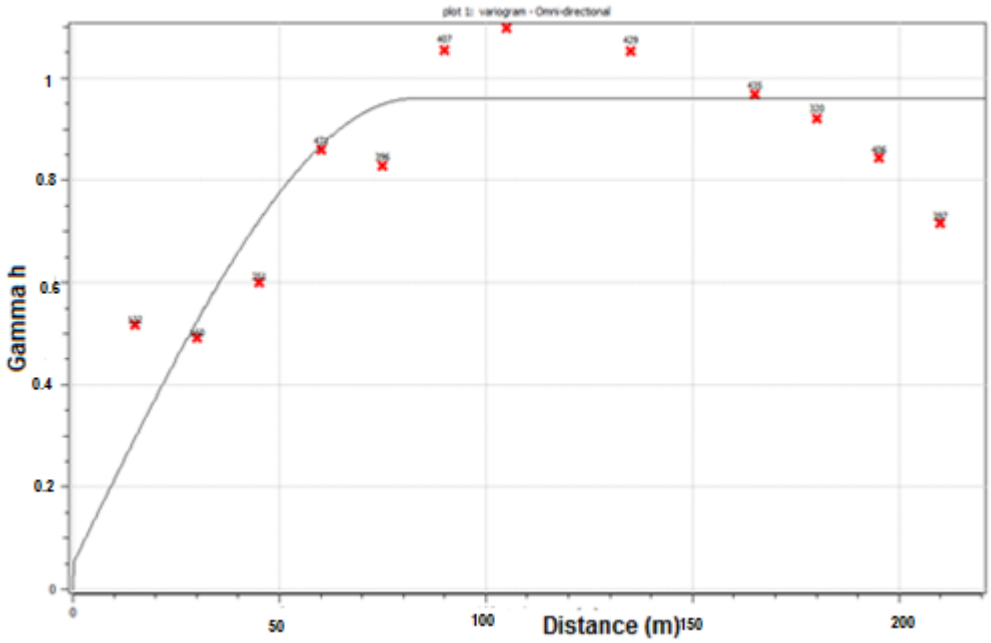

Figure 16: Model variogram parameters for Spm^3 data from the domain, modelled in Gaussian space.

SK with a mean of 0 was performed on the NS Spm^3 point data. The next step was to back transform the NS kriged data back to the original units. This was also done using Histogram transformation algorithm of the SGeMS program. Figure 17 (viewed from the top) shows the back-transformed kriged data and compares it with the OK untransformed kriging. The back-transformed simple kriging results data appeared

less smoothed compared to the OK results. The high grade area in the South West using NS is more much more-well defined forming a North West- South East linear feature. Figure 18 attempts to show the extent of the high grade area at depth. The high Spm^3 estimate seemed to be confined close to the surface (about 30m) and does not continue at depth where the region is generally poorly sampled. At this stage however, the back- transformation returned an average Spm^3 average which is comparable to the OK mean. It is therefore the author's opinion that the back-transformation in SGeMS is able to return the back-transformed mean. The performance of the algorithm in returning the corresponding back-transformed variances that can be used for accessing uncertainty will be investigated and discussed in Section 6.

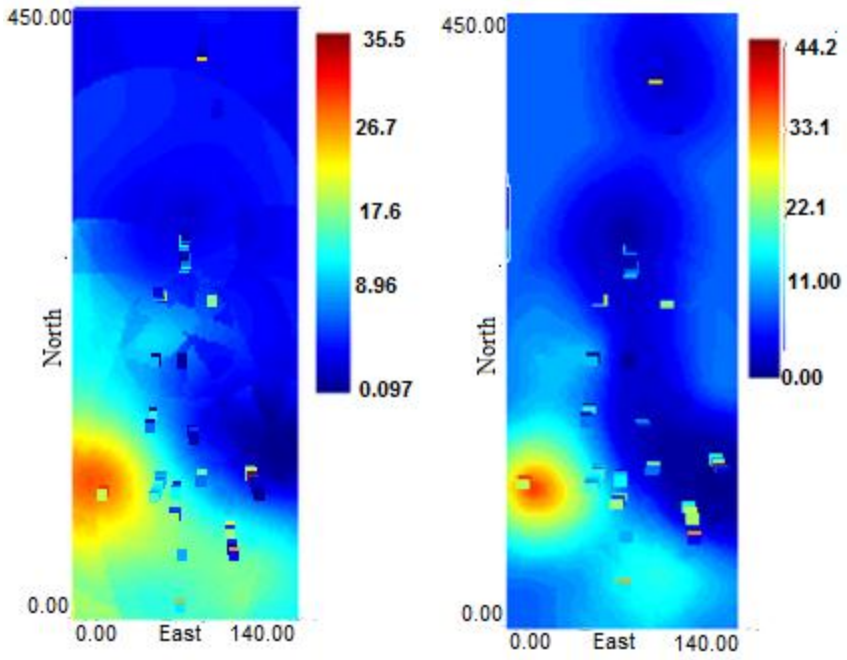

Figure 17: Comparison of untransformed OK (left) and gaussian (NS) back-transformed kriging map outputs (right)

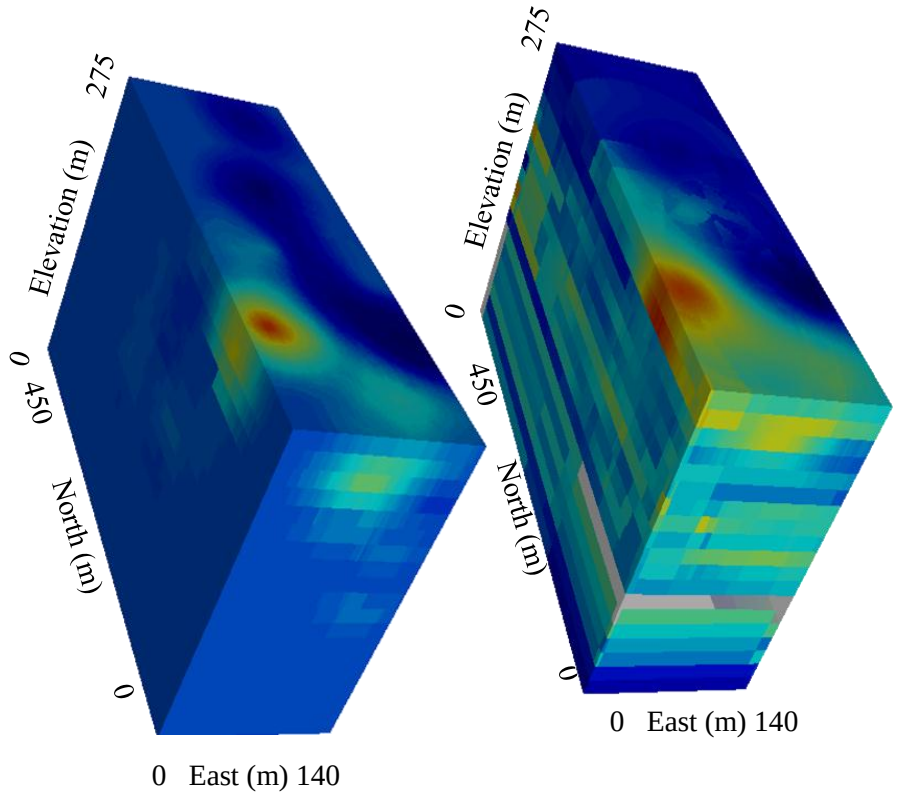

Figure 18: KIMB4 domain OK results (right) and SK back-transformed kriging results (left) viewed from the SW

4.3 Indicator Kriging of Spm^3 variable

Indicator kriging (IK) of the Spm^3 was investigated in an attempt to define the high Spm^3 values in the KIMB4 domain. Indicator Kriging (IK) was introduced in the geostatistical sphere by Journel in 1983 as a technique in resource estimation. The original intention of Journel, based on the work of Switzer (1977) and others, was the estimation of local uncertainty by the process of derivation of a local cdf. The original attraction of IK was that it was non-parametric and it did not rely upon the assumption

of a particular distribution model for its results. IK has grown to become one of the most widely-used algorithms and it is the prime non-linear geostatistical technique used today in the minerals industry (Blackney and Glacken, 1998). The essence of the indicator approach is the binomial coding of data into either 1 or 0 depending upon its relationship to a cut-off value, z_k. For a given value z(x),

$$I(x; z_k) = \begin{cases} 0 \ if & z(x) \leq z_k \\ 1 \ if & \text{Otherwise} \end{cases}$$

Then, the semivariogram (ɣ (h)) is used to express the spatial structure of indicator codes, written as follows:

$$\gamma(h) = \frac{1}{2N(h)} \sum_{i=1}^{N(h)} [I(x_i; z_k) - I(x_i + h; z_k)]^2$$

h is the distance between locations x_i and $x_i + h$ and N(h) is the number of pairs (x_i, $x_i + h$). The ccdf at the unsampled location at x can be obtained by the IK estimator:

$$F[z_k; x|(n)] = I^*(x_i; z_k)$$

$$= \sum_{i=1}^{n} \lambda_i I(x_i; z_k)$$

where λ_i are the weights and (n) is the set of n observed data points used.

This is a non-linear transformation of the data value, into either a 1 or a 0. Values which are much greater than a given cut-off, z_k, will receive the same indicator value as those values which are only slightly greater than that cut-off. Hence indicator transformation of data can be an effective way of limiting the effect of very high values. SK or OK of a set of indicator-transformed values will provide a resultant value between 0 and 1 for each point estimate. This is in effect an estimate of the

proportion of the values in the neighbourhood which are greater than the indicator or threshold value.

The transformations are also able to derive local distributions of uncertainty which lead to a practical estimate of resources above a range of cut-off grades. These estimates called 'recoverable resources', while representing the correct support for mining still need to be subjected to the reserve process. On the downside, the IK method has since attracted considerable debate as to whether or not it is a valid technique. A particular issue is that indicator variograms tend towards pure nugget effect as the threshold increases. Other problems with datasets for example change of sample support (Chilès and Delfiner, 2012), or clustering of data (Isaaks and Srivastava., 1989) can also prevent the application of indicator kriging. However these problems are not present in the KIMB4 data set.

In order to get an indication of cut-off values that define high and low Spm^3 values in KIMB4, a number of different cut-off values of Spm^3 were investigated. Estimates were performed using the 12 Spm^3 cut-off and they are presented in Figure 19 and the rest are shown in Appendix III.

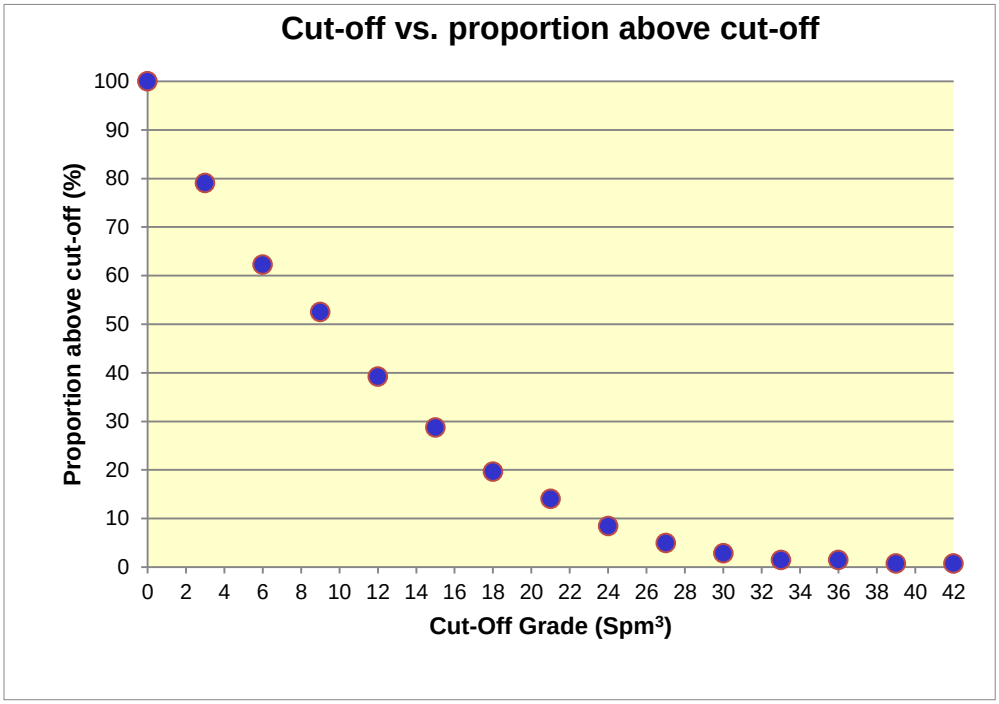

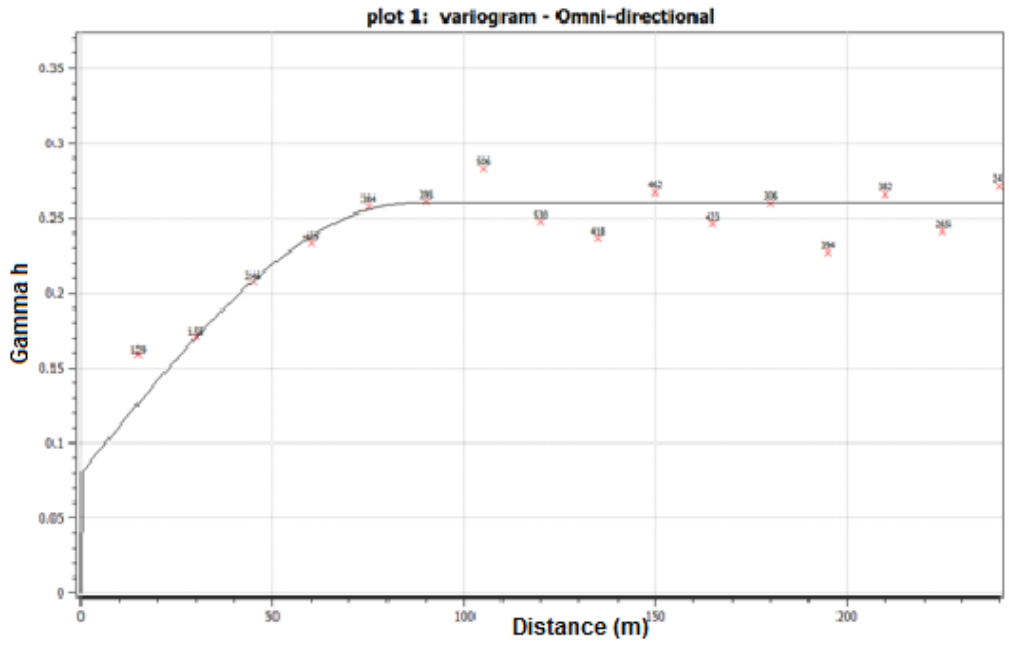

Figure 19: Relationship between various cut-offs of Spm^3 and the proportion above cut-off (top) and the model indicator variogram at a cut-off of 12 Spm^3.

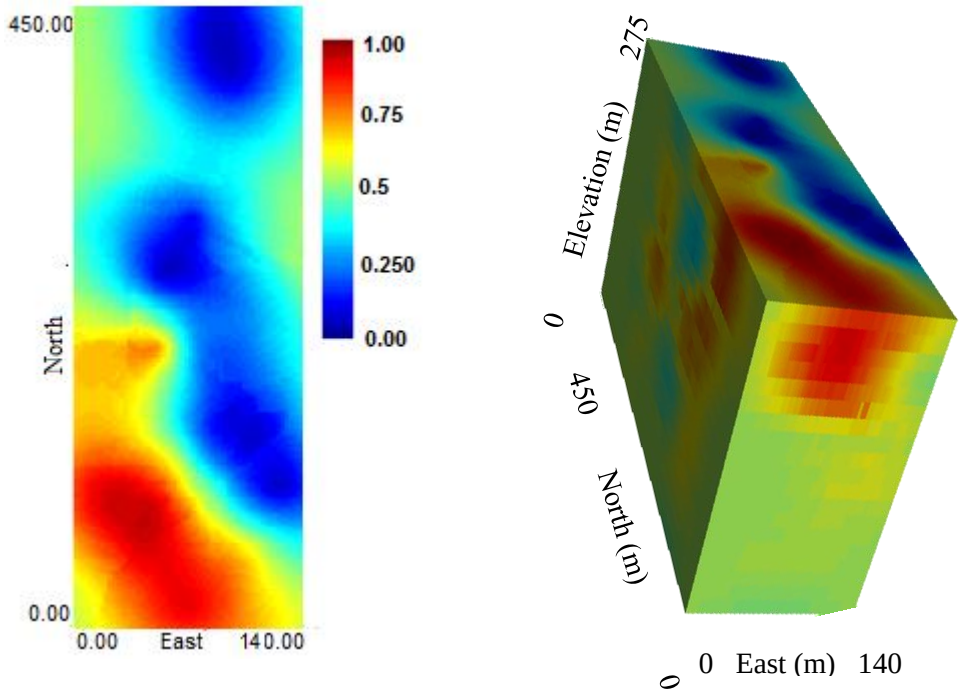

Figure 20: Kriged map of Spm^3 >12 viewed from the top, as well as the block model of the KIMB4 domain.

Figure 20 shows the kriged map of Spm3 >12 viewed from the top as well as the block model of the KIMB4 domain.

5 CONDITIONAL SIMULATION OF THE SPM^3 VARIABLE OF THE KIMB4 DOMAIN

The direct block simulation (DBSIM) method has been proposed as an alternative to conventional SGS. The method considerably reduces computational time. DBSIM simulates the internal points of each block and when the simulated block is calculated the point values are discarded. The simulated block value is then added to the conditioning dataset. To integrate the block support conditioning data the algorithm has been developed in terms of a joint simulation, where the second variable relates to the block values sequentially derived through the simulation process. The algorithm simulates several hundreds of blocks per second and is considerably faster than any point conditional simulation combined with re-blocking. Furthermore Dimitrakopoulos, et al., (2002), show that in addition being substantially faster and more efficient in terms of computing requirements, the DBSIM method is equally reliable in terms of reproduction of the sample statistics.

However because simulating points using SGS with the aim to re-block so as to yield a block value had the added advantage of getting the point estimates as well, for the current study this approach was preferred over the block simulation method. The approach was proposed by Deutsch and Journel in the 1990s and was accepted by several authorities (e,g. Dimitrakopolous, et al., 2002). The block simulations were therefore done using point simulations followed by averaging to the mining block sizes (re-blocking).

5.1 The Theory of Sequential Gaussian Simulation

Like kriging the theory of simulations has been documented by authors such as Deutsch and Journel (1998) and Chilès and Delfiner (2012). While this technique ensures reproduction of spatial data, it is also founded on a very strong assumption of

stationarity just like kriging where in particular, the mean is assumed to be the same at every location in the field. Domains are generally used to constrain fields with a common mean; yet, when no hard boundary between varying means exists, such as when there is a continuous trend in data, the stationarity assumption however cannot be maintained.

Kriging and conditional simulation differ fundamentally although differences between them can be subtle at times. The main differences between the two are that:

- The aim of kriging is to provide the best linear unbiased estimate (BLUE) of the variable, without consideration of the spatial statistics of all the estimates collectively. The focus is on local accuracy as opposed to spatial continuity. (Deutsch and Journel, 1998).
- Conditional simulation presents a more accurate picture of the true variance within a dataset compared to kriging. Simulations in general focuses on more correct spatial continuity

The theoretical explanation of the mathematical fundamental principles of the SGS technique to be briefly discussed in this section was taken from Delfiner and Chiles (2012). The theory considers as a vector-valued random variable Z (Z_1, Z_2,...,Z_N) for which a realization of the sub vector (Z_1,Z_2,...,Z_M) is known and equal to (z_1,z_2,..., z_M) ($0 \leq M < N$). The distribution of the vector Z conditional on $Z_i = z_i$, i=1, 2,...,M, can be factorized in the form:

$$\Pr\{z_{M+1} \leq Z_{M+1} < z_{M+1} + dz_{M+1}, \ldots\ldots\ldots, z_N \leq Z_N < z_N + dz_N \mid z_1, \ldots\ldots\ldots, z_M\}$$

$$= \Pr\{z_{M+1} \leq Z_{M+1} < z_{M+1} + dz_{M+1} \mid z_1, \ldots\ldots\ldots, z_M\}$$

$$\times \Pr\{z_{M+2} \leq z_{M+2} < z_{M+2} + dz_{M+2} \mid z_1, \ldots\ldots\ldots, z_M, z_{M+1}\}$$

$$\vdots$$

$$\times \Pr\{z_N \leq Z_N < z_N + dz_N \mid z_1, \ldots\ldots\ldots, z_M, z_{M+1}, \ldots\ldots\ldots, z_{N-1}\}$$

The vector Z is sequentially simulated by randomly selecting Z_i from the conditional distribution $Pr\{Z_i<z_i|\ z_i,\ldots\ldots..,z_{i-1}\}$ for i = M+1,……,N and including the outcome Z_i in the conditioning dataset for the next step. In the case of a Gaussian random vector, the conditional probabilities can be calculated.

If the above method is applied to the simulation of a Gaussian random function the simulation is SGS. If the Gaussian RF has a known mean, the conditional distribution of Z_i therefore is Gaussian, with mean z_i and variance σ^2_{ki}. Here Z_i is the SK of Z_i from $\{Z_i:j<i\}$, and σ^2_{ki} is the associated kriging variance.

The sequences of steps to generate an SGS are as follows:

- Transform data to Gaussian space.
- Compute and model the variogram of the transformed data.
- Define a random path that passes through each node of the grid representing the deposit.
- Krige the normalised value at the selected node and obtain the kriged value
- The simulated value could also be obtained by drawing from a normal distribution using the kriged estimate and the kriging variance as the mean and variance respectively.
- Add the new simulated point to the conditioning data set, move to the next node and repeat the kriging and random sampling of the resultant

The SGS method has several advantages which include:

- Sequential simulations are easy to understand
- A variety of algorithms exist for its implementation
- Conditioning and simulations are part of an integrated process
- Anisotropies are handled automatically
- Applicable to any covariance function

5.1.1 Validation of the simulations

Several aspects that can be considered in order to evaluate the performance of the simulations include:

- Gaussian statistics: How close are the Gaussian mean and variance to zero and one?
- Raw univariate Statistics: How close are the back-transformed mean and variance of the simulations to the original data?
- Histograms: How well do the histograms of the variable reproduce the histogram of the drillhole data?
- Correlation coefficients: How well do the simulation reproduce the correlation coefficient of the drillhole data?
- Scatterplots: Are the scatterplots of the simulations comparable to those of the drillhole data?
- Variograms: Are the experimental variograms of the simulations comparable to those of original data?
- Spatial patterns: Do the graphical images of the simulations represent geologically plausible spatial patterns? Are there any obvious visual artifacts or errors such as elevated grades?
- Space of uncertainty: Could the true grades be outside the range of the grades simulated?

5.2 The application of sequential gaussian simulation to the Spm3 variable

This section will produce realisations of the Spm^3 variable on a point support scale using the sequential gaussian simulation method. To incorporate the change of support, the blocks were discretised into a point scale grid and the nodes then simulated by point simulation. The point simulations were then averaged out on block scales using the Block Upscaling (Block Averages) Menu.

This approach was preferred for this study as it offers two advantages:

- Both the point and the block simulations are obtained. For example in simulation of mining methods, an additional reconnaissance survey (e.g. pre-mining drill-holes) and mining blocks (selection units) can be simulated at the same time.
- It is very fast to generate a simulation for a new block size, or simulate blocks of variable dimension.

The KIMB4 domain is approximately 140m x 450m x 275m (X, Y, Z). In this study, the fifty realizations were simulated within the KIMB4 domain by discretising the mining block into 2.5m x 2.5m x 15m grid per regularised (SMU) block (25m x 25m x 15m) and then simulated by point simulation. This grid size was considered to be small enough to accommodate SGS, yet is large enough for timely processing and avoided subsampling as well. The simulation grid required 1 node for each block. The total number of nodes therefore required for the simulation was thus 184800.

The conditional Sequential Gaussian Simulations generated as part of this study were performed using the following steps:

- Transforming of the raw drill hole data into Gaussian space using the Histogram Transformation algorithm in SGeMS.
- Modelling the variogram using the Gaussian space data using the variogram module in SGeMS. This and the previous step have already been undertaken in the kriging using Normal Scores section of the study
- Running a total of 50 simulations using the SGS algorithm in SGeMS. Various authors have used different numbers of realisations to model uncertainty. Dimitrakopoulos, et al., (2002) considered that 50 realisations were sufficient for their purposes while Goovaerts (1997) makes reference to 100 realisations.

- However a balance is required between reducing the number of realisations, and thus the computing time, without compromising the validity of the simulated model. To determine the number of realisations that would be required to obtain a reliable uncertainty model, the number of realisations are plotted against the progressive mean and progressive coefficient of variation (COV) (Appendix IV). This approach was adopted from Robin (2006) and 50 realisations were optimal for this case.
- Kriging points from the surrounding data at each simulation node using simple kriging (mean=0 and variance = 0.95)
- Back-transformation of the gaussian conditionally simulated values to raw space.
- Verifying the conditional simulation by comparing the variogram of the input sample data against variograms of individual point simulations and by comparing the base statistics of the sample data against those of the conditional simulation and kriged output.

5.2.1 Validation of the Spm^3 variable simulation

The following observations were made with regards to the aspects that need to be considered to validate the simulations

- A mean of 0.04 and variance of 0.91 (compared to 0.95 variance of the Gaussian transformation) was obtained for all the simulations collectively.
- The NS histograms statistics were reproduced and Figure 21 show the cumulative frequency of 10 randomly selected realisations (in blue) compared to the input data (in red)

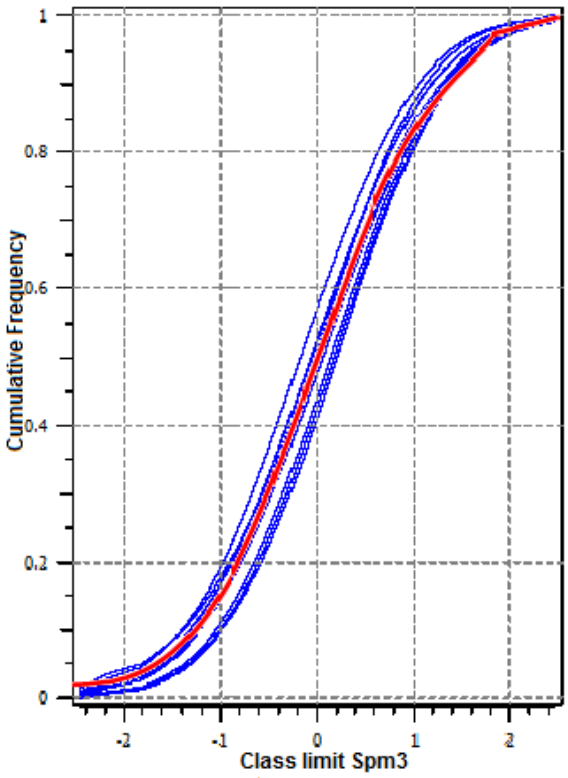

Figure 21: Cumulative frequency distribution of 10 randomly selected realisations in NS (in blue) compared to the cumulative frequency of the input data (in red)

- The global characteristics also did not vary much between the individual realisations. The individual back-transformed realisations reproduced the histograms and frequency distribution of the input sample data (Figure 22 and Figure 23).
- To further compare the global statistics, an approach adopted from De-Vitry (2010) was adopted. Firstly the mean and variance of the individual realisations were divided by the mean of the drill hole data and multiplied by 100 to give a ratio. Realisations that have means above 100% are generally over simulated while those below 100% are under simulated. The ratios of the means and variances of the realisations produced were calculated for the Spm^3 variable. The means were close to 100% while the variances were an average of 5% above the 100% ratio.

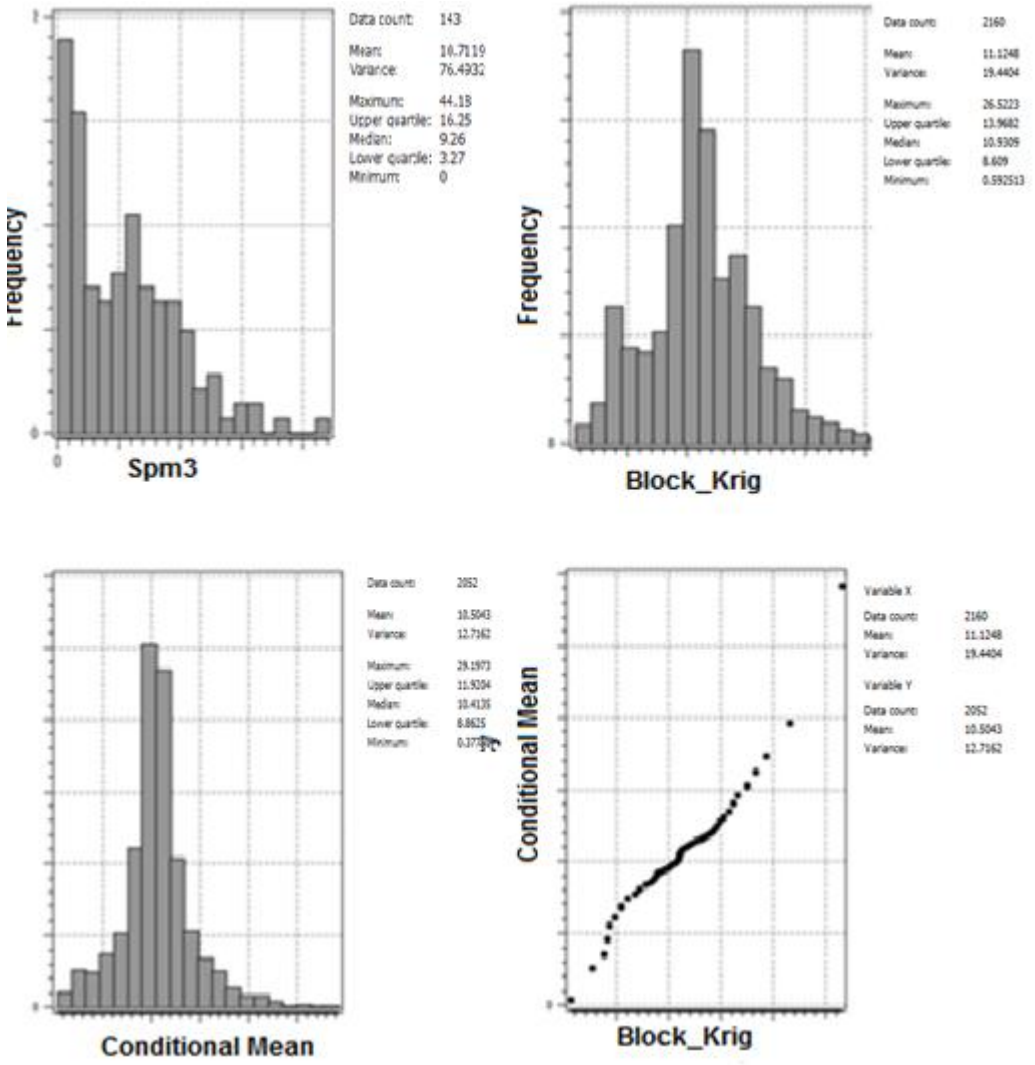

Figure 22: The univariate statistical parameters of randomly selected histograms generated from the Sequential Gaussian simulation of Spm^3 compared to those of the sample data (bottom left).

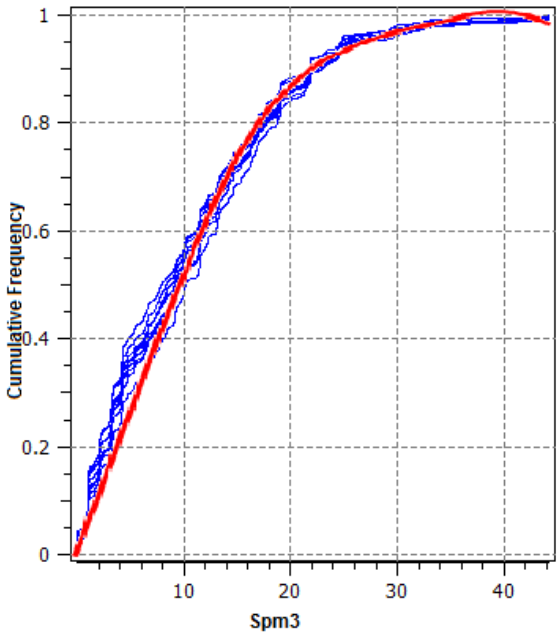

Figure 23: Frequency distribution of 10 randomly selected back-transformed realisations (in blue) compared to the raw Spm3 data (in red)

- Correlation coefficients are an effective summary of how well the simulated Spm^3 variable correlated to the raw drill hole data.
- Absolute differences between the correlation coefficients of the realisations and the correlation coefficients of drillhole data were calculated. The absolute difference is a measure of how closely the simulations reproduced the drillhole coefficients. A value close to 0 (zero) is desired and an average of 0.14 was obtained in this case. Nineteen realisations had these differences above the 0.14 average.
- The scatter plot of the correlation coefficients of the realisations and the correlation coefficients of the drillhole data were generally characterized by a few outlying points. It was observed that other realisations outside the 19 (above the 0.14 average) had more pronounced outlying points.
- The sills of the experimental back- transformed variograms (about 10 randomly selected realisations were used) plotted slightly below that of the

sample data (Figure 24), suggesting much lower variability. Ergodic fluctuations or discrepancies between simulations and model statistics are a common feature in simulation studies (Deutsch and Journel, 1998).

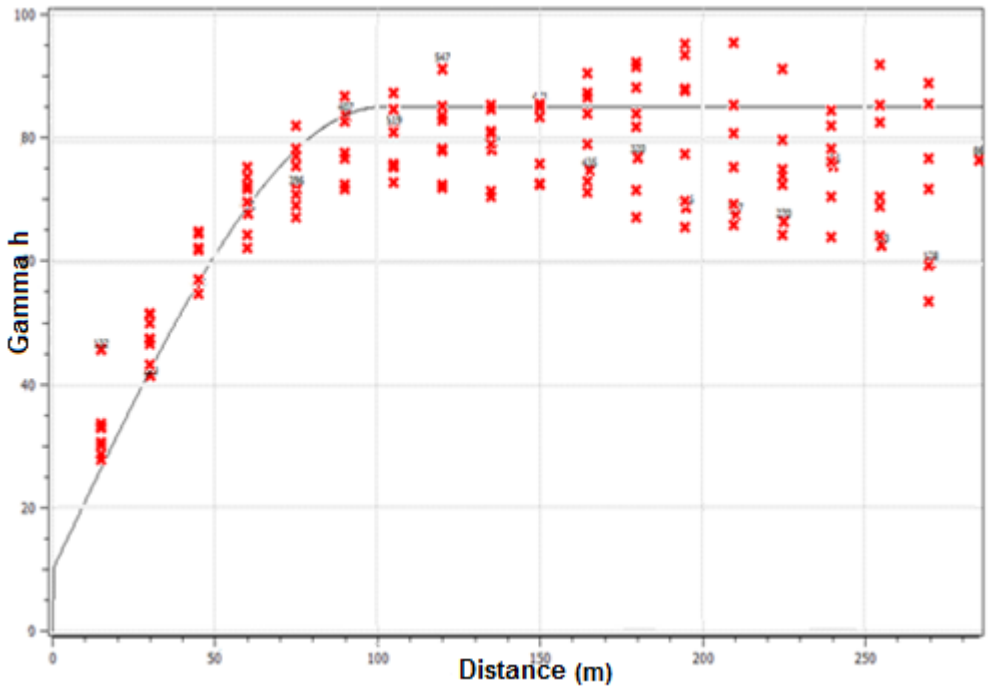

Figure 24: Experimental variograms of randomly selected realisations (crosses) compared to the model of the input data (solid line)

- The spatial patterns of the individual realisations did not considerably differ from each other. The high and low value areas were generally maintained in the realisations. The map output of the average realisations was similar to the kriged map output. There were no obvious geologically unreasonable patterns e.g. sudden areas of elevated or inflated grades (Appendix V). The overall result of the simulations was therefore considered realistic.

6 ASSESSING UNCERTAINTY IN THE KIMB4 DOMAIN

Deutsch (2011) devised a workflow to assess uncertainty of variables over an area of interest using kriging and conditional simulation means and variances. This approach involves evaluating the kriging means and their associated variances and conditional means and conditional variances using map outputs to delineate areas of low and high variances. The conditional kriging variances are able to give a visual indication of local uncertainty via the conditional variance maps output.

In kriging with the NS data, the kriging variances become data-value dependent unlike using the original data where the estimates are dependent on the configuration of the sampling points. Some geostatistical software are equipped with algorithms which can back-transform the NS kriging estimates back to their original units. The processes behind the back transformation have been discussed. With the conditional distributions back in original units, the mean and variance are also back in original units but they are now dependent on the data values.

While kriging variance map outputs generally show strong dependency on the data configuration where values are lowest at the data points (regardless of the values) and increase away, the original units conditional variance show dependency on the data values. The variances can be uniformly higher in high point value areas or more uniformly lower in generally lower point value areas. Therefore the conditional variances are much more trustworthy. These areas are therefore "certain" or are areas of low uncertainty. There will still be areas where it is not clear whether they are high or low variance areas. These will be areas where uncertainty is highest.

This approach was used in this study to help delineate areas within the KIMB4 domain which have surely high and low variance as well as those where it is difficult to tell and therefore present areas of high uncertainty in the grade estimates.

6.1 Measures of uncertainty

A variety of summary statistics and uncertainty measures such as conditional variances, IQR, Conditional COV (CCOV) and probability intervals can be derived from the resulting cdf and used to support decision making. The conditional variance measures the spread of the cdf around its mean value $Z^{*:}$

$$CVar(x)=\sum_{k=1}^{k+1}[\bar{Z}_k - Z_E(x)]^2.\,[F(x;\,Z_k)-F(x;\,Z_{k-1})]$$

where:

- z_k, k=l,...K, are K threshold values discretising the range of variation of *z* values
- $\bar{z}_k$ is the mean of the class z_{k-1}, $(z_{k-1},\, z_k)$which in case of a within class linear interpolation model corresponds to $z_k = (\, z_{k-1} + z_k)\,/2$
- $z_E^*\,(x)$is the expected value of the cdf approximated by the discrete sum:

$$z_E^*\,(x)=\sum_{k=1}^{k+1}\bar{z}_k\ .[F(x;z_k)-F(x;z_{k-1})]$$

The conditional coefficient of variation (CCOV) or relative conditional standard deviation corresponds to the conditional standard deviation divided by the mean. The CCOV expresses variability as a percentage of the mean, and is calculated as follows:

$$CCOV(x)=\frac{\sqrt{[\bar{z}_k - z_E(x)]^2.\,[F(x;\,z_k)-F(x;z_{k-1})]}}{Z_E^*(x)}$$

The conditional interquartile range (IQR) is defined as the difference between the upper and the lower quartiles of the normal distribution:

$$IQR = q_{0.75}\,(x) - q_{0.25}\,(x) = F^{-1}(x, 0.75) - F^{-1}(x, 0.25)$$

The accompanying realisation map outputs or images from the simulations can also be visually compared among themselves and against the kriging maps. Spatial features are deemed to be "certain" if they are present in most of the simulated maps and "uncertain" if they only appear on relatively few simulated maps. Probability type information and map outputs are instrumental in establishing the probability of variables to be above certain thresholds as well as how the distribution of the areas changes with the different thresholds.

6.2 Point kriging model

The final point kriged model contained back-transformed NS kriging of the Spm^3 variable, conditional means and variances, IQR, 0.05, 0.5 and 0.95 quantiles, CCOV and the probability that the grade would be greater than 0.2ct/t.

Point kriging of the Spm^3 variable was done in Section 4 where initially, OK was used to obtain the estimate of the Spm^3. This was followed by SK using normalised Spm^3 values. According to Deutsch (2011), SK with normal scores (NS) with a mean of zero can be equated to computing a conditional mean and a conditional variance by solving normal equations. In line with Deutsch's workflow, the variography and kriging were carried out NS with a mean of 0 and variance of 0.95. The NS kriged estimates of Spm^3 variable were then back-transformed to the original units. The gaussian values (-2.46 to +2.46) were back-transformed using the Histogram Transformation algorithms of the SGeMs software. The initial transformation targeted the raw Spm^3 distribution thereby conditioning the estimates to the point distribution. Using the Post Kriging algorithm of the SGeMS program, the conditional mean and variances, IQR as well as quantiles, probability of being over or below the mining grade cut-off were then computed.

The back-transformed map output showed slight disparities when compared to the respective kriged NS conditional map and OK output (Figure 25) but the high Spm^3 (>12 Spm^3) areas to the South Western edge of the domain remained high, and the low values elsewhere remaining low in all the three outputs.

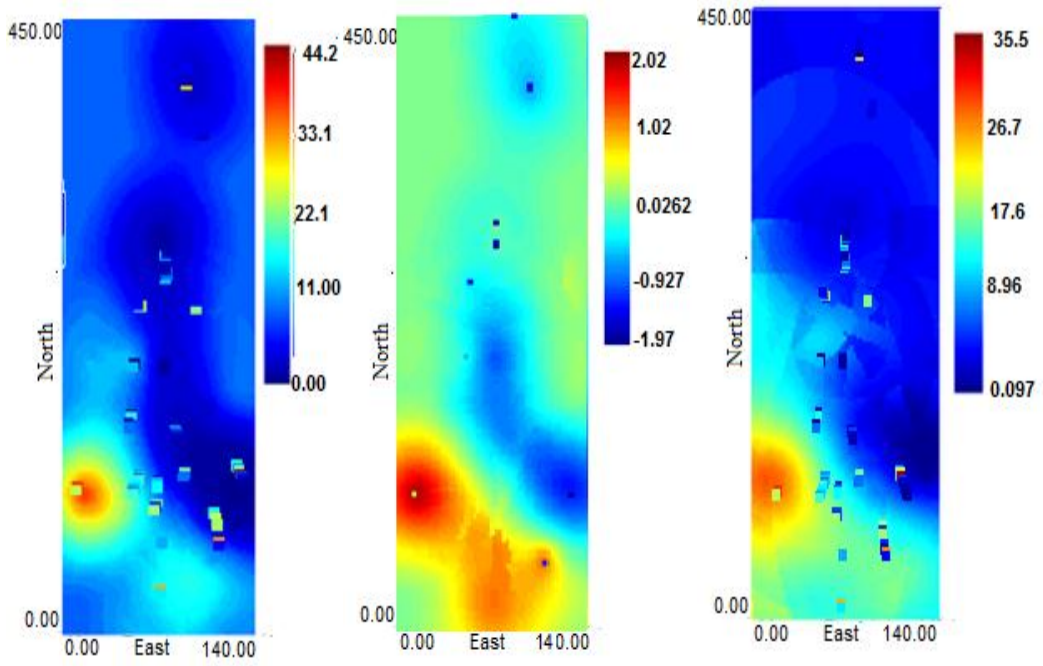

Figure 25: Map outputs of back-transformed NS kriging (left) compared to kriging in NS with mean of zero (middle) and OK (right) showing the high grade area to the South West of the domain and low grades estimates elsewhere.

The variances, unlike the kriged estimates behaved differently. The variances of the back-transformed Spm^3 values were significantly lower (+11.1 to +21.8) compared to the OK variances (+17 to +170). The spatial patterns on the map output of the back-transformed data also looked identical to the variance map output of the NS variance (Figure 27). However the histogram returned by the back-transformed variances had an 'unusual' distribution which did not mimic that of OK.

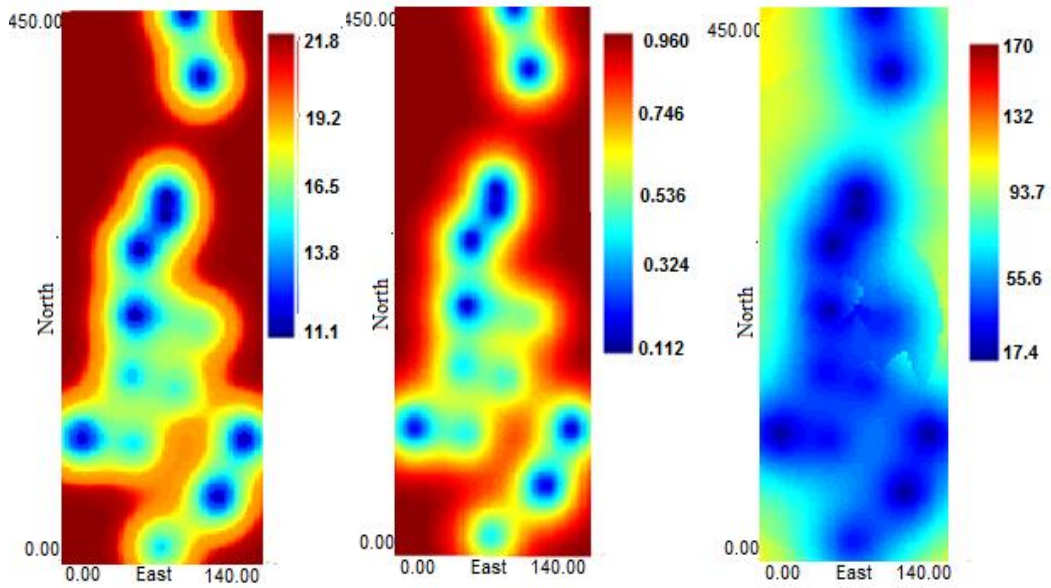

Figure 26: Back-transformed NS Variance (left) compared to the Kriging variances in NS with mean of zero (middle) and OK (right)

The data distribution and kriging showed that there are fairly high values on the SW margin of the domain and relatively low values elsewhere. The conditional variances however showed a poor correlation with the Spm^3 variable because low variance values related to both high and low Spm^3 values (Figure 27). The unusual distribution of the back-transformed variance and conditional variance may therefore indicate the limitation of SGeMS in back transforming NS variances to be used in assessing uncertainty.

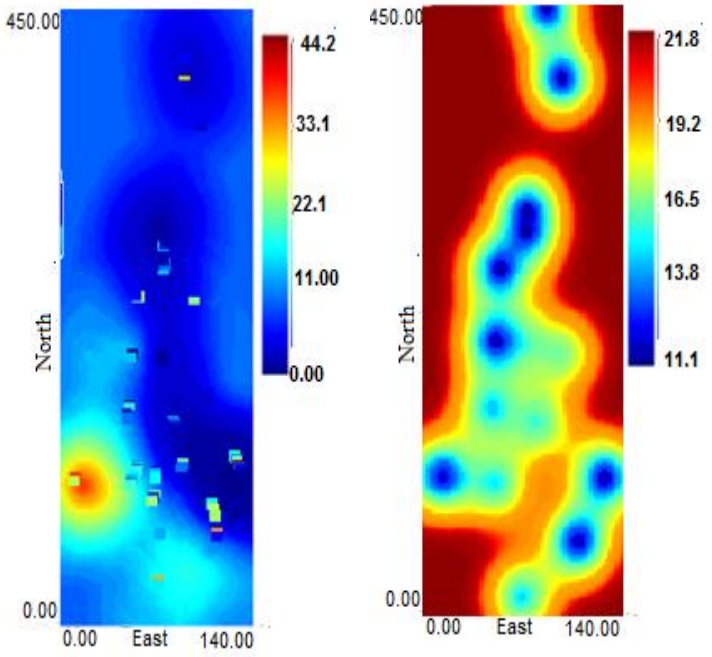

Figure 27: NS Back-transformed mean map (right) compared to back-transformed variances (left)

6.3 Quantile and Probability Maps

According to Deutsch (2011), quantile maps can be equated to probability maps (P maps). Low quantile e.g. of 0.05 correspond to and identifies areas that are surely high grade because every single grid cell of the low quantile has a 95% chance that the true value is higher than the values on the map. Likewise the high quantile (0.95)/ P95 map identifies areas that are surely low in a variable or grade with each grid having a 95% chance of that the true value is lower than the values on the map. The 0.5 quantile/P50 map looks almost identical to the kriging map. However the quantile map is a map of local medians and it does not represent the means like kriging. More often than not, the kriging means are less than the P50 values. Using the quantile

maps, areas that are surely high and surely low can be flagged and an indication of uncertainty over an area can be obtained.

Three maps at 0.05, 0.5, and 0.9 quantiles were produced in addition to the NS back-transformed map and the results are shown in Figure 28.

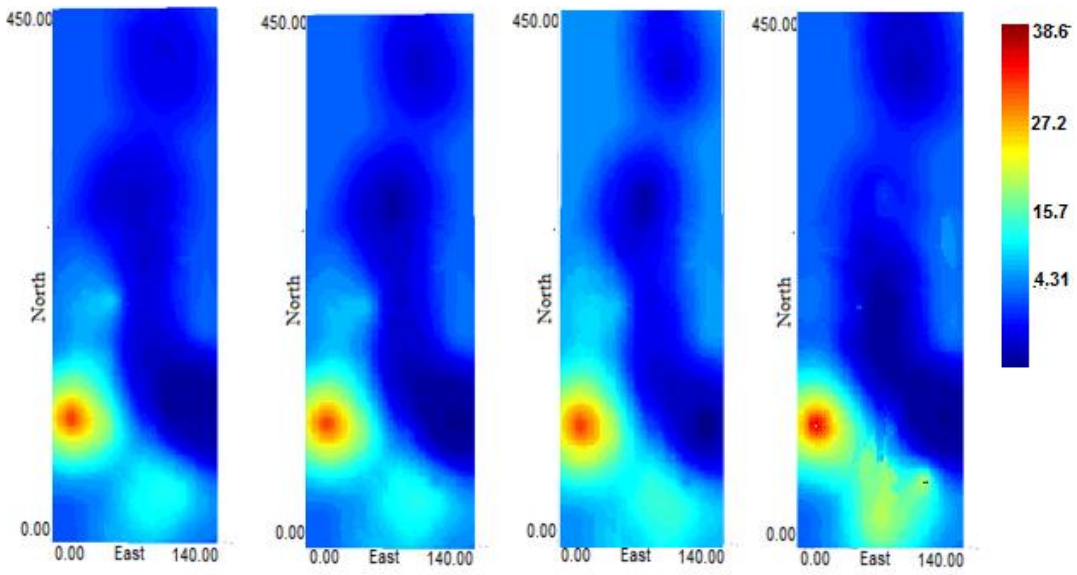

Figure 28: 0.05 (extreme left), 0.5 (middle left), 0.9 (middle right) probability maps and NS back-transformed map (extreme right)

The low quantile (0.05) or P5 map corresponds and identifies areas that are surely high grade because every single grid cell on the P5 map, has a 95% chance that the true value is higher than the values on the map. Likewise the high quantile map (0.9)/ P90 map identifies areas that are surely low in Spm^3 with each grid having a 90% chance of that the true value is lower than the values on the map**.**

The quantile map outputs all look very identical when they are compared among themselves and to the kriging map output. The lowest Spm^3 region seems to be consistently delineated to the east of the domain and these regions continue even at

depth while the high value area consistently maps to the SW. Areas where the estimates are uncertain are rather difficult to delineate. One may suggest the regions highlighted in a lighter blue to the SE of the high value area but this is also very subjective.

An attempt to summarise the local distributions of uncertainties by their means and their variances is presented above. However the measures did not allow for the assessment of local uncertainty and delineations of the different zones of uncertainty. Both the conditional mean and variance maps were very identical to the kriging and kriging variance maps. More importantly the back-transformation of the NS kriging variances in SGeMS for assessing uncertainty was inadequate. As a result a measure of variance that is trustworthy and dependable as well as conditional both to data values and configuration could not be obtained.

6.4 Point Simulation Model

In Section 5 sequential gaussian simulation of the Spm^3 variable in the KIMB4 domain was carried out and validated. A total of 50 point realisations were computed and back-transformed to the original units.

The initial intention of simulation was to take the workflow devised by Oritz and Deutsch (2003) to block scale by simulating blocks. However because the NS variances and means did not perform well in determining the local uncertainty within the KIMB4 domain, the local uncertainty will be investigated using the point simulations following the same work flow as in the kriged model.

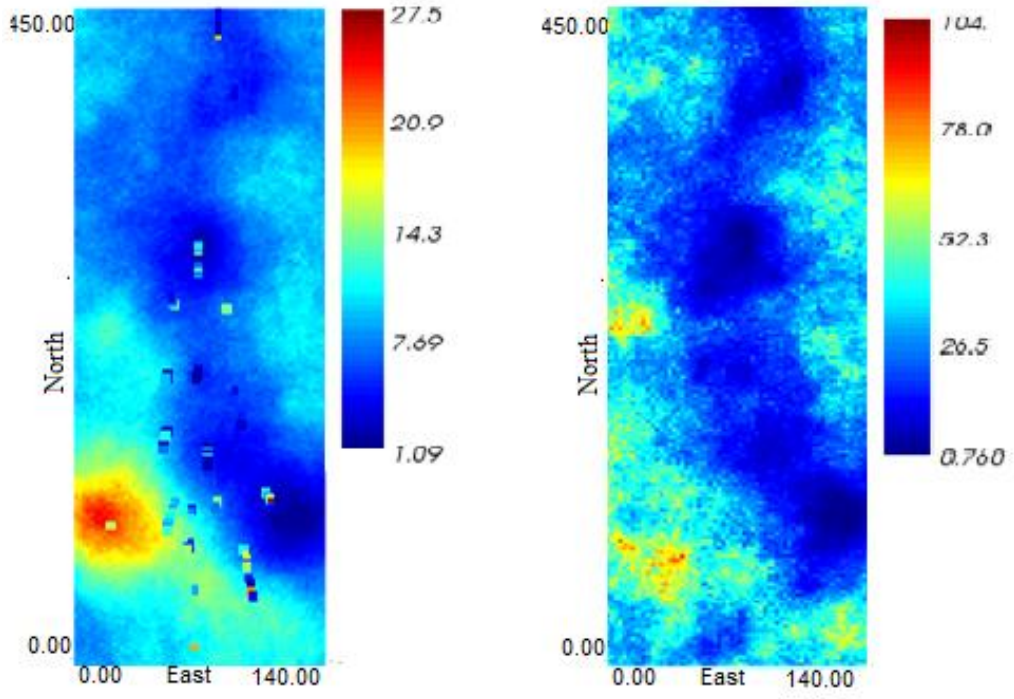

Figure 29: Map of conditional means (left) and conditional variances (right)

The POSTSIM algorithm of the SGeMs program allows for the computation of the conditional mean and variances of the computed realisations. In this case the 50 realisations were passed on to the algorithm and the respective conditional mean of 10.91 and variance of 67.8 were obtained. The respective map outputs are shown on Figure 29. Unlike in the kriging model, the high variances are found where the high conditional mean values are positioned. Conversely, the low means are positioned where the kriged variances are low with the exception of the unsampled edges of the domain. The simulation model therefore seems to be more appropriate in assessing uncertainty than the kriged model.

Three probability maps P10, P50 and P90 were produced as shown in Figure 30 and compared to the Conditional mean map. As in kriged model, the low quantile (in this case we used the 0.1 or P10 map) corresponds and identifies areas that are surely high

grade and the high quantile map (0.9)/ P90 map identifies areas that are surely low in Spm^3. The 0.5 quantile/P50 map remains identical to the kriging mean map.

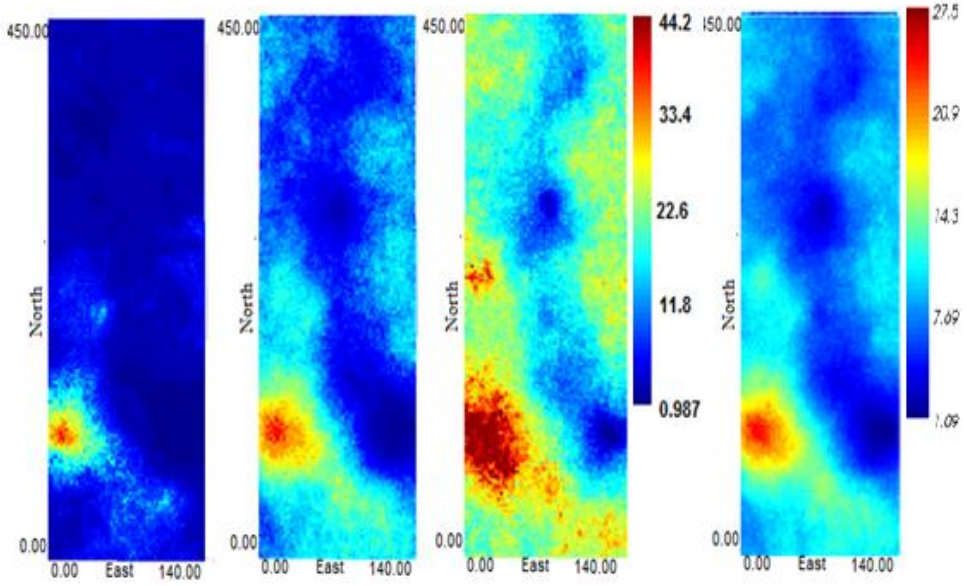

Figure 30: Map outputs of probability maps at 0.1 quantile (extreme left), 0.5 quantile (middle left), 0.9 quantile (middle right) compared to the conditional mean map (extreme right)

The 0.5 quantile/P50 map remains identical to the kriging mean map. Right from the visual onset, the quantile maps are very different. The 0.1 quantile maps delineate the truly high value area to the SW margin of the domain. The surely low value areas persistently lie to the East of the domain with other portions in the middle and to the extreme North of the domain. The areas where the estimates are uncertain lie in between low value areas and to the SW of the truly high value area (Figure 31).

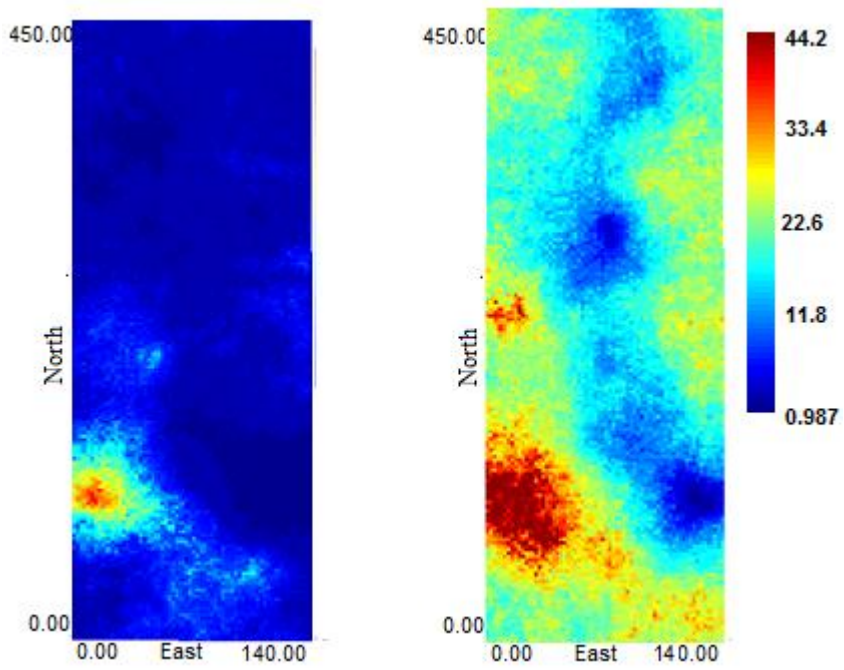

Figure 31: P10 and P90 maps flagging areas that are surely high (right) and areas that are surely low in Spm^3 estimates (left).

The economic cut-off grade in K1 is 0.2ct/t. The equivalent Spm^3 value can be easily determined since the MSS and density are known (0.0767ct/stn and $2.64t/m^3$ respectively). This was worked out to be $6.84Spm^3$. The probability of the grade being above $6.84Spm^3$ was investigated and Figure 32 shows the model of the probability of the grade being above $6.84Spm^3$. The SW region still has the highest probability of being above the cut-off grade while the portion to the east which coincides with the surely low Spm^3 area has the lowest and intermediate values in between.

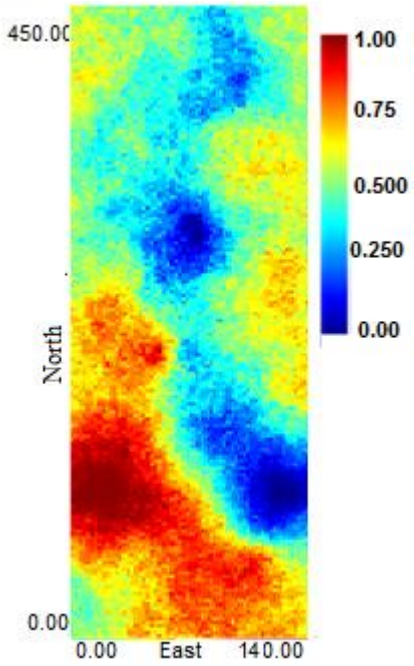

Figure 32: Probability of Spm^3 values above 0.2ct/t cut-off.

The interquartile range (IQR) is a relative measure and as such does not use the mean as the centre of the distribution. This measure ignores the internal distribution of probability grade, leading to over representing uncertainty. Therefore it was not considered for this study.

6.5 Presentation of the block model

The block simulations were obtained from point scale realisations averaged into blocks (25m x 25m x 15m). The final model contained fields for 50 grade block average realisations, conditional means and variances, 0.05, 0.5, 0.95 quantiles, Coefficient of Variation and Probability that the grade would be greater than 0.2cpt/t.

The univariate statistical parameters generated from the block simulations are illustrated in Figure 33 and compares against those of the sample data and the kriged output.

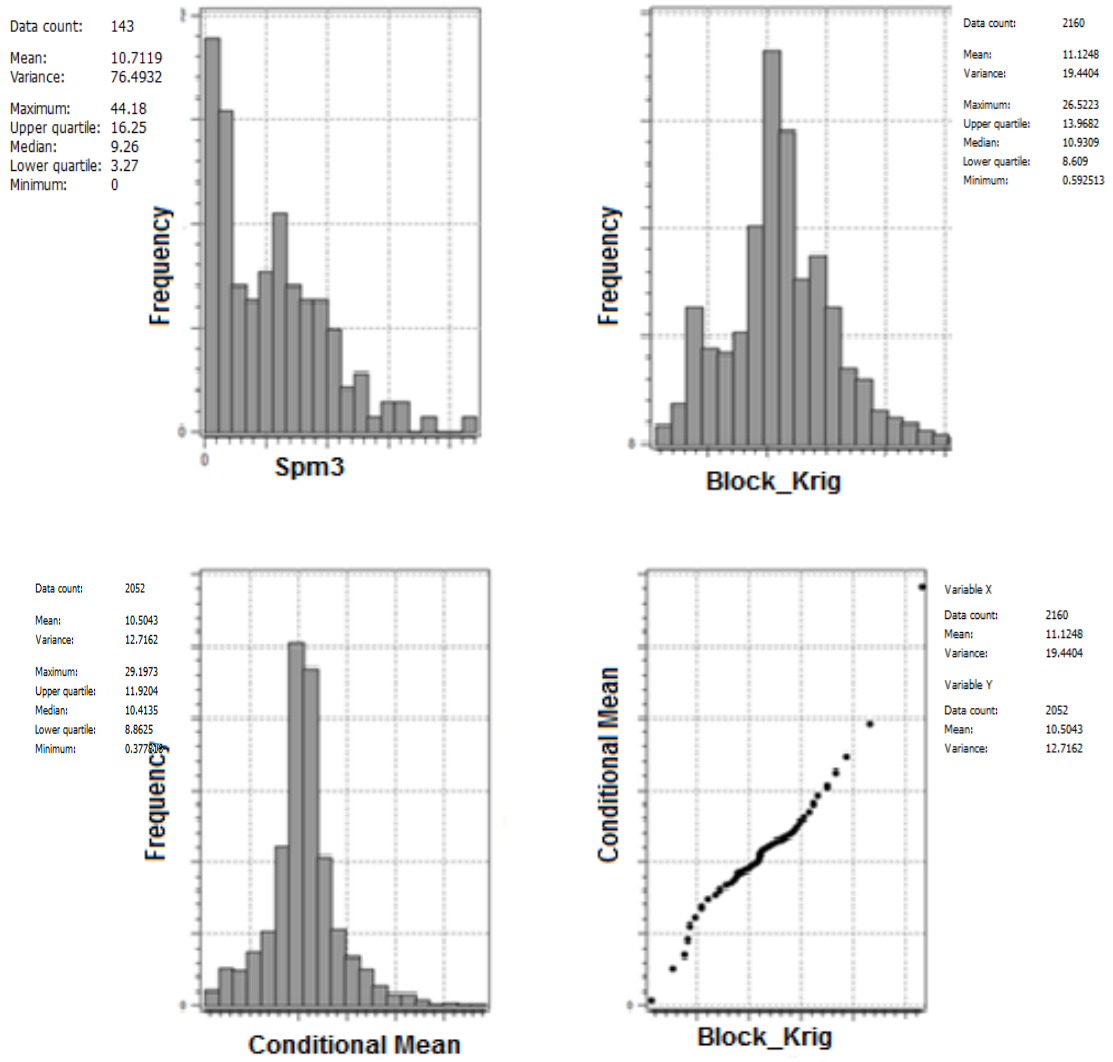

Figure 33: Comparison of univariate statistical parameters of the Spm[3] sample data (top left) against those of the ordinary kriged estimates (top right) and mean of the simulations (bottom left). The output from the kriging and simulation is also compared using a quantile-quantile plot (bottom right) where ordinary kriged estimates are plotted on the X-axis and the Conditional mean of the simulations on the Y-axis.

The univariate statistics from the kriging and the average of the simulations are similar. This is also evident when examining a quantile-quantile plot showing the output from the kriging and the mean of the simulations. Figure 34 shows map output from the different techniques used to model the variability and estimate the Spm^3 variable of the KIMB4 domain. The angled view attempted to capture and show the variability in this unit.

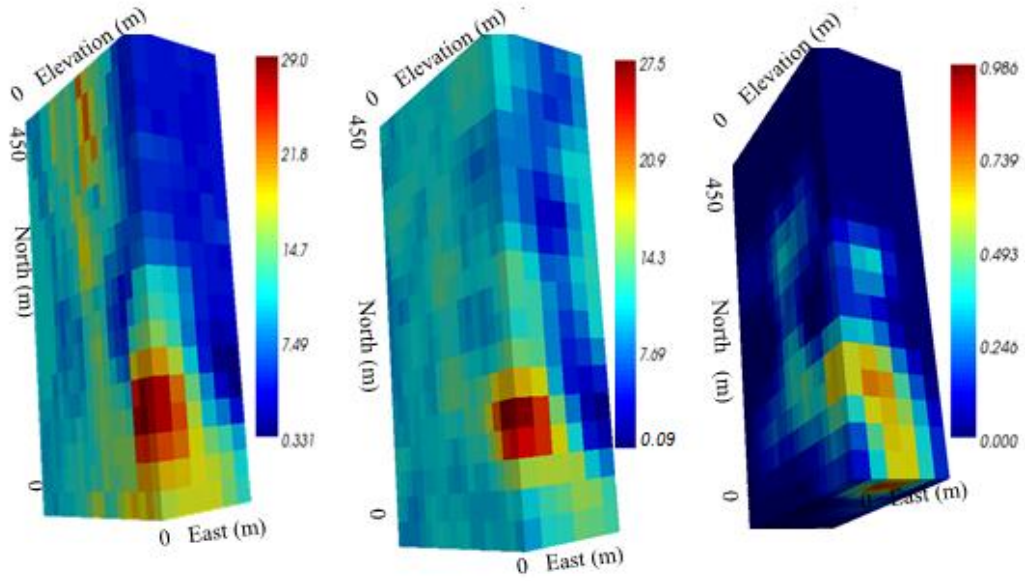

Figure 34: Output from the different techniques generated by Kriging (left), SGS (middle) and indicator kriging results (Prob Z*>12) right

The 50 realisations were passed on to the POSTSIM algorithm and the respective conditional mean of $10.78Spm^3$ and variance of $44.73Spm^3$ were obtained. The respective map outputs are shown on Figure 35. The high conditional means and variances for the block simulations remain confined to the South West of the domain. The variances remain fairly low elsewhere besides the unsampled edges of the domain.

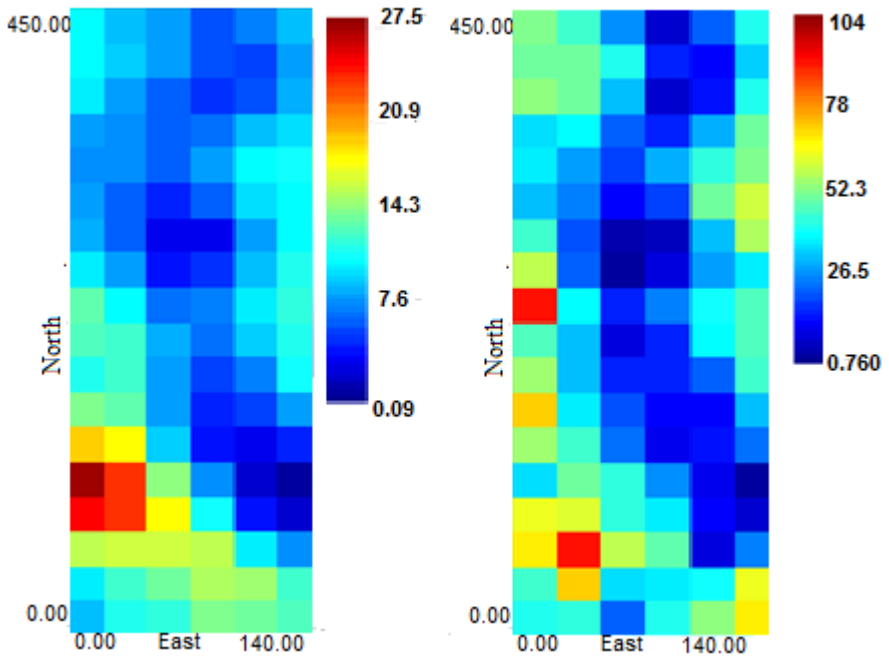

Figure 35: Map of Conditional means (left) and conditional variances (right)

Three probability maps P10, P50 and P90 were produced as shown in Figure 36 and compared to the Conditional mean map. Blocks in the SW margin of the domain remain truly high value blocks while blocks that are low lie to the South East of the domain with other blocks in the middle and to the extreme North of the domain. Blocks where the estimates are uncertain lie in between low value blocks and to the SE of the truly high value blocks.

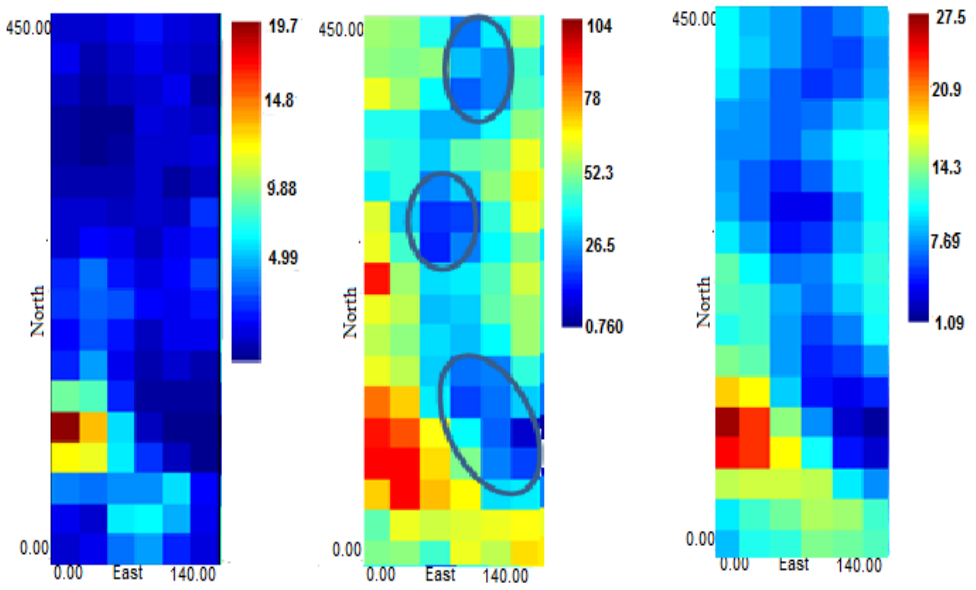

Figure 36: P10 (left) and P90 (middle) maps flagging blocks that are surely high and blocks that are surely low in Spm^3 estimates blocks where there is high uncertainty - broken line (left) and conditional mean map (right).

The SW margin of the domain remains truly a high value area (Figure 36). The surely low value blocks lie to the east of the domain and blocks where the estimates are uncertain lie to the SE of the truly high value blocks.

In order to assess the effect of using the conditional coefficient of variation (CCOV) for improving the classification of KIMB4 resource; statistics were generated for the CCOV per recoverable resource classification category of the domain as indicated on Table 6. The thresholds

Table 6: Base statistics for CCOV and classification category

Classification	CCOV	Number of blocks	% of blocks
Measured	0-2	248	0.12
Indicated	2-4	651	0.317
Inferred	4-8.18	1153	0.561

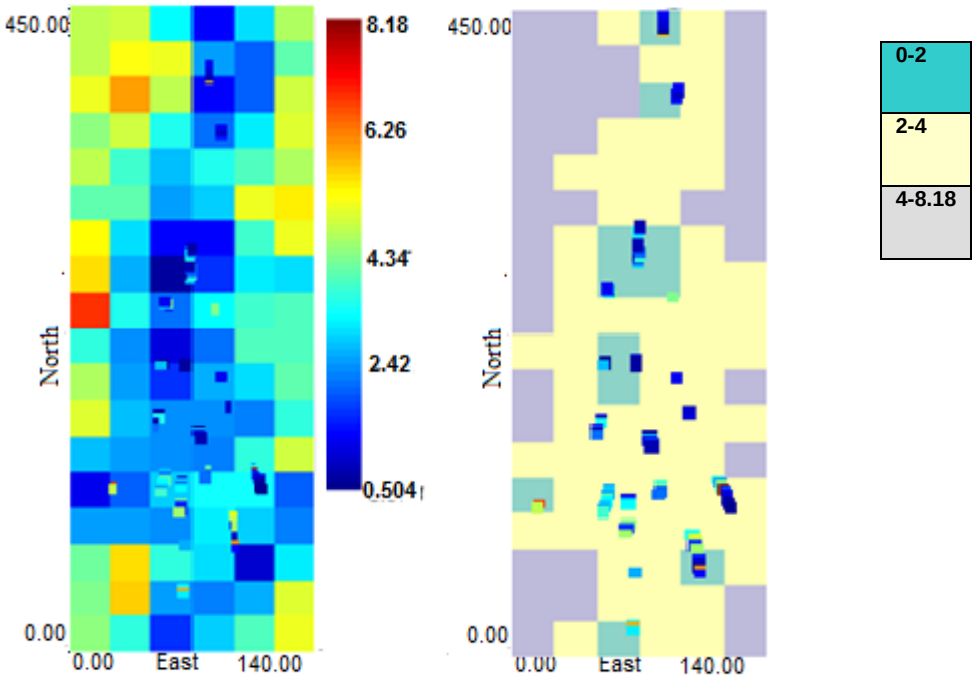

Figure 37: Block coefficient of variation and resource classification

The dark blue blocks coincide with drillhole points and it is evident that zones of high confidence (low uncertainty) correspond well with these points, while zones of high uncertainty correspond with zones that have been insufficiently sampled (Figure 37). Colouring the simulation model on CCOV will allow for the targeting of specific zones of highest CCOV and place lower importance on zones with lowest CCOV. In

this way expenditure on future drilling programmes would thus be optimised to gain maximum benefit.

The decision to allocate blocks to Inferred, Indicated or Measured resource category at Murowa remains the responsibility of the competent person. However, using the CCOV as a measure provides a good, semi quantitative method to use as an aid, which with similar measures on other variables will make quantitative classification possible. The coefficient of variation seems to provide a reliable indication of uncertainty in the simulated grade and is perhaps a more reliable tool for confirming, or even improving, the classification within the KIMB4. Furthermore, it perhaps is the best tool to direct drilling programmes in zones that require additional sample information.

This resource classification criterion is based on the uncertainty measures derived from the cdf of each block in the resource model. The criterion requires the selection of a threshold value that reflects the error tolerance that is acceptable for the block estimate. Therefore for given thresholds, the KIMB4 block can be classified at a Measured, Indicated or Inferred level of confidence depending on whether the CCOV is less than or greater than the thresholds. The thresholds are user-defined and in this case the thresholds values ranging from 0 to 2, 2-4 and 4-8.18 were used. In Figure 37 the darker blue coloured blocks representing low CCOV values have been classified at a Measured resource category while the pale blue blocks are Indicated and the pales greens and yellows are Inferred.

KIMB4 domain's CCOV values have highlighted the potential to convert Indicated material to a Measured status. This is particularly applicable to the central zones where the classification by T&I may have been too stringent. The Murowa Mine has not been supplied with this uncertainty model to assist with the planning of additional drilling aimed at converting Indicated material to Measured status.

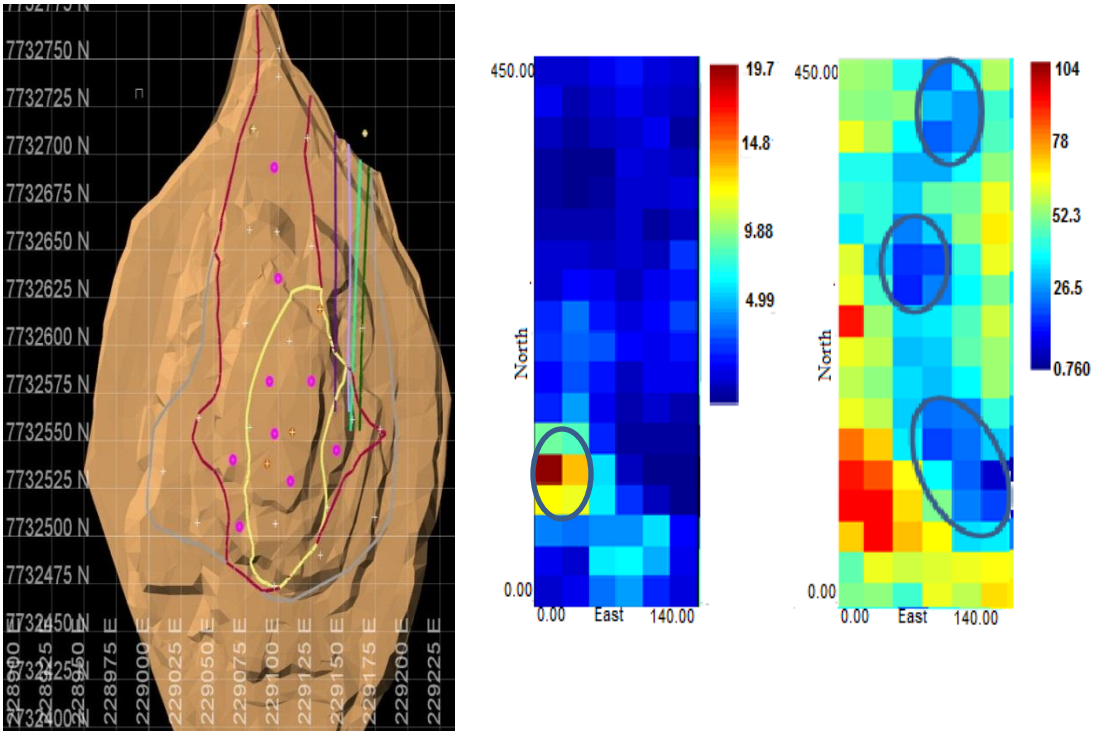

Figure 38: Proposed LD holes (pink) and P10 and P90 maps flagging blocks that are surely high and blocks that are surely low in Spm^3 estimates and blocks where there is high uncertainty -broken line (middle and right). The magenta line outlines the KIMB domains, the yellow line- weathering and the blue the MPZ.

However some drilling to define the resource at depth has been proposed in 2010. A total of eight holes i.e. 5 x 300 m and 3 x 250 m LDRC holes were proposed to confirm the measured resource at K1. Generally, the results of the uncertainty model are not too removed from the proposed holes (Figure 38).

7 DISCUSSION

Flagging high and low value areas is essential in making decisions which areas need additional drilling. These areas are where the uncertainty is highest. In the K1 kimberlite one of the issues that has been raised before was the concern over the relatively low density of the drilling and relatively small number of samples used in the evaluation of the K1 kimberlite particularly after the deficit in the reconciliation of 2009. The KIMB4 domain being the most voluminous of the other domains, carries the bulk of the resource and it is vital to establish where additional drilling can be done in order to increase the confidence of the estimates.

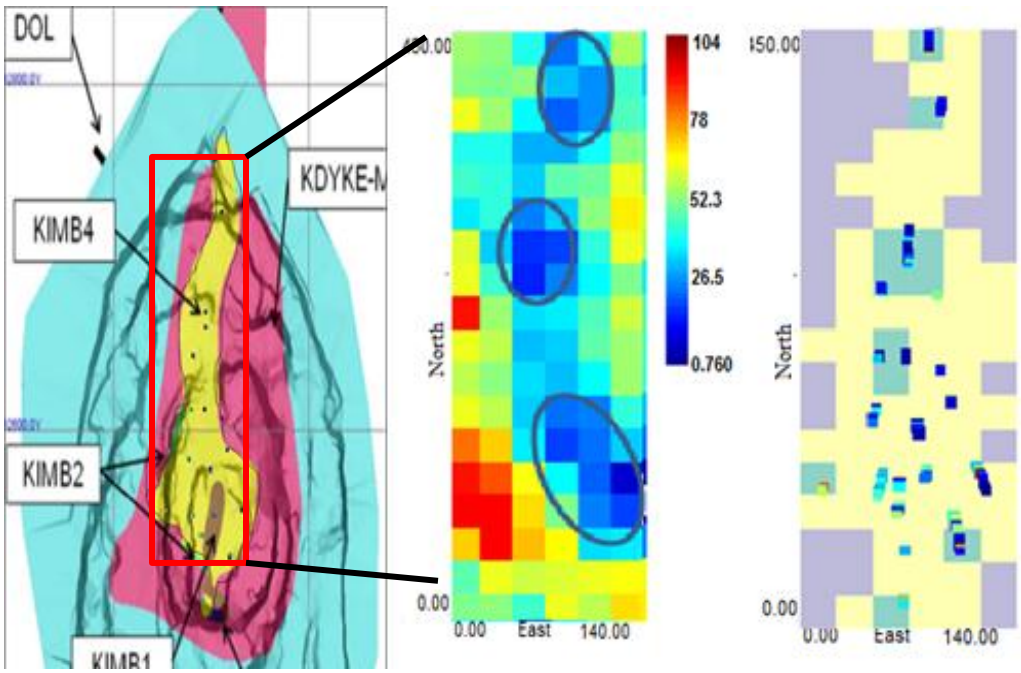

Figure 39: Post plots of Spm^3 values on the geological model in relation to the areas of high and low uncertainty and resource classification based on COV.

Referring to the post plot in Figure 39 (right), the surely high value area is based on a single drill hole with high value samples, while SW trending high uncertainty area seems to have a number of drill-holes but closer under scrutiny, it becomes clear the

drill holes are rather widely spaced and the drilling density can potentially be increased. The area to the north of the high value sample also has a paucity of drill holes. Drilling density can be increased in these areas.

Of equal interest to delineating areas of high and low uncertainty in grade estimates would be quantifying the uncertainty. Uncertainty around estimates such as grades in a deposit can be quantified on a variety of scales such as over regions that represent set production periods, mining units (SMUs and benches), or over the entire pipe (Harrison et al 2009). One way of quantifying the risk associated with such estimates is using the range of grades calculated from the realisations at a particular scale. The mean grade of each realization at that scale is calculated, realizations are ranked and ranges of uncertainty can be calculated at preferred confidence limits that can be generated around the mean of the realisations. In this way high and low estimates can also be obtained for mine design or pit optimisation.

Uncertainty ranges for the KIMB4 domain were investigated at a 15 m bench scale using the block model. Twenty realisations were selected and their means calculated per 15m bench. 15% limits about the mean were selected as they define the limit of acceptable variability for an Indicated resource status (Figure 40). The 15% limits were exceeded for a considerable number of the benches although it becomes worse from about the 12th bench (555m).

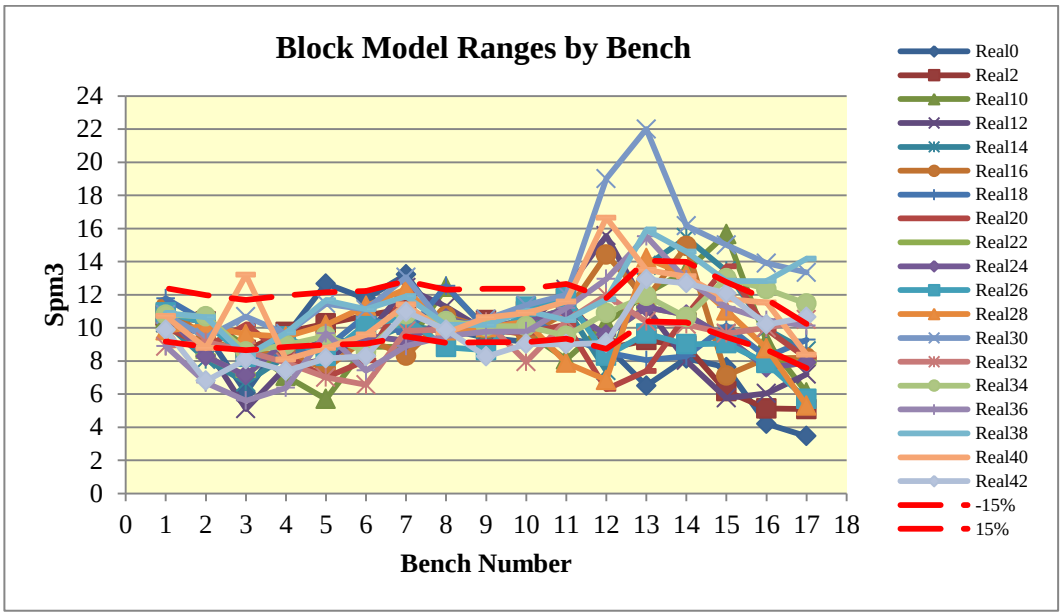

Figure 40: Comparison of the output of nineteen individual conditional simulations. The ±15% envelope about the mean is shown as a reference.

This increased noise at depth seems to be associated with the paucity of sample data over the last few benches (Appendix V11). This is consistent with the T&I classification in 2009 where the resource above 545m was classified in the Indicated Category and below as Mineral Inventory.

Figure 41 shows the mean conditionally simulated Spm^3 per bench (representing all the realisations) along with the 95% confidence limits. This is compared with kriging. The conditional mean is consistently slightly lower than the kriging although the two estimates compare very well throughout all the benches. Both the kriging and the mean of the simulations are also remarkably constrained within the ±15% envelope about the mean even at depth. Another observation is the elevated average Spm^3 values between benches 13 and 14 that are followed by a steep decrease. The maps comparing kriging with realisations are shown in Appendix VII.

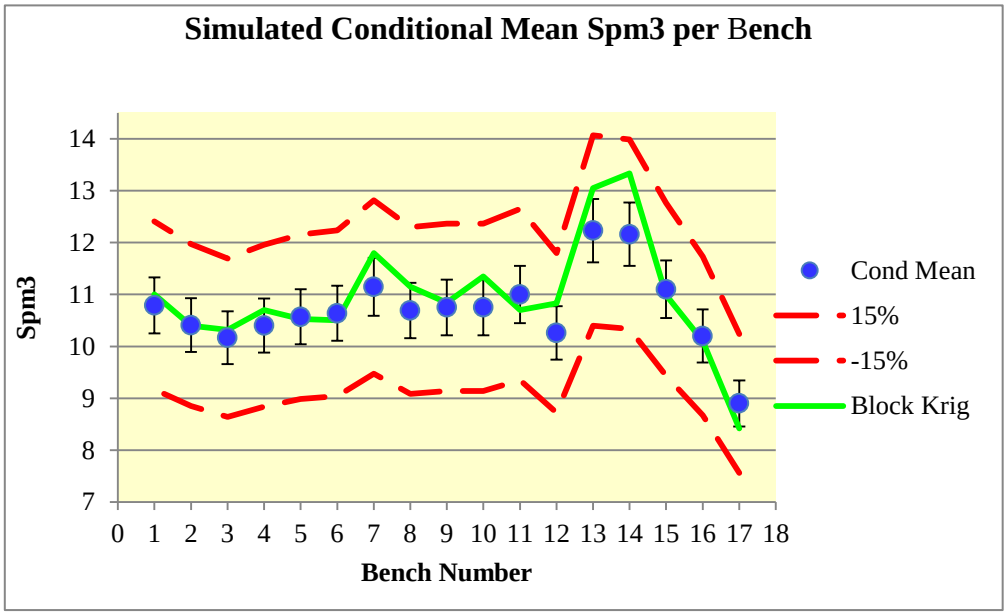

Figure 41: Spm^3 Conditional simulated mean per bench along with the 95% confidence limits.

8 CONCLUSIONS AND RECOMMENDATIONS

The KIMB4 domain of the K1 pipe carries the bulk of the resource and therefore the greatest risk with respect to the grade estimates. The poor grade reconciliation of 2009 compared to the predicted resource model grade necessitated the need to investigate the geological model and grade estimates and provide an indication of uncertainty around the grade in this unit.

Both the practices of kriging (to a lesser extent) and simulations via conditional means, variances, and CCOV were able to provide measures and indication of uncertainty in the estimates in the KIMB4 domain. Areas of high uncertainty could be delineated and these areas can be targeted for additional drilling to increase the confidence and reduce the uncertainty in the estimates. The paucity of sample data coupled with increased uncertainty in the estimates from about 545m was indicated.

Having an accurate assessment of uncertainty arising from grade variability in the ore reserve allows risk in a mining project to be quantified and considered in decision-making processes. This knowledge adds value to a project before the ore reserve is depleted and before development capital is committed to the project. Although basic, the uncertainty-based diamond grade models presented in this study are consistent with standard geostatistical modelling practices. They take into account a variety of additional factors including global statistics, the representative histogram, and the model variogram. Of the measures evaluated the CCOV provided a good measure to use for resource classification and although the method remains semi-quantitative it was possible to use a CCOV value to assign resource categories in this unit.

The quantification of uncertainty and risk also has major implications for open-pit design and production scheduling as it relates to the management of cash flows which at Murowa is in the order of millions of dollars.

For any open-pit design uncertainty over grades, tonnages or geology can be readily modelled and integrated into the optimization and design process so as to provide accurate modelling and quantification of uncertainty and risk, rather than a single estimate assessment. Simulations therefore have the ability to develop more technically sound, and robust risk-based approach to valuing mineral deposits, as well as quantify, and thus minimize, risk in selection of an appropriate pit design.

8.1 Recommendations for Future Work

Based on the work performed in this study, the SGS approach not only performed well but can be a recommended approach for simulating grade in the Murowa kimberlite.
The SGS was easy to implement and produced results that can be defended.
Realisations obtained from this study can be combined with those that can be obtained from the MPZ and KIMB1 domains in the K1 and utilised in pit optimisation. The uncertainty models presented here were modelled using SGeMS, geostatistical open-source three-dimensional software. Therefore another step that can be taken would be to simulate the boundaries of the domains in the K1 pipe and generate multiple interpretations using software such as Vulcan. The use of kriging means and variances suffered from the limitation of the software in terms of the inability to perform adequate back transformations.

Assessing the uncertainty in the grade estimate for the KIMB4 domain has indicated that this is a worthwhile exercise to run on all the domains on the KI pipe. Furthermore it would be relatively easy to rerun this exercise including the additional sample information that will be gained from the proposed additional drilling.

9 REFERENCES

Blackney, P.C.J and Glacken, I.M. (1998) A practitioner's implementation of indicator kriging. Submitted for Publication in The Geostatistical Association of Australasia "Beyond Ordinary Kriging" Seminar Perth, Western Australia.

Bush, D. (2010) An overview of the estimation of kimberlite diamond deposits, South African Institute of Mining and Metallurgy, Source to use, pp.73 - 86.

Chilès, J-P and Delfiner, P. (2012) *Geostatistics-Modelling Spatial Uncertainty* John Wiley & Sons, New York, pp.489.

Deutsch, C. V. and Journel, A G. (1998) *Geostatistical Software Library and User's Guide*, Second Edition, Oxford University Press, Applied Geostatistics Series, pp.13-131.

Deutsch, C. V. and. Lyster, J. M. (2004) PostMG: A Postprocessing Program for Multigaussian Kriging Output.

Deutsch, C. V. (2011) Unpublished document from the Citation Course in Geostatistics, under the auspices of the Geostatistical Association of Southern Africa, Johannesburg.

De-Vitry, C. (2010) Simulation of correlated variables: A comparison of approaches with a case study from the Yandi Channel Iron deposit. A research project submitted to the Faculty of Engineering, Computer and Mathematical Studies University Adelaide, Adelaide, in partial fulfilment of requirements for the degree of Master of Science in Engineering.

Dimitrakopoulos, R., Farelly, C. T. and Godoy, M. (2002) Moving forward from traditional optimisation grade uncertainty and risk effects in open-pit design, Transactions of the Institutions of Mining and Metallurgy, Section A: Mining Technology, 111, January to April 2002, pp. A82 - A88.

Dohm, C.E., (2010) Course Notes: Geostatistical Methods in Mineral Resource Evaluation, GDE, University of the Witwatersrand.

Duffin A C. (2000) Murowa Diamond Project Feasibility Study Report – Volume 1 – Resource Estimate.

Goovaerts, P. (1997) *Geostatistics for Natural Resources Evaluation*. Oxford University Press, Applied Geostatistics Series, pp.483.

Harrison, S., Leuangthong, O., Crawford, B. (2009) Uncertainty-based grade modelling of kimberlite : A case study of the Jay kimberlite pipe, EKATI Diamond Mine, Canada. Extended abstract and poster submitted to the Ninth International Kimberlite Conference, Frankfurt, Germany.

Isaaks, E. H. and Srivastava, R. M. (1989) *An Introduction to Applied Geostatistics*. Oxford University Press, New York, USA. Applied Geostatistics Series.

Journel, A.G. (1983) Non-parametric estimation of spatial distributions, Mathematical Geology 15, pp.445 – 468.

Moss, S. W., Hetman, C. M. and Webb, K. J.(2010) Geology of the Murowa K1 Kimberlite. Report No. MSC10/051R, Mineral Services of Canada Inc.

Mtetwa, S.; Chipfunde, L. and Makwanise, R. (2002) Establishment of biomonitoring reference sites for Zimbabwe-A tool for effective integrated catchment management.

Proceedings of the 3rd WaterNet /Warfsa Symposium: 'Water demand management for sustainable development', Dar es Salaam.

Ortiz, J. M. and Deutsch, C. V. (2003) Uncertainty Upscaling. In *Centre for Computational Geostatistics*, Volume 5, Edmonton, AB.

Parker, H. M. (1991) Statistical treatment of Outlier Data in Epithermal Gold Deposit Reserve Estimation, Mathematical Geology vol 23, No2.

Platell, R. (2011) Murowa Resource Update. A Report Prepared by Rio Tinto Technology and Innovation, Perth, Australia for Tim Biddulp Project Manager for Murowa Expansion Project.

Smith, C.B., Sims, K., Chimuka, L., Duffin, A., Beard, A.D., and Townend, R., (2004). Kimberlite metasomatism at Murowa and Sese pipes, Zimbabwe: Lithos, Vol. 76, pp219 - 232.

Switzer, P. (1977) Estimation of spatial distributions from point sources with application to air pollution measurement. *Bulletin of the International Statistical Institute*,Vol 47 (2), pp.123 – 127.

Robins, S. P. (2006) The quantification of grade uncertainty and associated risk, and their influence on pit optimization for the Sadiola Deep Sulphide Prefeasibility Project. MSc Dissertation submitted to the Faculty of Engineering and the Built Environment, University of the Witwatersrand, Johannesburg, in partial fulfilment of requirements for the degree of Master of Science in Engineering.

Roscoe, W. E. and Postle, J. T. (2005) Diavik Diamond Mine Mineral Reserves and Mineral Reserves audit report, prepared for Aber Diamond Corporation, NI 43-101 Report.

Vann J; Jackson S and Bertolli O. (2003) Quantitative Kriging neighbourhood analysis for the mining geologist- a description of the method with worked case examples. 5th International Mining Geology Conference, Melbourne. The Australasian Institute of Mining and Metallurgy, pp.215 – 223.

APPENDIX I- EXTRACT FROM THE JORC CODE: REPORTING OF DIAMOND EXPLORATION RESULTS, MINERAL RESOURCES AND ORE RESERVES

40. Clauses 40 to 43 of the Code address matters that relate specifically to the Public Reporting of Exploration Results, Mineral Resources and Ore Reserves for diamonds and other gemstones. Unless otherwise stated, Clauses 1 to 36 of this Code (including Figure 1) apply. Table 1, as part of the guidelines, should be considered persuasive when reporting Exploration Results, Mineral Resources and Ore Reserves for diamonds and other gemstones
For the purposes of Public Reporting, the requirements for diamonds and other gemstones are generally similar to those for other commodities with the replacement of terms such as 'mineral' by 'diamond' and 'grade' by 'grade and average diamond value'. The term 'quality' should not be substituted for 'grade,' since in diamond deposits these have distinctly separate meanings. Other industry guidelines on the estimation and reporting of diamond resources and reserves may be useful but will not under any circumstances override the provisions and intentions of the JORC Code.
A number of characteristics of diamond deposits are different from those of, for example, typical metalliferous and coal deposits and therefore require special consideration. These include the generally low mineral content and variability of primary and placer deposits, the particulate nature of diamonds, the specialised requirement for diamond valuation and the inherent difficulties and uncertainties in the estimation of diamond resources and reserves.

41. Reports of diamonds recovered from sampling programs must provide material information relating to the basis on which the sample is taken, the method of recovery and the recovery of the diamonds. The weight of diamonds recovered may only be omitted from the report when the diamonds are considered to be too small to be of commercial significance. This lower cut-off size should be stated.

The stone size distribution and price of diamonds and other gemstones are critical components of the resource and reserve estimates. At an early exploration stage, sampling and delineation drilling will not usually provide this information, which relies on large diameter drilling and, in particular, bulk sampling.

In order to demonstrate that a resource has reasonable prospects for economic extraction, some appreciation of the likely stone size distribution and price is necessary, however preliminary. To determine an Inferred Resource in simple, single-facies or single-phase deposits, such information may be obtainable by representative large diameter drilling. More often, some form of bulk sampling, such as pitting and trenching, would be employed to provide larger sample parcels. In order to progress to an Indicated Resource, and from there to a Probable Reserve, it is likely that much more extensive bulk sampling would be needed to fully determine the stone size distribution and value. Commonly such bulk samples would be obtained by underground development designed to obtain sufficient diamonds to enable a confident estimate of price.

In complex deposits, it may be very difficult to ensure that the bulk samples taken are truly representative of the whole deposit. The lack of direct bulk sampling, and the uncertainty in demonstrating spatial continuity of size and price relationships should

be persuasive in determining the appropriate resource category.
42. Where diamond Mineral Resource or Ore Reserve grades (carats per tonne) are based on correlations between the frequency of occurrence of micro-diamonds and of commercial size stones, this must be stated, the reliability of the procedure must be explained and the cut-off sieve size for micro-diamonds reported.
43. For Public Reports dealing with diamond or other gemstone mineralisation, it is a requirement that any reported valuation of a parcel of diamonds or gemstones be accompanied by a statement verifying the independence of the valuation. The valuation must be based on a report from a demonstrably reputable and qualified expert. If a valuation of a parcel of diamonds is reported, the weight in carats and the lower cut-off size of the contained diamonds must be stated and the value of the diamonds must be given in US dollars per carat. Where the valuation is used in the estimation of diamond Mineral Resources or Ore Reserves, the valuation must be based on a parcel representative of the size, shape and colour distributions of the diamond population in the deposit.

APPENDIX II– EXPERIMENTAL HORIZONTAL VARIOGRAMS

1. Screenshot of experimental variograms of azimuths 0° to 55° at 5° intervals

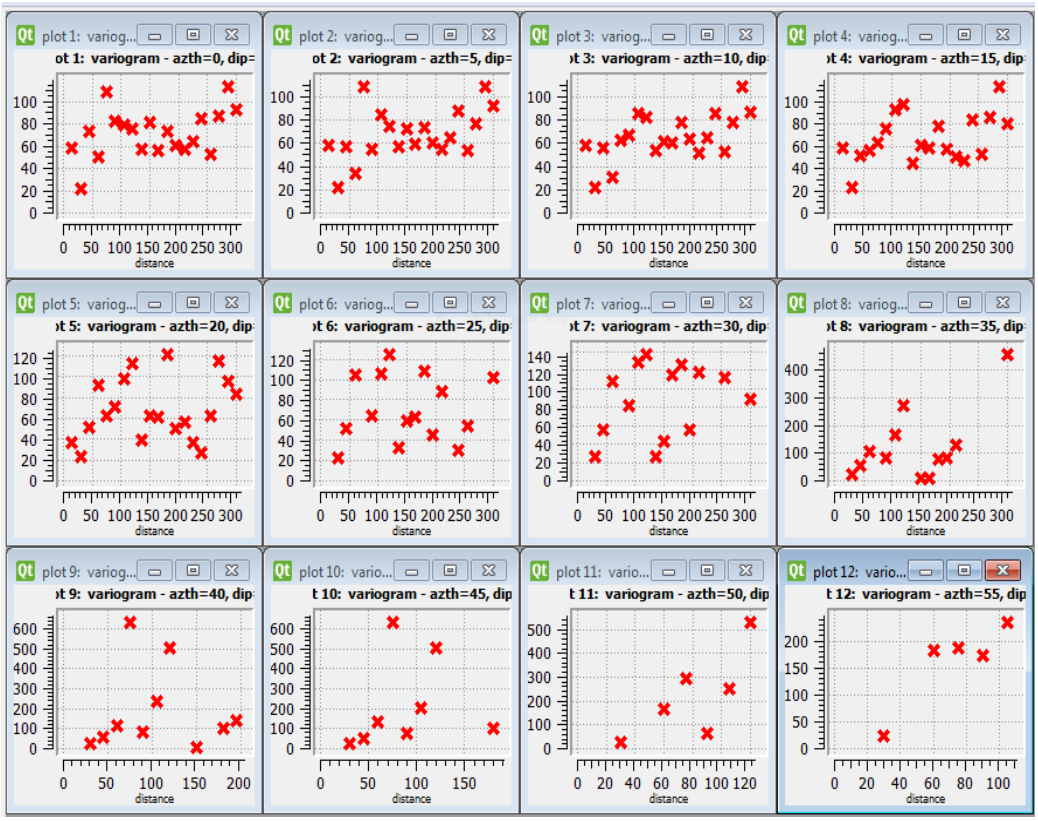

2. Screenshot of experimental variograms of azimuths 60° to 115° modelled at 5° intervals

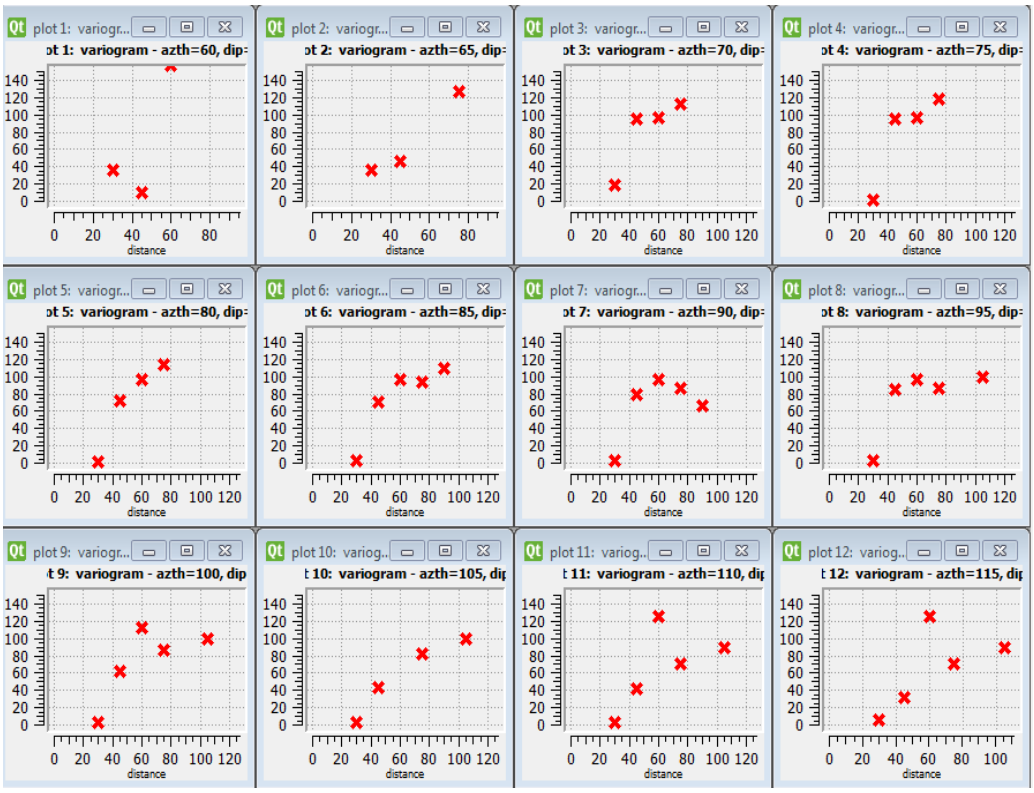

3. Screenshot of experimental variograms of azimuths 120° to 175° modeled at 5° intervals

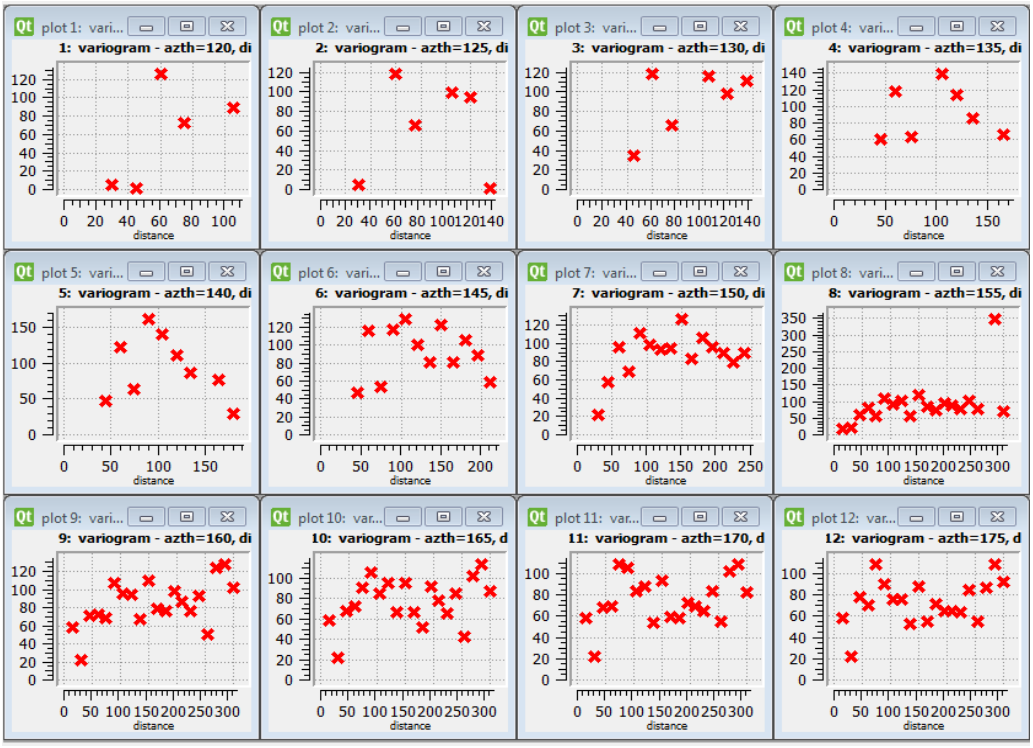

APPENDIX III – INDICATOR VARIOGRAM MODELS FROM SPM^3 > 5 TO SPM^3 >26 THRESHOLDS

1.Spherical variogram model at >5 Spm^3 cut-off and resepctive map output. Nugget, sill contribution and range modelled at 0.03, 0.245 and 108.75m respectively

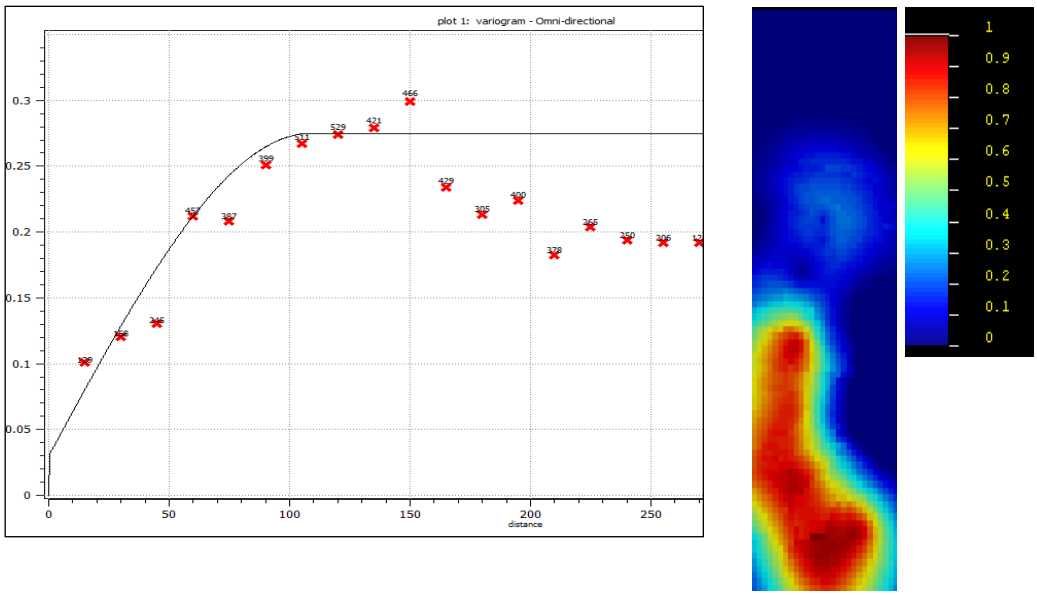

2. Spherical variogram model at >6 Spm^3 cut-off. Nugget, sill contribution and range modelled at 0.03, 0.24 and 101.75m respectively

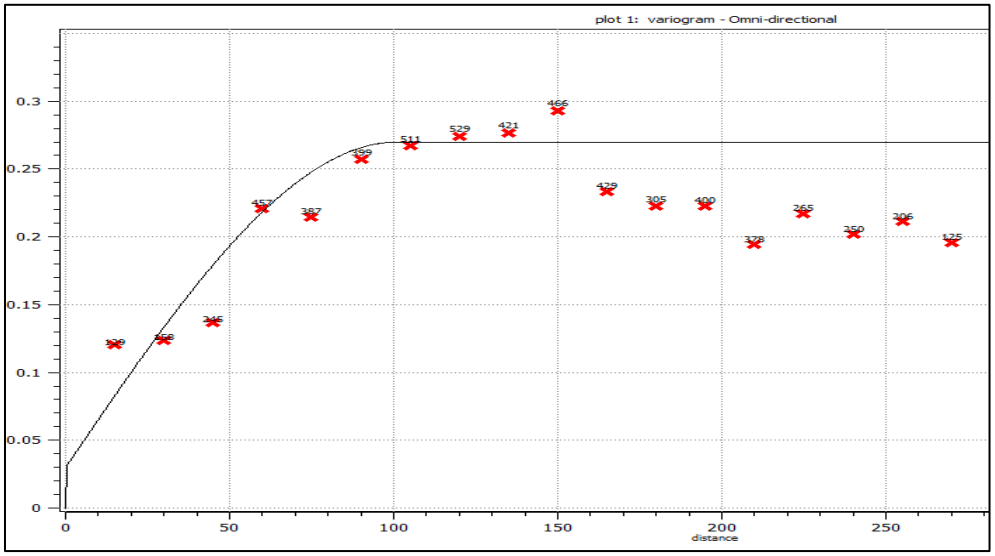

3.Spherical variogram model at >7 Spm^3 cut-off and resepctive map output. Nugget, sill contribution and range modelled at 0.03, 0.25 and 101.75m respectively

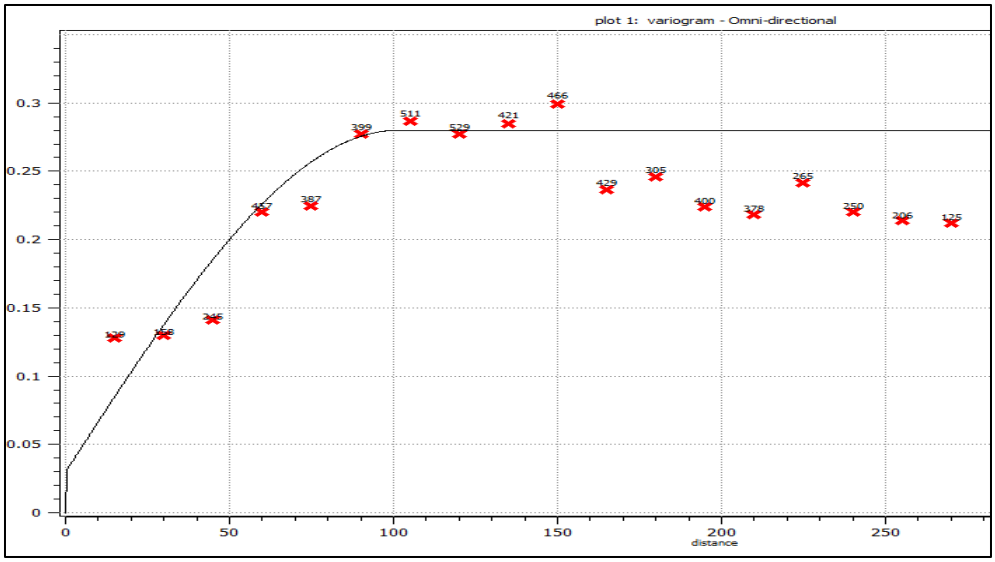

4.Spherical variogram model at >8 Spm^3 cut-off. Nugget, sill contribution and range modelled at 0.05, 0.23 and 108.75m respectively

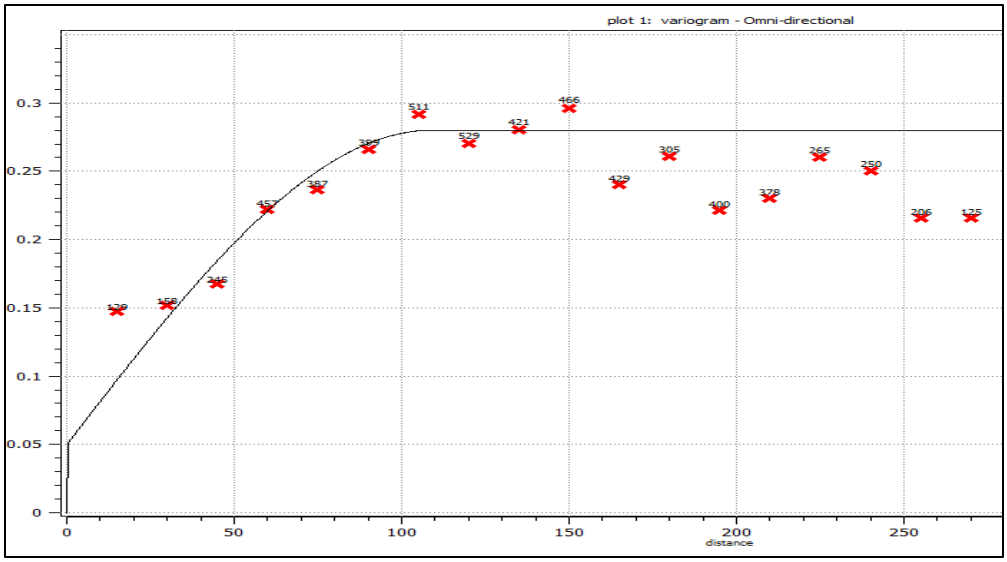

5. Spherical variogram model at >9 Spm^3 cut-off. Nugget, sill contribution and range modelled at 0.05, 0.22 and 101 m respectively

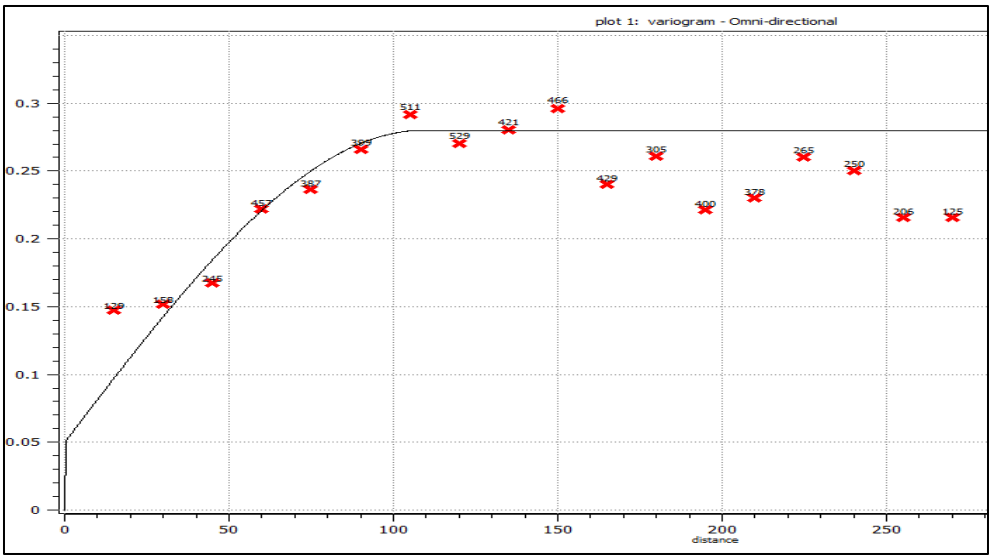

6. Spherical variogram model at >10 Spm^3 cut-off. Nugget, sill contribution and range modelled at 0.05, 0.22 and 101 m respectively

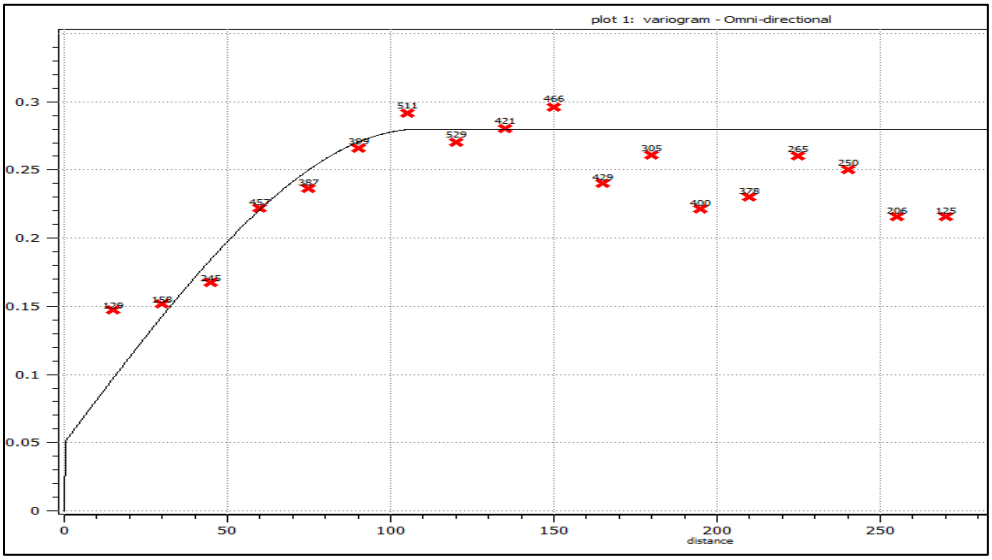

7. Variogram at >11 Spm^3 Cut-off Nugget, sill contribution and range modelled at 0.09, 0.179 and 97 m respectively.

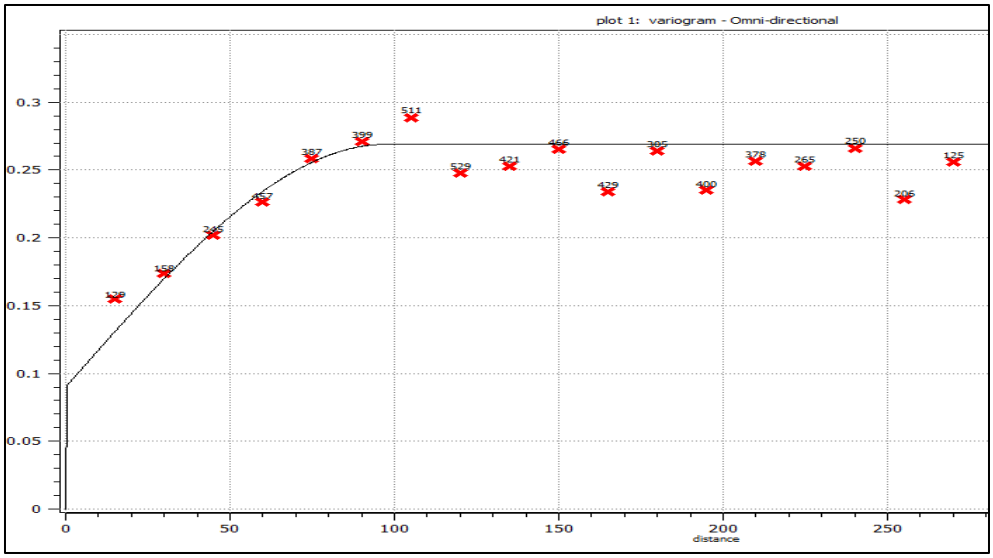

8. Variogram at >13 Spm^3 Cut-off. Nugget, sill contribution and range modelled at 0.09, 0.18 and 97m respectively

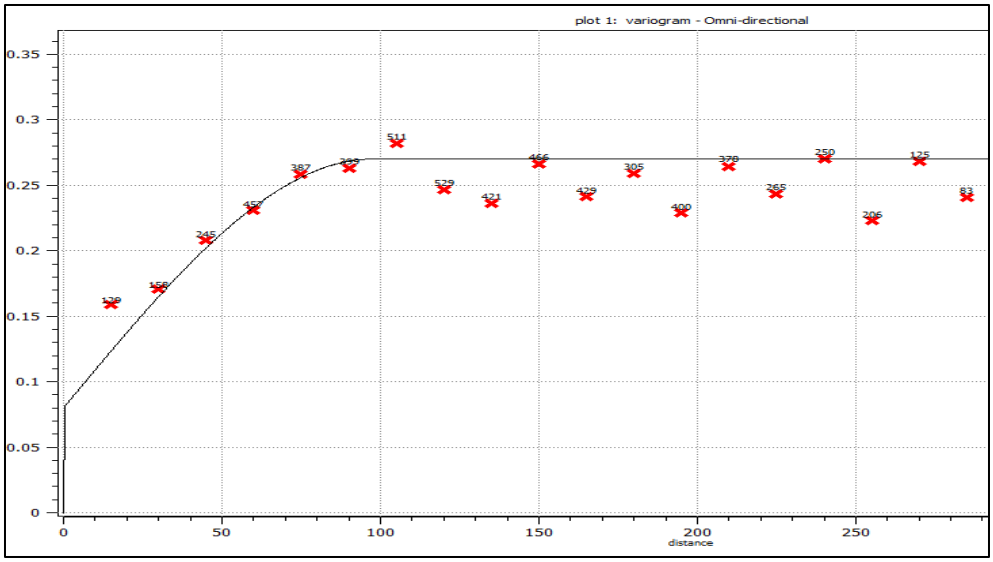

9. Variogram at >14 Spm^3 Cut-off. Nugget, sill contribution and range modelled at 0.1, 0.13 and 78.5 m respectively

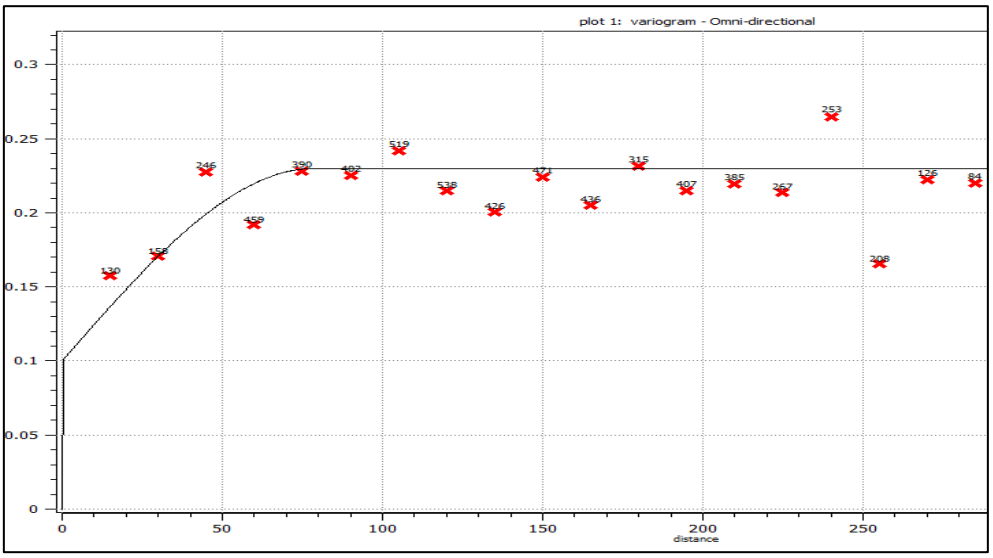

10.Variogram at >15Spm^3 Cut-off. Nugget, sill contribution and range modelled at 0.1, 0.115and 101 m respectively

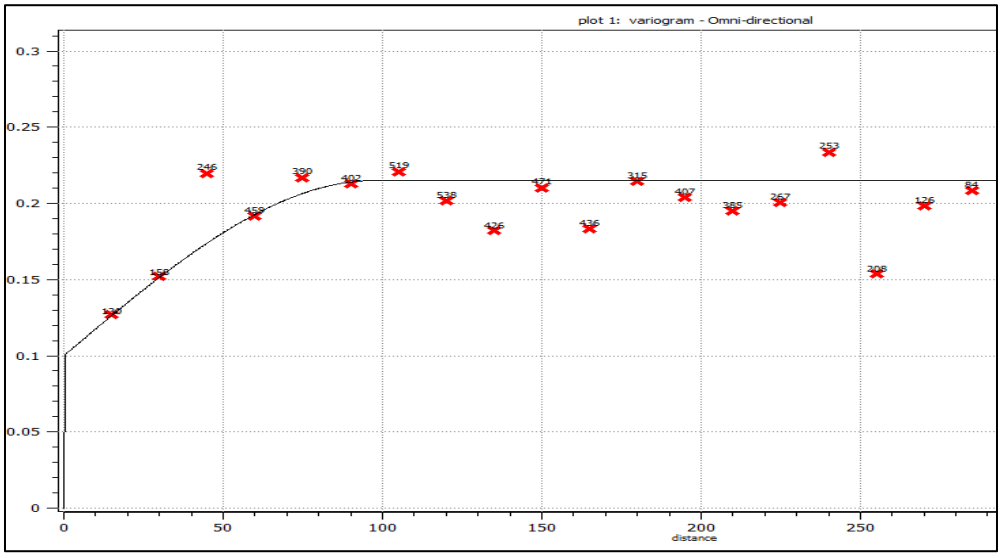

11. Variogram at >16 Spm^3 Cut-off. Nugget, sill contribution and range modelled at 0.1, 0.105 and 90 m respectively

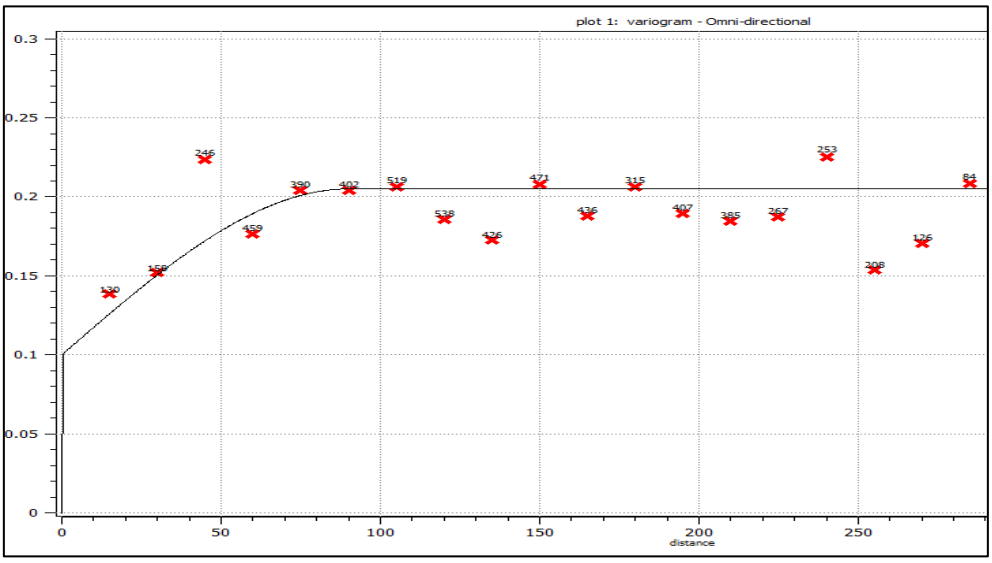

12. Variogram at >17 Spm^3 Cut-off. Nugget, sill contribution and range modelled at 0.105, 0.07 and 97 m respectively

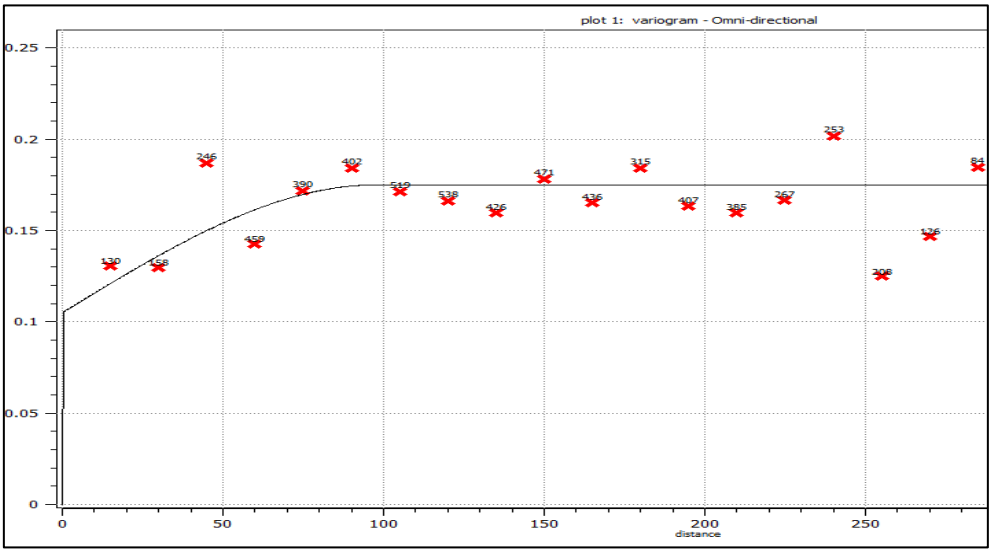

13. Variogram at > 18Spm^3 Cut-off. Nugget, sill contribution and range modelled at 0.085, 0.08 and 90 m respectively

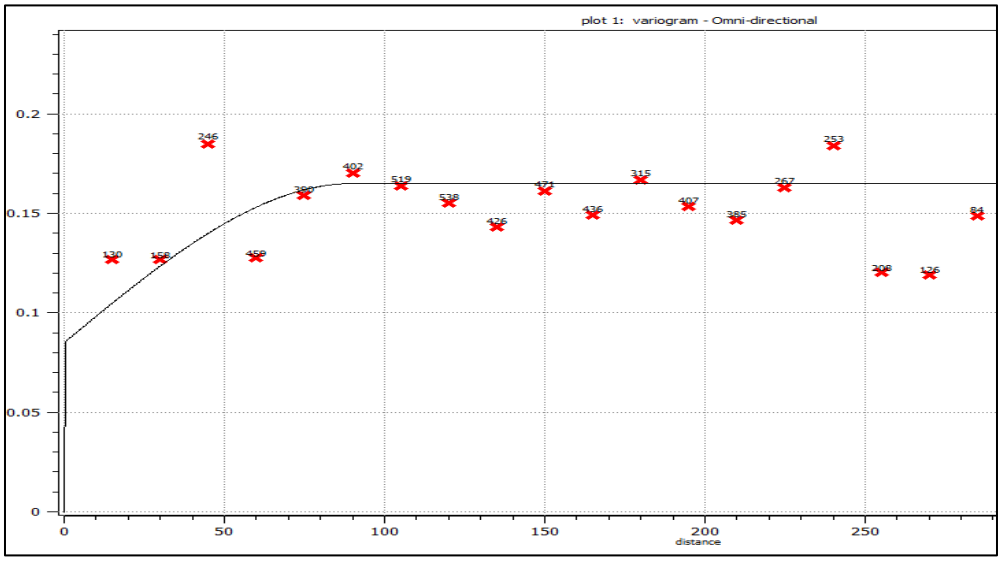

14. Variogram at >19 Spm^3 Cut-off. Nugget, sill contribution and range modelled at 0.08, 0.06 and 71m respectively

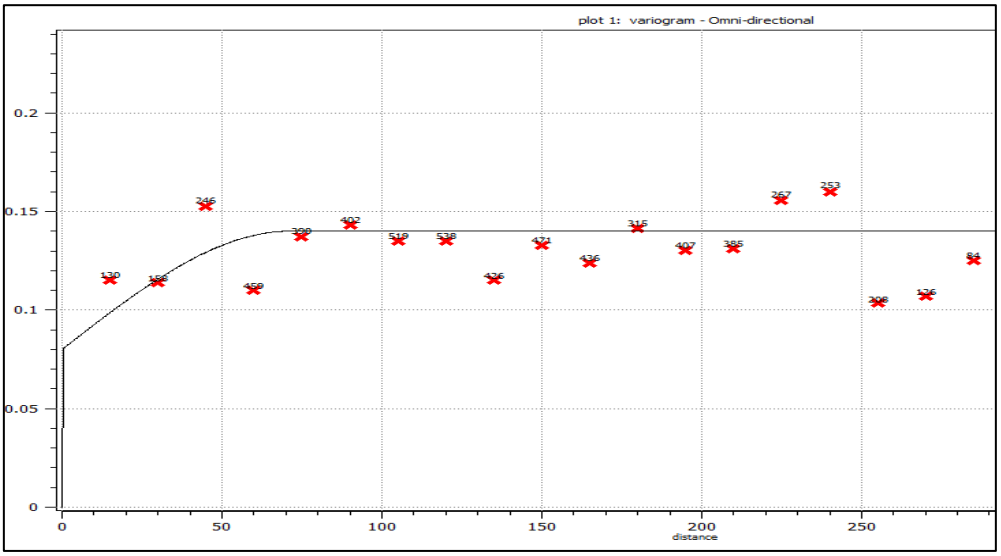

15. Variogram at >20 Spm^3 Cut-off and repective map output. Nugget, sill contribution and range modelled at 0.08, 0.04 and 75 m respectively

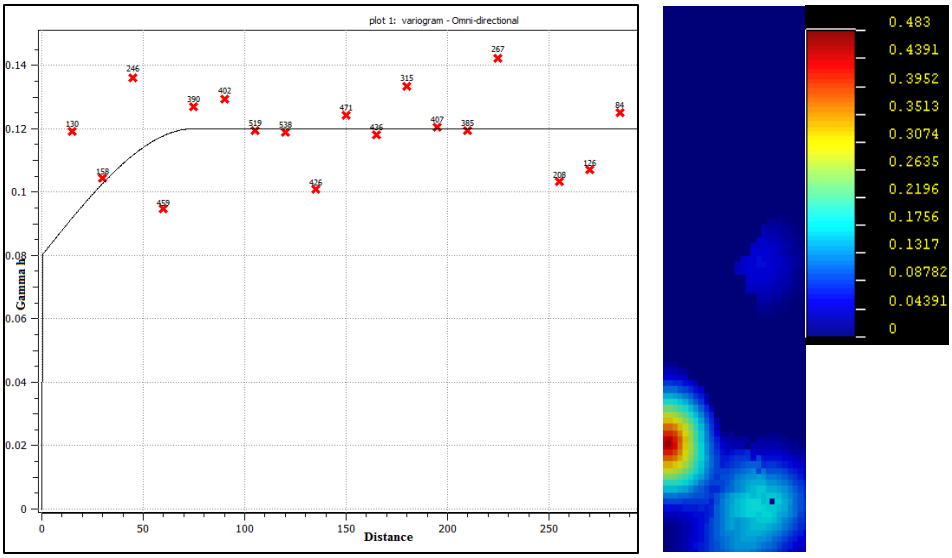

16. Variogram at >21 Spm^3 Cut-off. Nugget, sill contribution and range modelled at 0.04, 0.05 and 97.5 m respectively

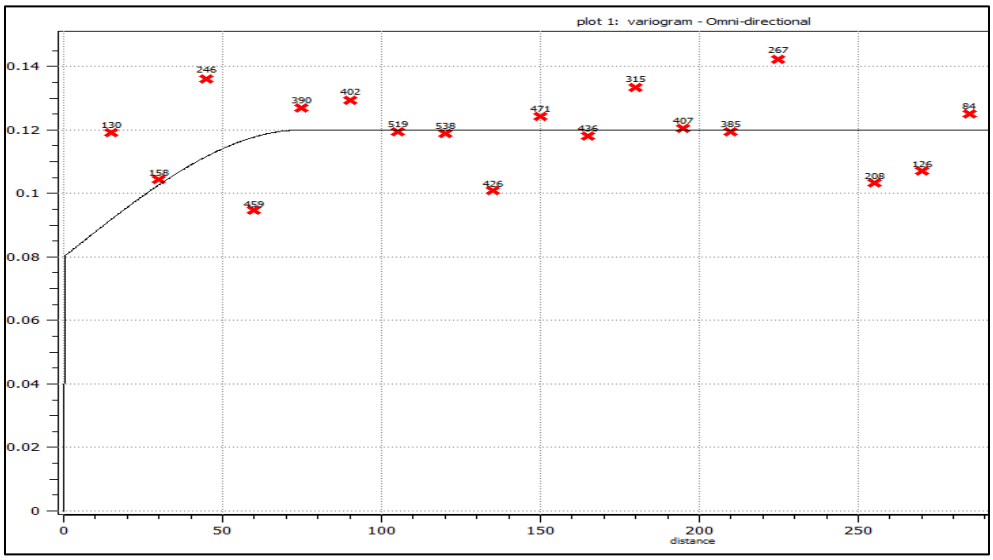

17. Variogram at >22 Spm^3 Cut-off. Nugget, sill contribution and range modelled at 0.04, 0.05 and 97.5 m respectively

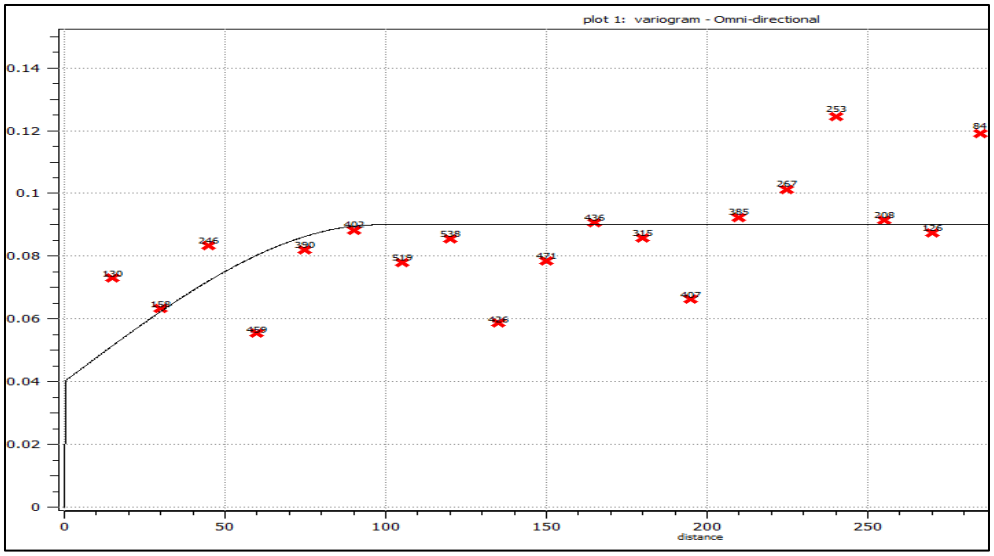

18. Variogram at >23 Spm^3 Cut-off. Nugget, sill contribution and range modelled at 0.028, 0.05 and 97.5 m respectively

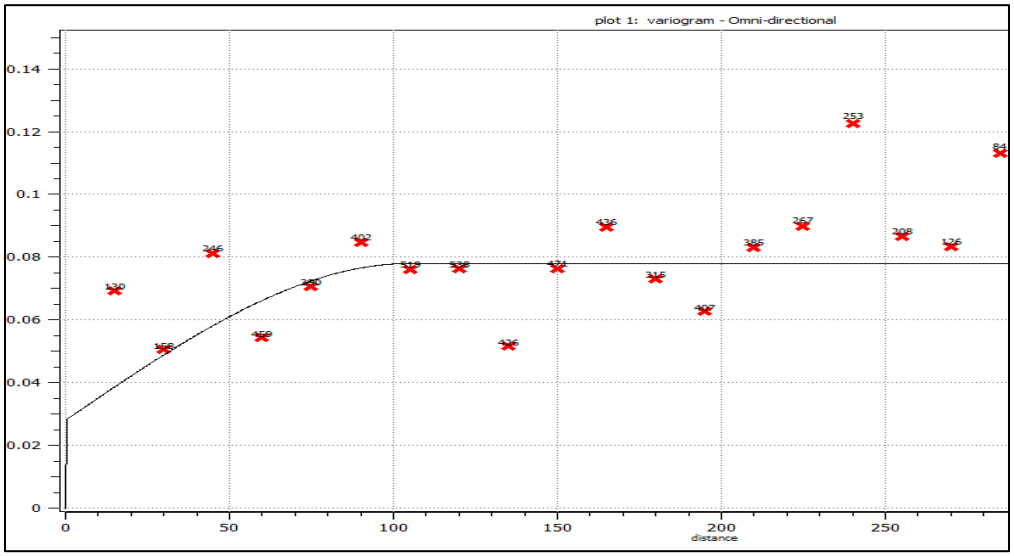

19. Variogram at >25 Spm^3 Cut-off. Nugget, sill contribution and range modelled at 0.04, 0.05 and 97.5 m respectively

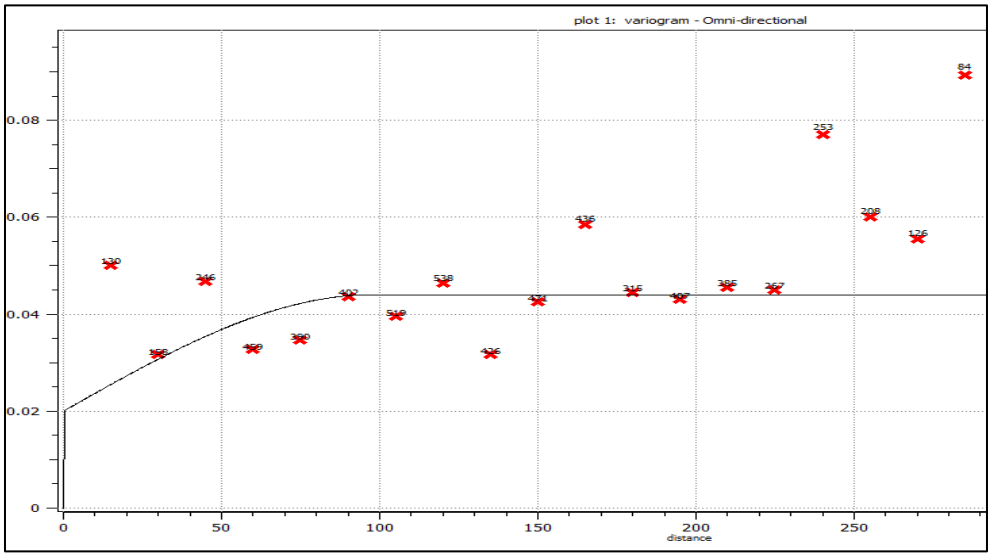

20. Variogram at >26 Spm^3 Cut-off and respective map output. Nugget, sill contribution and range modelled at 0.004, 0.04 and 97.5 m respectively

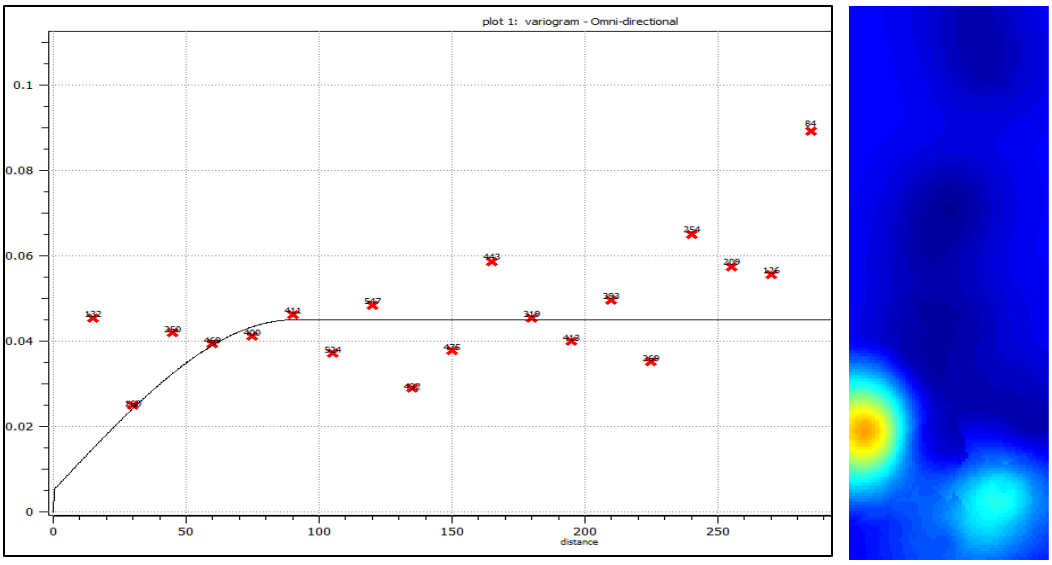

21. Variogram at >27 Spm^3 Cut-off. Nugget, sill contribution and range modelled at 0.004, 0.04 and 97.5 m respectively

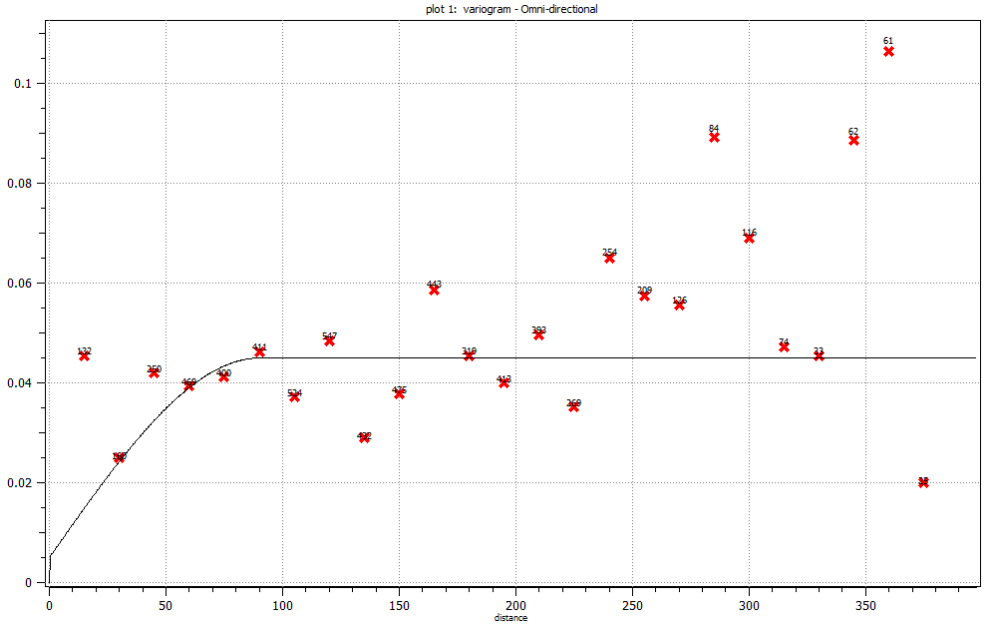

APPENDIX IV-PROGRESSIVE STATISTICS DATA

Realisation	No of Points	Blocks Estimated	Mean of Point Simulation	Var of Point Simulations	Point Sim Std Dev	Point Simulations COV	Mean Blk Simulations	Var BLK Simulations	Std Dev of Blk Simulations	BLK COV	Mean Raw Data	Var Raw Data	Std Dev Raw Data	COV Raw data
0	205200	2052	10.79	79.597	8.92	1.21	10.21	52.78	7.26	1.41	10.7	79.5	8.9	1.20
1	205200	2052	10.79	79.597	8.92	1.21	10.79	58.03	7.62	1.42	10.7	79.5	8.9	1.20
2	205200	2052	10.89	79.597	8.92	1.22	10.89	54.12	7.36	1.48	10.7	79.5	8.9	1.20
3	205200	2052	10.79	79.597	8.92	1.21	10.79	54.20	7.36	1.47	10.7	79.5	8.9	1.20
4	205200	2052	10.79	79.597	8.92	1.21	10.79	56.36	7.51	1.44	10.7	79.5	8.9	1.20
5	205200	2052	10.79	79.597	8.92	1.21	10.79	57.70	7.60	1.42	10.7	79.5	8.9	1.20
6	205200	2052	10.79	79.597	8.92	1.21	10.79	54.39	7.37	1.46	10.7	79.5	8.9	1.20
7	205200	2052	10.79	79.6694	8.93	1.21	10.79	58.44	7.64	1.41	10.7	79.5	8.9	1.20
8	205200	2052	10.79	79.597	8.92	1.21	10.79	53.95	7.35	1.47	10.7	79.5	8.9	1.20
9	205200	2052	10.79	79.597	8.92	1.21	10.79	54.07	7.35	1.47	10.7	79.5	8.9	1.20
10	205200	2052	10.79	79.597	8.92	1.21	10.79	53.36	7.30	1.48	10.7	79.5	8.9	1.20
11	205200	2052	10.80	80.61	8.98	1.20	10.80	56.99	7.55	1.43	10.7	79.5	8.9	1.20
12	205200	2052	10.79	79.73	8.93	1.21	10.79	56.99	7.55	1.43	10.7	79.5	8.9	1.20
13	205200	2052	10.79	79.597	8.92	1.21	10.79	52.93	7.27	1.48	10.7	79.5	8.9	1.20
14	205200	2052	10.79	79.597	8.92	1.21	10.79	56.09	7.49	1.44	10.7	79.5	8.9	1.20
15	205200	2052	10.79	79.597	8.92	1.21	10.79	55.70	7.46	1.45	10.7	79.5	8.9	1.20
16	205200	2052	10.79	79.597	8.92	1.21	10.79	51.88	7.20	1.50	10.7	79.5	8.9	1.20
17	205200	2052	10.79	79.597	8.92	1.21	10.79	52.87	7.27	1.48	10.7	79.5	8.9	1.20
18	205200	2052	10.79	79.597	8.92	1.21	10.79	55.11	7.42	1.45	10.7	79.5	8.9	1.20
19	205200	2052	10.80	80.57	8.98	1.20	10.80	59.05	7.68	1.41	10.7	79.5	8.9	1.20
20	205200	2052	10.79	79.597	8.92	1.21	10.79	56.01	7.48	1.44	10.7	79.5	8.9	1.20
21	205200	2052	10.79	79.6365	8.92	1.21	10.79	56.04	7.49	1.44	10.7	79.5	8.9	1.20
22	205200	2052	10.79	79.61	8.92	1.21	10.79	55.18	7.43	1.45	10.7	79.5	8.9	1.20
23	205200	2052	10.79	79.597	8.92	1.21	10.79	52.13	7.22	1.49	10.7	79.5	8.9	1.20
24	205200	2052	10.79	79.597	8.92	1.21	10.79	54.73	7.40	1.46	10.7	79.5	8.9	1.20
25	205200	2052	10.79	79.597	8.92	1.21	10.79	51.37	7.17	1.51	10.7	79.5	8.9	1.20
26	205200	2052	10.79	79.597	8.92	1.21	10.79	56.63	7.53	1.43	10.7	79.5	8.9	1.20
27	205200	2052	10.79	79.597	8.92	1.21	10.79	55.17	7.43	1.45	10.7	79.5	8.9	1.20
28	205200	2052	10.79	79.597	8.92	1.21	10.79	56.17	7.49	1.44	10.7	79.5	8.9	1.20
29	205200	2052	10.79	79.597	8.92	1.21	10.79	54.27	7.37	1.46	10.7	79.5	8.9	1.20
30	205200	2052	10.79	79.597	8.92	1.21	10.79	54.39	7.37	1.46	10.7	79.5	8.9	1.20
31	205200	2052	10.79	79.597	8.92	1.21	10.79	54.43	7.38	1.46	10.7	79.5	8.9	1.20
32	205200	2052	10.79	79.9064	8.94	1.21	10.79	55.64	7.46	1.45	10.7	79.5	8.9	1.20
33	205200	2052	10.79	79.597	8.92	1.21	10.79	55.25	7.43	1.45	10.7	79.5	8.9	1.20
34	205200	2052	10.79	79.597	8.92	1.21	10.79	51.69	7.19	1.50	10.7	79.5	8.9	1.20
35	205200	2052	10.79	79.597	8.92	1.21	10.79	53.28	7.30	1.48	10.7	79.5	8.9	1.20

Realisation	No of Points	Blocks Estimated	Mean of Point Simulation	Var of Point Simulations	Point Sim Std Dev	Point Simulations COV	Mean Blk Simulations	Var BLK Simulations	Std Dev of Blk Simulations	BLK COV	Mean Raw Data	Var Raw Data	Std Dev Raw Data	COV Raw data
36	205200	2052	10.79	79.598	8.92	1.21	10.79	54.02	7.35	1.47	10.7	79.5	8.9	1.20
37	205200	2052	10.79	79.597	8.92	1.21	10.79	52.47	7.24	1.49	10.7	79.5	8.9	1.20
38	205200	2052	10.79	79.597	8.92	1.21	10.79	56.08	7.49	1.44	10.7	79.5	8.9	1.20
39	205200	2052	10.79	79.597	8.92	1.21	10.79	54.47	7.38	1.46	10.7	79.5	8.9	1.20
40	205200	2052	10.79	79.597	8.92	1.21	10.79	56.47	7.51	1.44	10.7	79.5	8.9	1.20
41	205200	2052	10.79	79.5986	8.92	1.21	10.79	53.87	7.34	1.47	10.7	79.5	8.9	1.20
42	205200	2052	10.81	81.06	9.00	1.20	10.81	58.81	7.67	1.41	10.7	79.5	8.9	1.20
43	205200	2052	10.79	79.597	8.92	1.21	10.79	57.00	7.55	1.43	10.7	79.5	8.9	1.20
44	205200	2052	10.79	79.597	8.92	1.21	10.79	55.88	7.48	1.44	10.7	79.5	8.9	1.20
45	205200	2052	10.79	79.597	8.92	1.21	10.79	54.75	7.40	1.46	10.7	79.5	8.9	1.20
46	205200	2052	10.79	79.597	8.92	1.21	10.79	54.40	7.38	1.46	10.7	79.5	8.9	1.20
47	205200	2052	10.79	79.597	8.92	1.21	10.79	54.53	7.38	1.46	10.7	79.5	8.9	1.20
48	205200	2052	10.79	79.597	8.92	1.21	10.79	56.10	7.49	1.44	10.7	79.5	8.9	1.20
49	205200	2052	10.79	79.597	8.92	1.21	10.79	54.19	7.36	1.47	10.7	79.5	8.9	1.20

Plot of progressive mean against the number of realisations for block Point and Block simulations

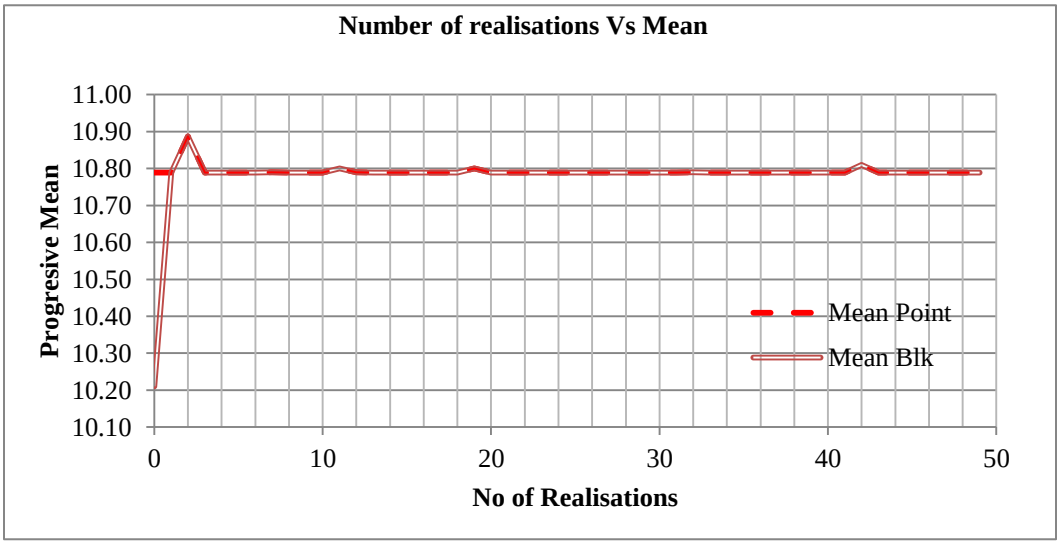

Plot of Progressive COV against the number of realisations for Raw data, Block and Point simulations

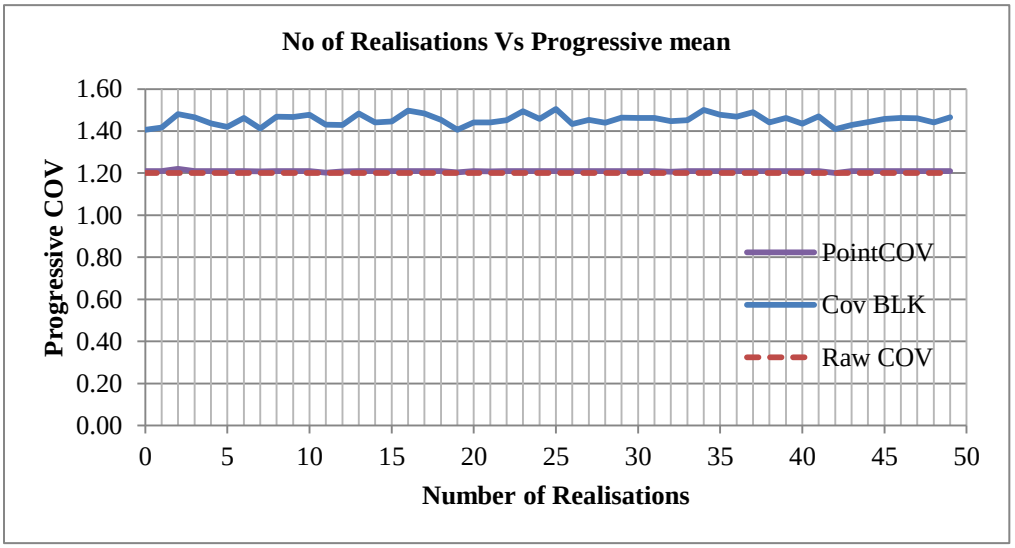

APPENDIX V-SUMMARY OF REALISATION STATISTICS

Realisation No	Gaussian Statistics		Back-transformed Stats		Histograms		Correlation Coefficient	Correlation coefficient differences
	Mean	Variance	Mean	Variance	Simulated Mean/Drillhole Average (%)	Simulated variance/Drillhole Variance (%)		
0	0.17	0.83	10.78	79.5	100.7	103.9	0.88	0.12
1	-0.03	1	10.78	79.5	100.7	103.9	0.89	0.11
2	0.03	0.88	10.79	79.6	100.7	104.1	0.87	0.13
3	-0.03	0.84	10.78	79.5	100.7	103.9	0.79	0.21
4	-0.016	0.97	10.79	79.6	100.7	104.1	0.86	0.14
5	-0.05	0.99	10.79	79.6	100.7	104.1	0.84	0.16
6	0.12	0.89	10.79	79.6	100.7	104.1	0.85	0.15
7	-0.014	1.1	10.79	79.7	100.7	104.2	0.86	0.14
8	0.08	0.86	10.79	79.6	100.7	104.1	0.83	0.17
9	-0.08	0.85	10.79	79.6	100.7	104.1	0.87	0.13
10	0.14	0.85	10.78	79.59	100.7	104.1	0.88	0.12
11	0.12	0.89	10.8	80.61	100.8	105.4	0.84	0.16
12	0.14	0.95	10.79	79.73	100.7	104.2	0.88	0.12
13	0.18	0.85	10.79	79.6	100.7	104.1	0.84	0.16
14	-0.057	0.94	10.79	79.6	100.7	104.1	0.85	0.15
15	-0.13	0.886	10.79	79.6	100.7	104.1	0.85	0.15
16	-0.1285	0.86	10.79	79.6	100.7	104.1	0.88	0.12
17	-0.03	0.84	10.79	79.6	100.7	104.1	0.85	0.15
18	-0.03	0.93	10.79	79.6	100.7	104.1	0.89	0.11
19	0.14	1.03	10.8	80.57	100.8	105.3	0.85	0.15
20	-0.058	0.94	10.79	79.6	100.7	104.1	0.86	0.14
21	-0.02	0.91	10.79	79.64	100.7	104.1	0.82	0.18
22	0.08	0.92	10.79	79.6	100.7	104.1	0.81	0.19
23	-0.03	0.83	10.79	79.6	100.7	104.1	0.86	0.14
24	0.12	0.87	10.79	79.6	100.7	104.1	0.87	0.13
25	0.26	0.8	10.79	79.6	100.7	104.1	0.85	0.15

Realisation No	Gaussian Statistics		Back-transformed Stats		Histograms		Correlation Coefficient	Correlation coefficient differences
	Mean	Variance	Mean	Variance	Simulated Mean/Drillhole Average (%)	Simulated variance/Drillhole Variance (%)		
26	0.04	1	10.79	79.6	100.7	104.1	0.85	0.15
27	-0.027	0.92	10.79	79.6	100.7	104.1	0.81	0.19
28	0.04	0.93	10.79	79.6	100.7	104.1	0.84	0.16
29	0.12	0.9	10.79	79.6	100.7	104.1	0.89	0.11
30	-0.17	0.91	10.79	79.6	100.7	104.1	0.85	0.15
31	0.01	0.91	10.79	79.6	100.7	104.1	0.84	0.16
32	0.25	0.94	10.79	79.9	100.7	104.5	0.89	0.11
33	0.013	0.89	10.79	79.9	100.7	104.5	0.88	0.12
34	0.05	0.79	10.79	79.6	100.7	104.1	0.87	0.13
35	0.019	0.86	10.79	79.6	100.7	104.1	0.84	0.16
36	0.21	0.84	10.79	79.6	100.7	104.1	0.84	0.16
37	0	0.81	10.79	79.6	100.7	104.1	0.85	0.15
38	-0.17	0.93	10.79	79.6	100.7	104.1	0.83	0.17
39	0.23	0.91	10.79	79.6	100.7	104.1	0.85	0.15
40	0.59	0.98	10.79	79.6	100.7	104.1	0.88	0.12
41	0.12	0.87	10.79	79.6	100.7	104.1	0.84	0.16
42	0.16	0.99	10.8	81.06	100.8	106.0	0.86	0.14
43	0.03	0.97	10.79	79.6	100.7	104.1	0.82	0.18
44	-0.002	0.95	10.79	79.6	100.7	104.1	0.86	0.14
45	0.002	0.88	10.79	79.6	100.7	104.1	0.83	0.17
46	0.08	0.92	10.79	79.6	100.7	104.1	0.88	0.12
47	0.09	0.88	10.79	79.6	100.7	104.1	0.88	0.12
48	0.03	0.99	10.79	79.6	100.7	104.1	0.83	0.17
49	-0.2	0.97	10.79	79.6	100.7	104.1	0.84	0.16

APPPENDIX VI- SELECTED INDIVIDUAL REALISATIONS

Realisation0	Realisation7	Realisation 15	Realisation 17	
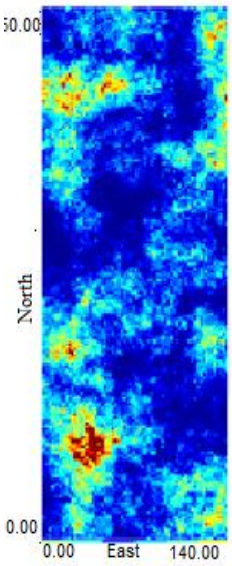	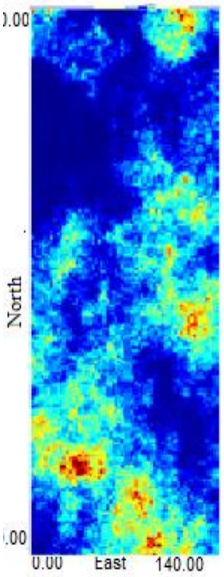	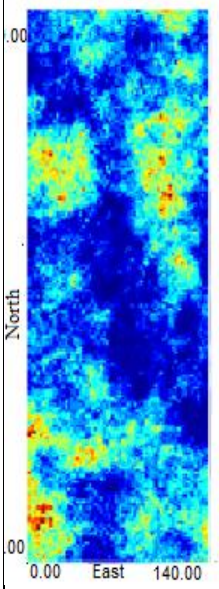	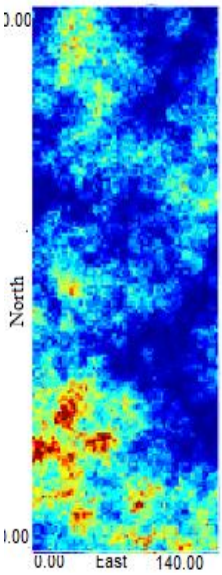	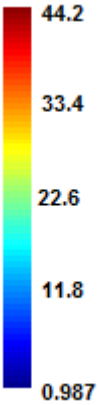
Realisation 23,	**Realisation27**	**Realisation 31**	**Realisation 39**	
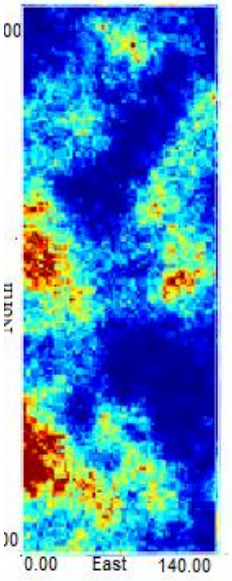	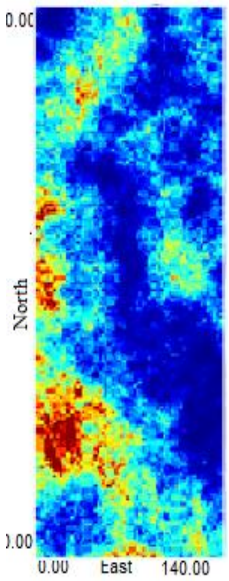	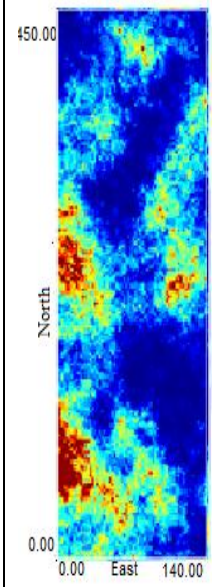	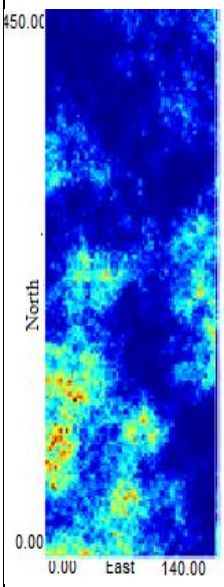	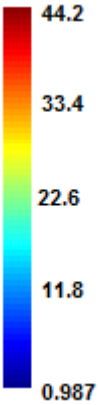

Realisation 40,	Realisation 45		
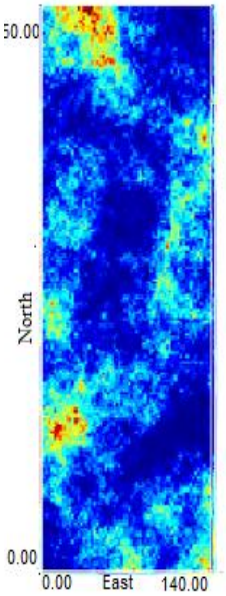	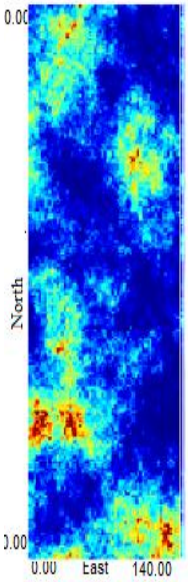		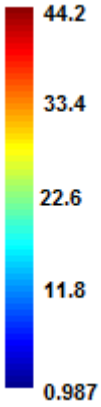

APPENDIX V11 –15m BENCH INTERVAL AND BLOCK KRIGING MAPS OUTPUT COMPARED TO SIMULATED MAPS OUTPUT PER BENCH INTERVAL

ELEVATION	BENCH
725	1
710	2
690	3
675	4
660	5
645	6
630	7
615	8
600	9
585	10
570	11
555	12
540	13
525	14
510	15
495	16
480	17
465	18

Kriging Map Outputs	Simulation Maps Output
1 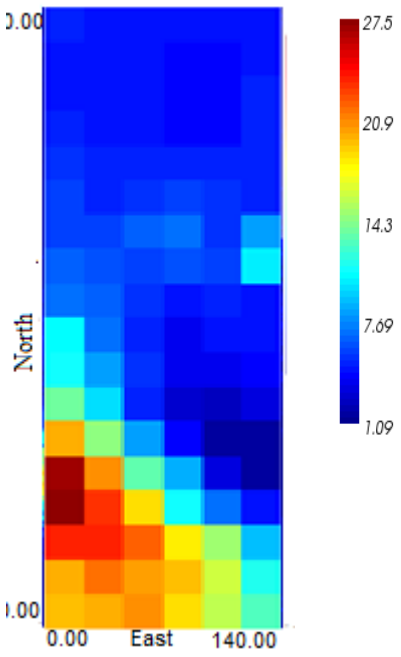	1 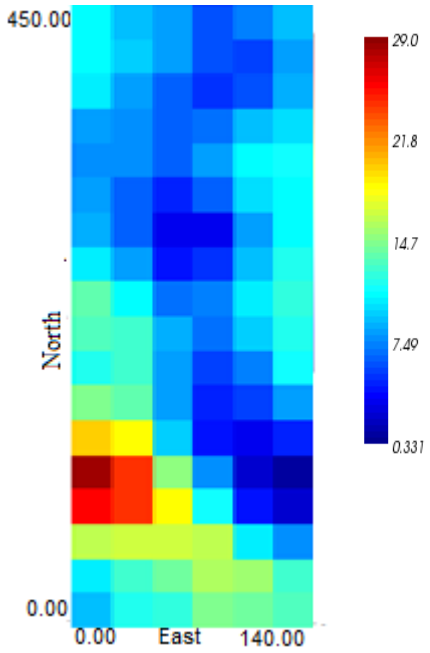
3 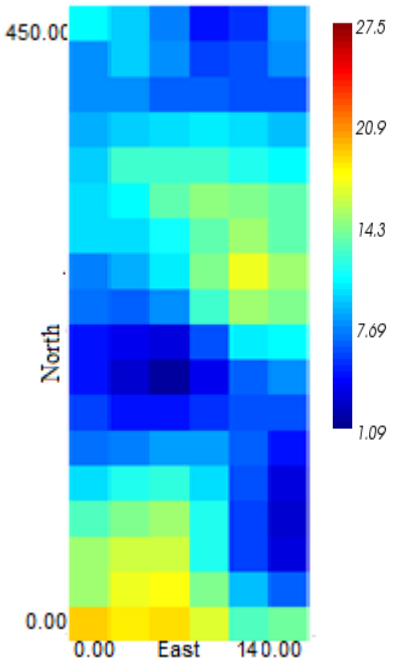	3 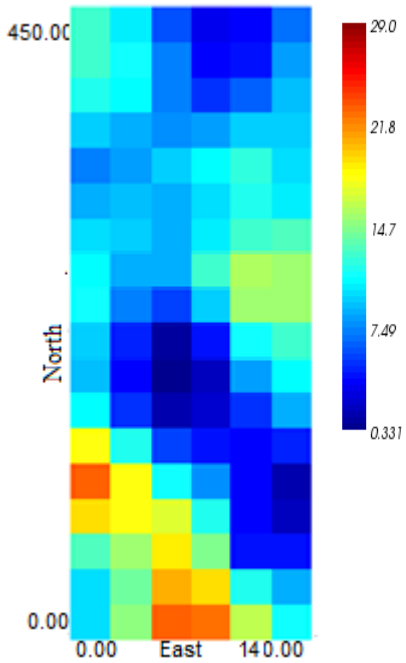

Kriging Map Outputs	Simulation Maps Output
5 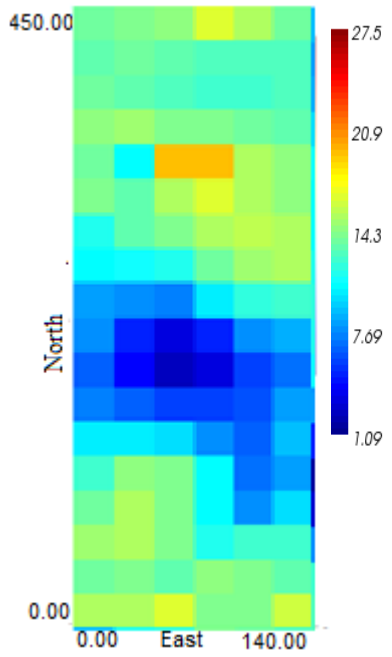	5 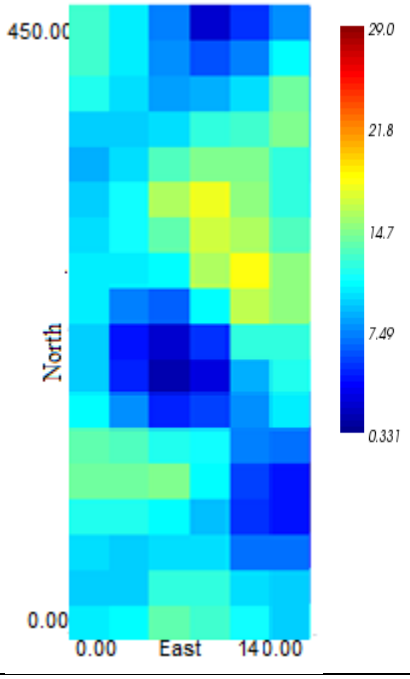
7 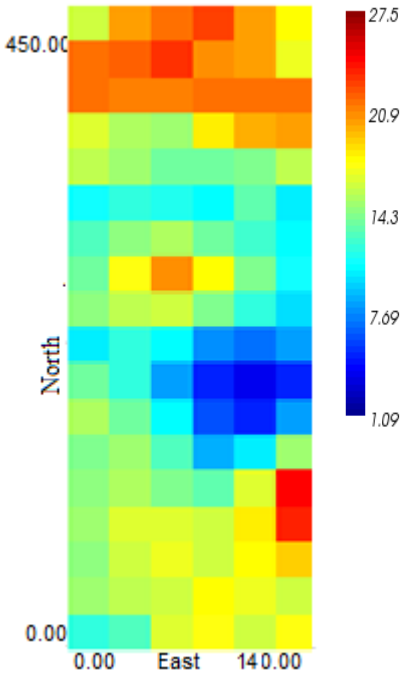	7 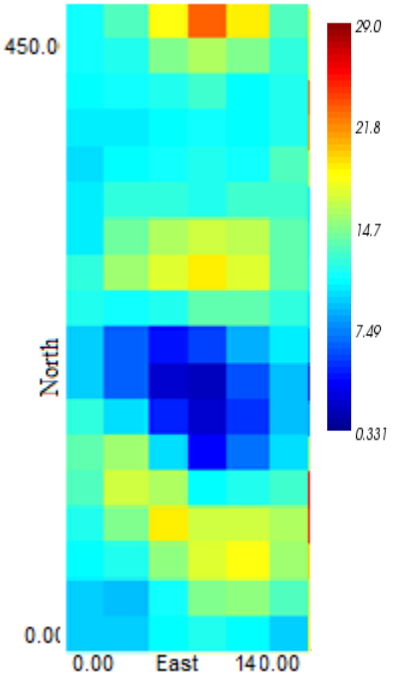

Kriging Map Outputs	Simulation Maps Output
9 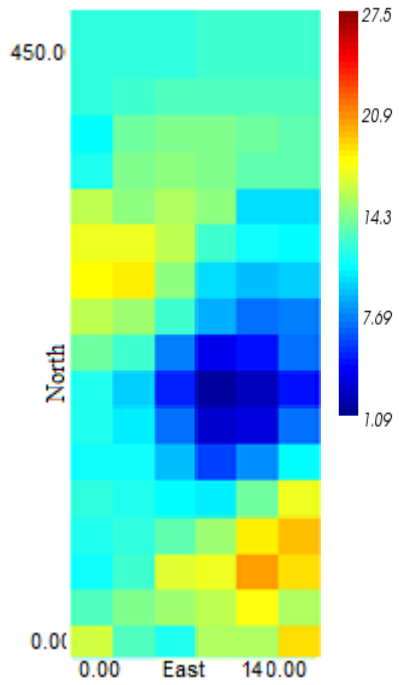	9 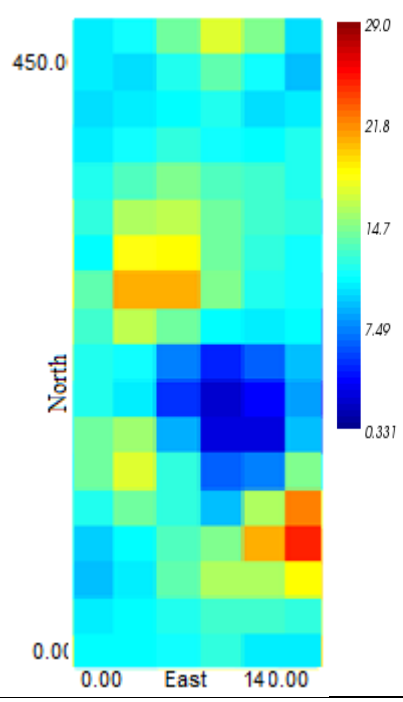
11 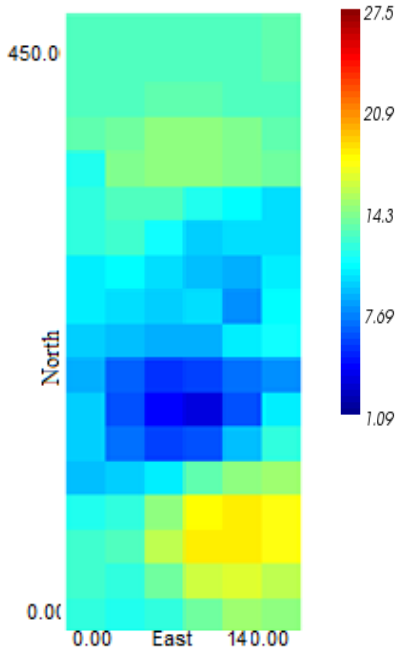	11 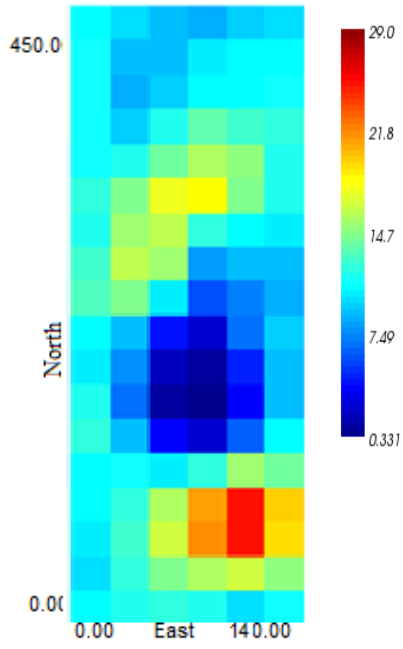

Kriging Map Outputs	Simulation Maps Output
13 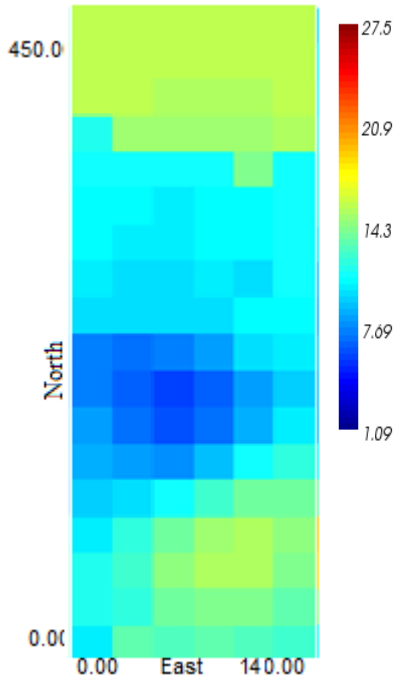	13 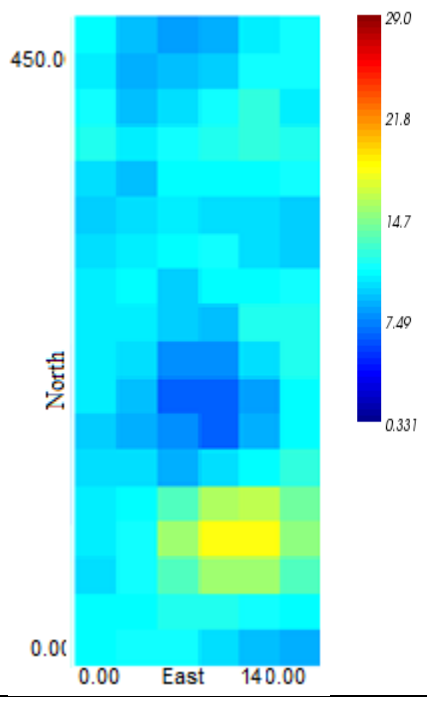
15 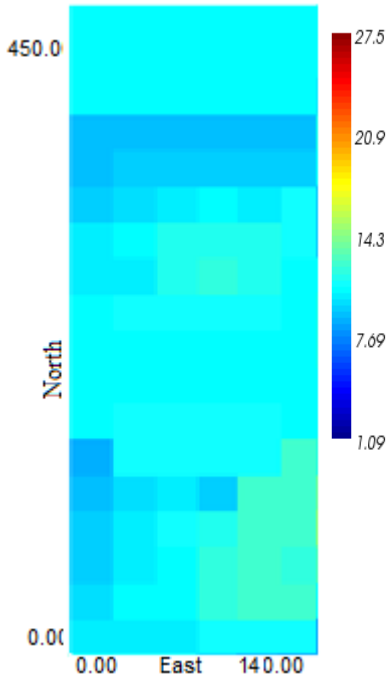	15 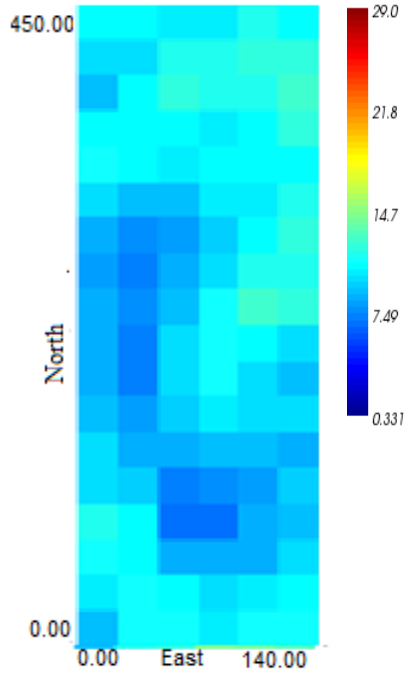

Kriging Map Outputs	Simulation Maps Output
17 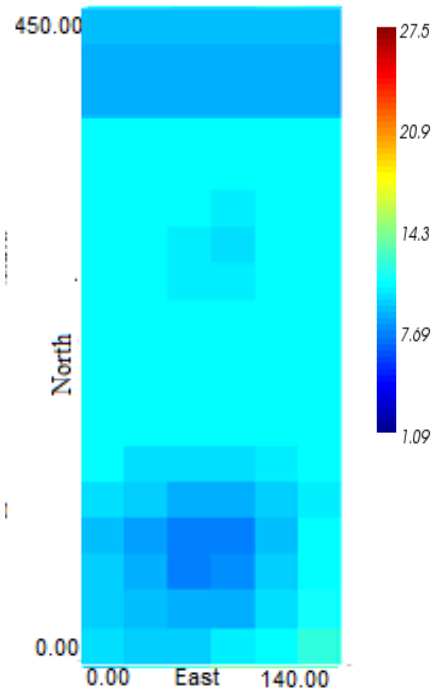	17 